Binding and Detection of Anions Using Tripodal Hosts

TODD, ADAM,MITCHELL

Binding and Detection of Anions Using Tripodal Hosts

A thesis submitted for the fulfillment of the requirements for the degree of

Doctor of Philosophy

In the faculty of Science of Durham University

by

Adam Mitchell Todd

Department of Chemistry

Durham University

South Road

Durham

2010

"I may not have gone where I intended to go, but I think I have ended up where I needed to be." **- Douglas Adams**

Abstract

The aim of this project was to investigate the anion-binding properties of a range of different receptor compounds. For the most part, the receptors reported here were tripodal in nature, wherein three hydrogen-bonding receptor groups, including amines, amides and ureas, are linked around a common structural core. In this study, a range of different cores were chosen, such as simple and flexible organic frameworks based on the tris(2-aminoethyl)amine (tren) precursor, conformationally-restricted and brightly coloured aromatic species based on the dye pararosaniline, and triply-ligated metal complexes of ruthenium(II).

In order to assess the anion binding abilities of these receptors, a range of different techniques were employed, with ^{1}H-NMR and UV/Visible spectroscopic titrations being the most common. Additionally, the incorporation of fluorescent pyrene moieties as a reporter group to some of the receptors allowed for the probing of anion binding via fluorimetric titrations in these cases.

During the course of the experiments, a number of interesting, and in some cases, unexpected, binding conformations were found – in particular, the interactions between many of the organic receptor compounds with the planar 1,3,5-benzenetricarboxylate (trimesylate) trianion, and the pH dependency of the colour of the pararosaniline-based receptors. Additionally, the range of cyclic thioether-capped ruthenium(II) receptor compounds reported here showed an unusually high resistance to degradation by solvent and guest when compared to similar receptors with aromatic-capped ruthenium, and successfully gave tripodal ML_3 complexes instead of the traditionally more stable ML_2X dipodal complexes.

Acknowledgements

First and foremost, I would like to thank my supervisor, Professor Jon Steed, for his help, guidance and direction these last years, and for giving me the opportunity to work on such an interesting and variable area of study. Thanks are also due to the members of Professor Steed's research group who have aided my work with their own experience and skills over the time I've worked alongside them. Particular thanks go to Adam Swinburne, for his invaluable assistance in the fluorometrics, and to the combined expertise of Drs Gareth Lloyd and Kirsty Anderson for their aid in the crystallography. In the same vein, additional thanks go to Dr Andres Goeta for taking the time to teach me how to collect and solve crystal data myself. Thanks also to Dr Martin Paterson of Heriot-Watt University for his assistance with the molecular modelling. Additionally, thanks also go to all of the members of the various analytical services at Durham, in NMR, mass spectrometry, crystallography, and elemental analysis for the collection of the majority of the analytical data. Also, thanks to the University of Durham as a whole, for giving me the chance to work amongst such people – it's become a home away from home, and it has been an honour to study and work here.

Personally, I would also like to thank my dear friends and family, for standing by me and supporting me throughout the last few years. It hasn't always been easy, but I believe it has been worthwhile. Finally, I would like to dedicate this work to my grandfather, Alexander Todd, who sadly passed away over the course of my time here and thus never got to see this finished product, though I know he was always proud of me.

1. Introduction

1.1 Background

The presence or lack of certain anionic species can have a detrimental effect on both health and the environment, and as such the ability to detect and perhaps influence anions within systems is desirable. The human body is dependent on anions (indeed, DNA is a polyanion) and an imbalance in the concentrations of these anions can lead to the development of a wide variety of medical complaints – for example, cystic fibrosis is a condition that is identified by the reduced ability of the body's cells to maintain a consistent chloride concentration.[1] Environmentally, many anions are viewed as contaminants, and efforts to remove them, or at least detect their presence, are driving the development of new and more effective anion sensors and receptor compounds.[2-5] There are a number of factors to consider, such as how do we attract the anion? How do we prove that the receptor has bound the anion? There are a number of answers to each question, and many of these will be discussed here. An obvious first step is to look at the various methods commonly used to attract and bind the anion.

1.2 Anion Binding Modes

1.2.1 Electrostatic Attraction

Perhaps the most obvious way to attract a negatively-charged species is by using a positively-charged receptor. One of the ways that this can be achieved is by protonation of an existing basic species within the receptor compound, typically a nitrogen lone pair. This technique has been used effectively by Park and Simmons,[6] who were among the first to detect anion encapsulation within katapinand azacages – tripodal cages consisting of two tertiary amines linked together by three aliphatic organic chains of varying length. Protonation of the amine nitrogen atoms using an acid such as HCl gives a dication with a chloride anion encapsulated within the cage (Figure 1.1). The selectivity towards anions in these cages is dependent on the size of the cavity, as anions which are too large are unable to fit inside the capsule.

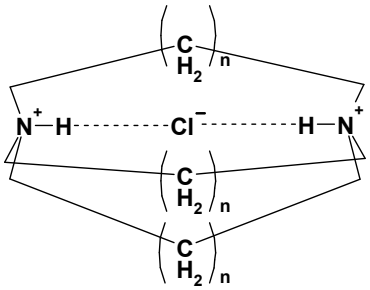

Figure 1.1 – General structure of katapinand azacages.

Linear biological polyamines have been well documented as anion receptors, showing a high affinity for phosphate and more complex polyanions even in water.[7] Combining the studies into azacages and their ability to encapsulate a guest well via coulombic attraction, and the idea that a polyammonium species is a good anion receptor, it becomes a logical step to combine as many ammonium functionalities as possible around a central receptor pocket, in order to maximise the attractive forces between host and guest. A range of macrocyclic polyammonium receptors were synthesised by Dietrich and Lehn with progressively larger, and thus more nitrogen-rich, cavities (Figure 1.2).[8-9] Their studies, combined with others on similar macrocyclic systems, indicated that the anion binding was driven primarily by electrostatic attraction, with the larger and more charged hosts showing increased stability constants in the majority of case. Little selectivity between anions is present, likely due to the inherently high flexibility of the host, which can fairly easily fold into a suitable shape for whatever guest species is present with little change in energy.

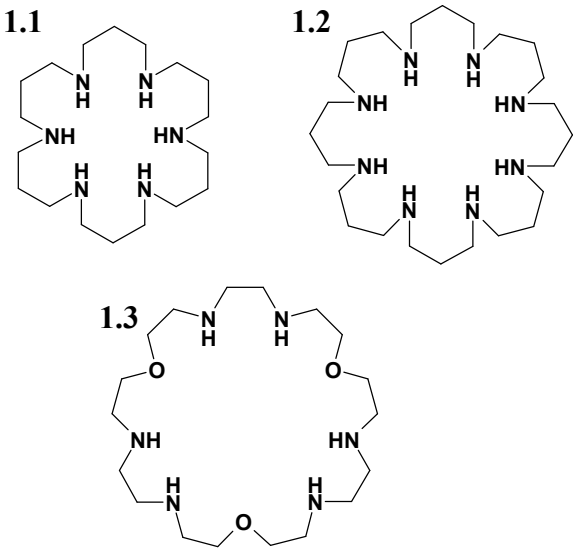

Anion	[1.1].6H$^+$	[1.2].8H$^+$	[1.3].6H$^+$
Oxalate^{2-}	3.8	3.7	4.7
Sulphate^{2-}	4.0	4.0	4.5
Fumarate^{2-}	2.2	2.9	2.6
Squarate^{2-}	3.2	3.6	3.4
Citrate^{2-}	4.7	7.6	5.8
Trimesylate^{3-}	3.5	6.1	3.8
$Co(CN)_6^{3-}$	3.9	6.0	3.3
AMP^{3-}	3.4	4.1	4.7
ADP^{3-}	6.5	7.5	7.7
ATP^{3-}	8.9	8.5	9.1

Figure 1.2 – Structure of azacrown macrocycles **1.1**, **1.2** and **1.3**, with a table of stability constants (log K values determined from pH titration methods in water).[8]

Following on from this work, Lehn then returned to the original idea of macrobicyclic systems developed by Park and Simmons, synthesising a range of cryptands, but with replacement of the hydrocarbon chains from the original studies with additional amine groups (Figure 1.3).[10-11] These cryptands, in acidic pH, undergo expansion by the electrostatic repulsion of the protonated ammonium groups, a process which allows the guest to enter. The anionic guest is bound by a mixture of electrostatic interaction and hydrogen bonding, with the latter being more important for the spherical halide ions than for the ellipsoidal anions, such as azide and dicarboxylates, which are a better fit for the pseudo-elliptical cavity formed by the receptor.

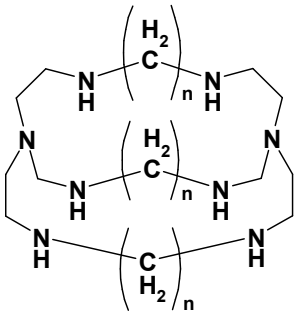

Figure 1.3 – Bicyclic azacryptands.

This method of protonated nitrogen-containing host compounds presents a significant limitation however: the host:guest system must be under rather acidic conditions, in order to ensure that all of the amino groups are fully protonated. Since pK_a values are dependent on the solvent system, it is extremely difficult to predict how the behaviours will change in different conditions, where fewer protonation sites are occupied. In an attempt to counteract this problem, Schmidtchen designed and synthesised the pseudo-tetrahedral quaternary ammonium hosts **1.4** and **1.5** (Figure 1.4).[12-13] It was hoped that these hosts would prove to be effective anion receptors, despite the lack of hydrogen bond donor groups, and indeed this was found to be the case, with a wide range of anions able to fit well in the cavity within the host, with internal diameters estimated as 4.6Å and 7.6Å for **1.4** and **1.5** respectively. Indeed, considering that the ionic radius of iodide is approximately 2.2Å, it was found that iodide in particular was an excellent guest for the smaller **1.4**, such that the host proved effective as a preferential transport for iodide across a membrane even in the presence of chloride.[14]

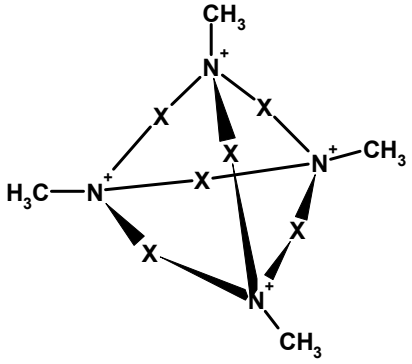

X = $(CH_2)_6$: **1.4**

$(CH_2)_8$: **1.5**

Figure 1.4 – Quaternary ammonium hosts.

The biggest difficulty faced by the use of primarily electrostatic interactions in host-anion chemistry is that often they lack a significant energetic driving force to association within the receptor. Much of the favourable energy change gained by complexation of the anion within the receptor cavity is balanced by the negative effect caused by the need for the anion to be desolvated before association can occur. Since many of the systems mentioned above are water-soluble, often the guest species is highly solvated by water molecules, so binding to the host, if it happens at all, is typically just as likely to occur on the outer surface of the host as within the cavity, since this binding mode reduces the need for desolvation to occur.

More effective cationic receptors result when the host relies less on purely electrostatic interactions, but also incorporates directionality by including some hydrogen bond donor groups. Extensive work by Sessler *et al*. has looked at the use of oligopyrroles such as porphyrin and various analogues,[15-18] using the innate preorganisation of the planar ring system as the basis for their hosts. Over the course of their studies, they were able to synthesise the di-protonated sapphyrin species **1.6**, and found it to be an excellent receptor for fluoride,[19] which was found to be the only anion of sufficiently small size to be included inside the plane of the ring. Other

anions, such as chloride and bromide, also bind to the receptor, but are too large to form the desired inclusion complex.

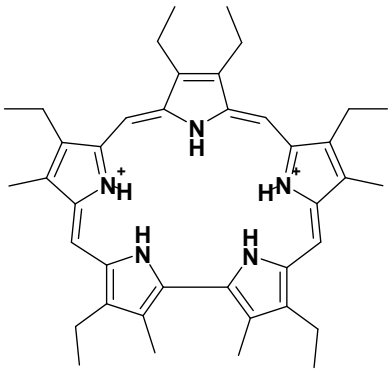

Figure 1.5 – Di-protonated sapphyrin **1.6**.

Other groups have also borrowed ideas from Nature by the use of guanidinium as a receptor group.[20] The guanidinium group is used in many enzymes as a binding group, particularly for many oxoanions, thanks to its ability to form two parallel hydrogen bonds to any guest species. This ability, coupled with the positive charge inherent to the guanidinium group, makes for an excellent anion binding species. Lehn continued his studies on macrocyclic systems by looking at the effect of incorporating guanidinium binding groups into the ring system[21] and found that complexation of anions, in particular phosphate, was driven primarily by electrostatic interactions. Further studies into the macrocyclic receptors **1.7** and **1.8** confirmed this, as the selectivity of the anion binding is dependent on the charge density of the anion.[22]

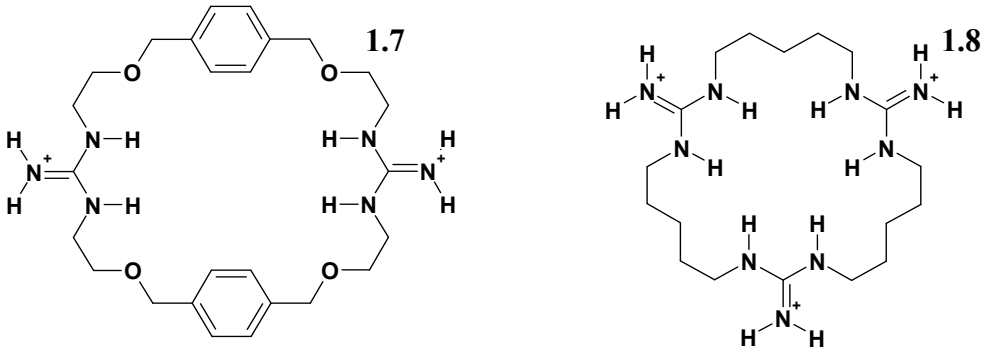

Figure 1.6 – Macrocyclic guanidinium receptors.

Others, such as Hamilton[23] and Göbel[24] have opted for simpler receptor compounds, synthesising cleft-shaped bis-guanidinium receptors based around a basic aryl or alkyl spacer group (Figure 1.7). These compounds have excited particular interest as enzyme mimics, with rate enhancements of 300 times being observed for **1.9**[25] and almost 5000 times being observed for **1.10**[26] in transesterification reactions compared to the uncatalysed reaction. These bis-guanidinium receptors also show superior catalytic behaviour over mono-guanidinium receptors, showing the improved complexation that can arise as a result of multiple binding groups leading to cooperative binding. In an attempt to design a receptor with even greater cooperative binding ability, Anslyn synthesised **1.11**,[27] and found that it showed significantly higher binding constants for phosphates than the more conformationally flexible hosts.

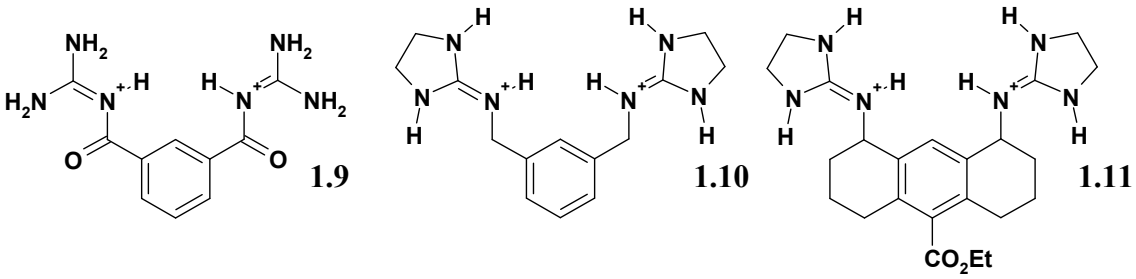

Figure 1.7 – Bis-guanidinium receptors.

Another way of creating a host compound with a cationic binding site is to incorporate a metal centre in some way. An effective way to achieve this is found by considering the system in a similar way to the aforementioned protonated hosts (Figures 1.1 - 1.4). For example, the azacrown ethers and cryptands shown earlier (Figures 1.1 – 1.3) can, in their basic form, be used to complex metal cations instead of protonation. Such systems then present an electropositive void at their centre, sandwiched between metal sites. The bis(tren) systems prove particularly effective at this arrangement, with the four amine nitrogen atoms in an ideal arrangement to complex to a metal such as copper, generating a cryptand such as **1.12**.[28]

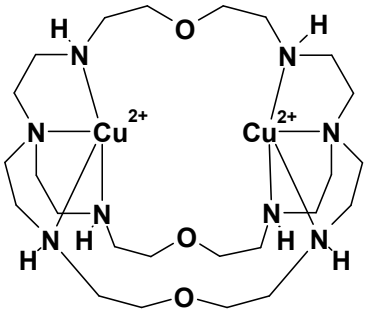

1.12

Figure 1.8 – Cu(II)-containing cryptand **1.12**.

This system showed excellent affinity for chloride, which is a good fit for the intermetallic spacing, and is believed to bind in bridging mode, since replacing one of the metal ions with two protons (thus maintaining the total charge) leads to a significantly weaker binding constant with chloride.

Another technique useful in incorporating a metal as part of the binding site is the use of cobaltocene or ferrocene. Cobaltocene ($[Co(Cp)_2]$) (Cp = cyclopentadienyl, $C_5H_5^-$) is the cobalt-containing analogue of ferrocene ($Fe(Cp)_2$), and is of virtually identical size and shape. Both are redox-responsive, particularly cobaltocene, which is more stable in the d^6 electronic configuration as cobaltocenium, containing Co(III). Incorporation of this species into the binding site of a receptor is synthetically easy, and allows for the metal centre to act as a redox probe. The positive charge of cobaltocenium is a useful anion-binding feature, although it alone is not sufficient to lead to any significant anion binding, with strong binding requiring the additional support of hydrogen-bonding groups. A number of cobaltocenium-containing receptors have been reported, the simplest being the bis-phenylamido compound **1.13** (Figure 1.9) synthesised by Beer.[29] This receptor uses the cobaltocenium unit as a structural feature, as well as taking advantage of the positive charge to assist in anion complexation. Similarly, the same group reported the related tripodal cobaltocenium receptor **1.14**,[30] this time using a simple aryl scaffold with the cobaltocenium groups incorporated as part of the receptor's arms. These systems were found to bind to anions in solvents such as acetonitrile or dimethyl sulphoxide, though they gave low binding constants and thus poor selectivity between anions.

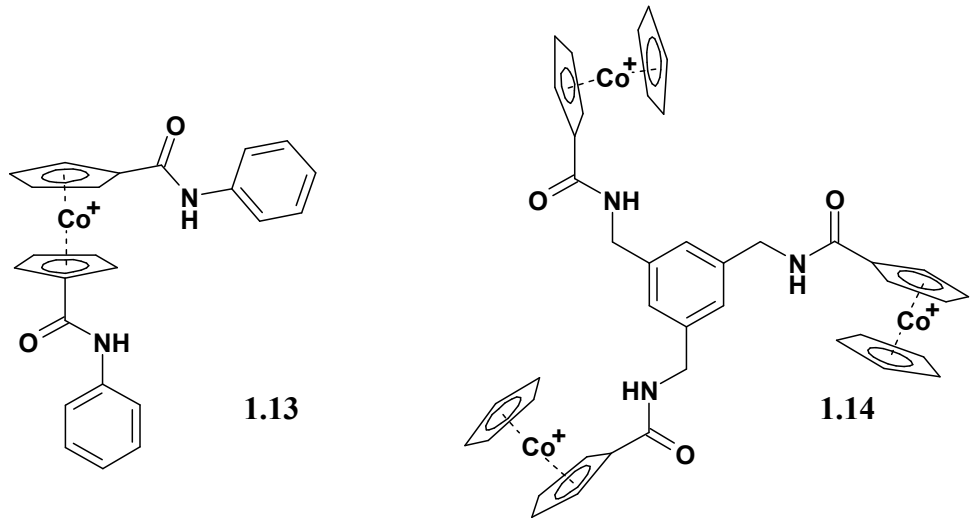

Figure 1.9 – Cobaltocenium-based receptors.

An interesting technique to incorporate a metal site into an anion receptor was employed by Atwood *et al*.[31-33] By taking macrocyclic cycloveratrylenes and calixarenes, which are ordinarily poor anion receptors due to their high electron density, and complexing metal fragments to the aromatic rings, it was possible to create an effective anion binding pocket within the bowl-shaped cavity inherent in such macrocycles (Figure 1.10). Upon coordination of the metal, typically ruthenium or iridium, electron density is drawn from the ring to the metal by π-metal interactions. This leads to a more electropositive central cavity which, in combination with the positive charge provided by the coordinated metal ions, proved extremely useful in the complexation of anions via anion-π interactions. Complexation of anions was found to occur via the cup form, with oxoanions such as trifluoromethane sulphonate ($CF_3SO_3^-$) binding with the hydrophobic region turned to the bottom of the cavity, exposing the hydrophilic anionic region to the solvent.[31]

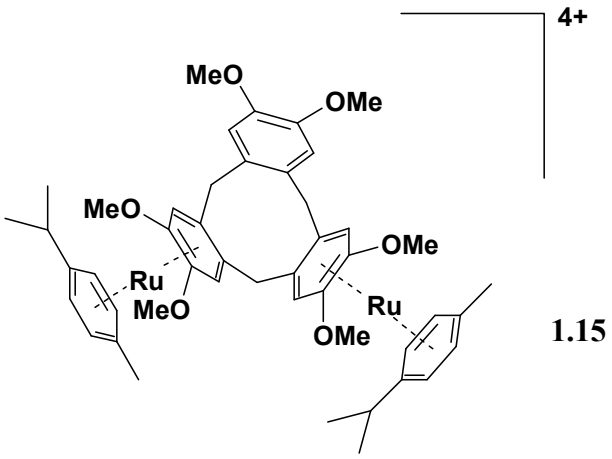

1.15

Figure 1.10 – Macrocyclic cycloveratrylene receptor **1.15**.

Anion binding using cationic receptors can be a powerful method, but in many cases, the electrostatic interactions alone are insufficient to encourage strong binding, as evidenced by the fact that many of the examples mentioned here are more complex macrocycles and cryptands. Those systems which show the highest affinity for anions typically contain more than just a positive charge in the binding site.

1.2.2 Neutral Hydrogen Bond Interactions

An alternative to receptor compounds based on a charged species is to employ a neutral receptor design. In this case, the receptor usually relies on hydrogen bonds alone to bind to a guest species, which can be advantageous since there is no need to consider the counter ion that is associated with a cationic receptor. The most common functional groups used in neutral anion receptors are amines, amides, ureas and thioureas. While less commonly used, amines represent the simplest form of neutral anion receptor. Primary amines in anion receptors are rare, as an amine is typically a more basic functional group and so make for better hydrogen bond acceptors than

donors. More common is the use of a secondary amine, especially when one or both of the substituents are electron-releasing. Perhaps the most common bonding group used in this case is pyrrole. Pyrrole is unique compared to other amines since the lone electron pair of the nitrogen can be delocalised into the ring system, thus being less available to accept a hydrogen bond. For example, Cheng and coworkers synthesised the tripodal receptor **1.16** (Figure 1.11) and studied its anion binding properties.[34] They found, as expected, that **1.16** showed a higher affinity for more basic anions such as $H_2PO_4^-$ and F^- due to the higher acidity of the pyrrolic N-H group.

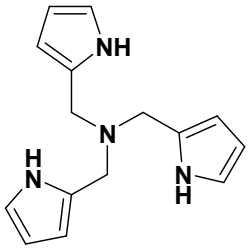

Figure 1.11 – Tris(pyrrole) receptor **1.16**.

Others have incorporated the pyrrole moiety into a macrocyclic receptor. Work by Sessler demonstrated the synthesis and anion binding properties of the calix[4]pyrrole **1.17** (Figure 1.12) which was found to bind fluoride selectively in dichloromethane solution.[35] Later work on **1.17** showed that this selectivity was very much dependent on the nature of the solvent, with the selectivity for fluoride lost in changing the solvent from dichloromethane to absolute acetonitrile.[36]

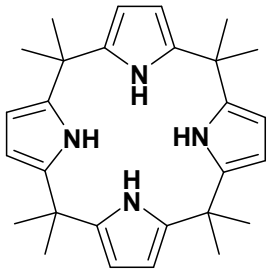

Figure 1.12 – Calix[4]pyrrole **1.17**.

Far more effective than most amines as anion receptors are those functional groups which contain more acidic hydrogen atoms, since more acidic hydrogens are stronger hydrogen bond donors. This can be achieved by functionalising the amine to an amide or urea, wherein the neighbouring carbonyl is able to delocalise the nitrogen lone pair. Because of the lower basicity of the nitrogen atom caused by this effect, amide and urea-based receptors are significantly more common. Anion receptors using amides as the binding group have been well documented,[37] and a large variety of compounds have been reported, while the urea is attractive since it contains two parallel hydrogen bond donors, in a similar fashion to the guanidinium group discussed earlier.

Throughout the history of anion binding chemistry, it has been noted that the urea moiety is an excellent hydrogen bonding group for carboxylate anions.[38-39] The structurally simple bis(4-nitrophenyl)urea **1.18** (Figure 1.13) was synthesised in order to test the stability of this interaction.[40] Following the complexation of acetate by UV/Visible absorption spectroscopy, it was possible to observe a distinct red shift of the absorption profile of the urea upon addition of acetate, to a maximum shift of ~50nm at a 1:1 stoichiometric ratio of urea:acetate. This shift was accompanied by a change in colour from pale to bright yellow. The more basic the anion, the greater the

change in colour – addition of fluoride to a solution of the receptor shows a two-step process: First, the colour deepens to yellow-orange as the first equivalent of fluoride is bound to the urea, forming a [ligand-H→F]$^-$ complex. Second, the colour deepens further to a dark red-orange as one of the N-H groups is deprotonated by a second equivalent of fluoride, leading to the formation of a [ligand→HF_2]$^{2-}$ complex.[41]

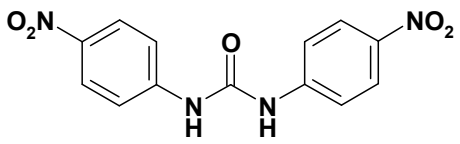

1.18

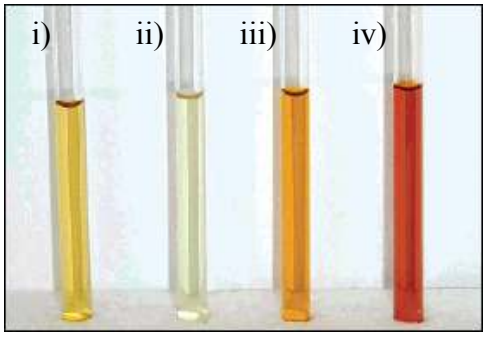

Figure 1.13 – Bis(4-nitrophenyl)urea **1.18**, and the colour changes observed upon addition of various anions in acetonitrile: i) **1.18** + 1 equiv. acetate; ii) Free **1.18**; iii) **1.18** + 1 equiv. fluoride; iv) **1.18** + 2 equiv. fluoride.[41]

Similarly, Gunnlaugsson *et al*. reported the synthesis of the urea-functionlised phenanthroline receptor **1.19** (Figure 1.14).[42] Rather than probe the anion binding through visible colour brought about by a change in absorption, this group observed the changes in the innate fluorescence emission of the phenanthroline functionality. It was found that **1.19** could strongly bind to a range of anions in solution, but showed a particular selectivity for chloride, since chloride led to the formation of a 2:1 host:guest complex in acetonitrile solution. Following the addition of anions to the receptor by fluorescence spectroscopy, it was noted that anions such as acetate, dihydrogen phosphate, and fluoride caused a quenching of the fluorescence band upon binding by photoinduced electron transfer between the trifluoro-*p*-tolyl group and the

fluorophore. The interesting result was found when chloride was the anion. In this case, quenching did not occur, but instead an enhancement in the fluorescence emission was observed, suggesting that the intramolecular quenching mechanism is disfavoured upon binding to chloride.

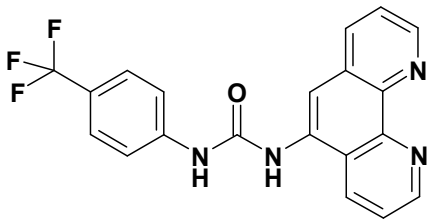

1.19

Figure 1.14 – Phenanthroline-based fluorescent sensor.

These systems highlight quite effectively the usefulness of the urea as an anion receptor group, and also contain inbuilt reporter functionality, allowing a visible response to binding of an anion. However, it seems obvious that a single urea (or amide) is not likely to be as effective an anion receptor as a host containing multiple binding groups. Gale and coworkers synthesised a series of amide and urea-based ditopic receptors (**1.20** and **1.21**, Figure 1.15) and studied their anion coordination potential.[43] Anion binding studies in deuterated dimethylsulphoxide containing trace H_2O showed that the bis-urea **1.21** confirmed the significantly higher selectivity for carboxylates over any other anion, while the amide **1.20** did not show the same effect.

1.20

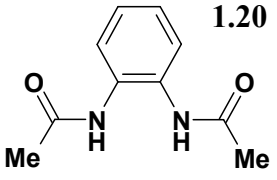

1.21

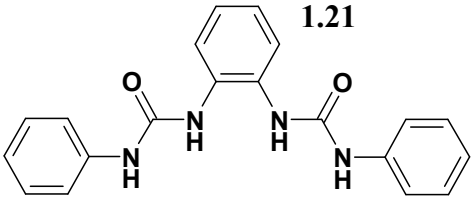

Figure 1.15 – Ditopic receptors **1.20** and **1.21**.

In a similar fashion, Reinhoudt and colleagues developed the ditopic bis-urea receptor **1.22** (Figure 1.16).[44] This receptor contains a greater degree of core flexibility than the receptors reported by Gale and coworkers, with additional *iso*-propyl groups to increase solubility in organic media. Binding studies performed in DMSO showed the highest affinity for dihydrogen phosphate, with no binding observed for weaker-binding anions such as chloride under these conditions.[44] In the same study, Reinhoudt's group expanded the receptor system to a number of tetrakis-urea receptor compounds, ranging from the acyclic, pincer-style receptors of general form **1.23** to the macrocyclic receptors generalised as **1.24** (Figure 1.16). Both of these expanded receptor series showed increased binding affinity for all anions in DMSO, indicating that complexation to an anion is enhanced by the addition of more binding groups within the cleft or binding pocket of a receptor.

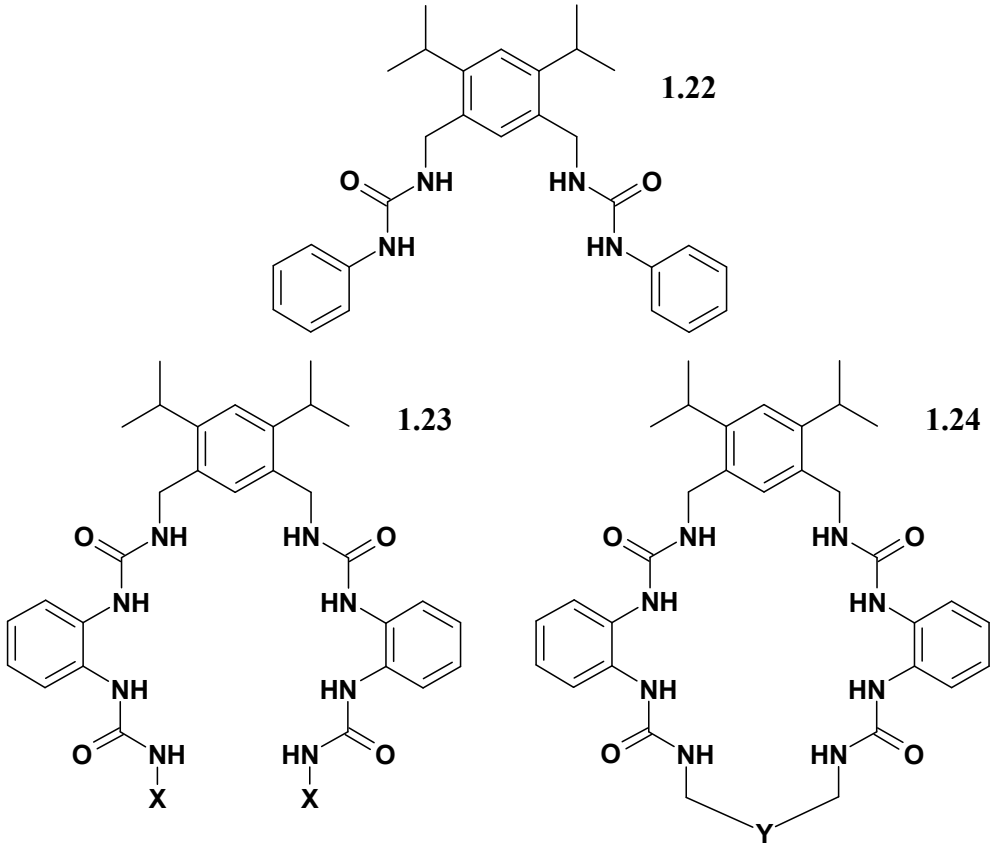

Figure 1.16 – Model receptor compound **1.22**, and tetrakis-urea acyclic receptors **1.23** and macrocycles **1.24**.[44]

Gale and coworkers expanded their earlier work on the bis-urea receptor **1.21** along a similar line by increasing the number of urea functionalities present. Receptors **1.25** and **1.26** (Figure 1.17) were reported and share structural features in common with the parent compound **1.21**.[45]

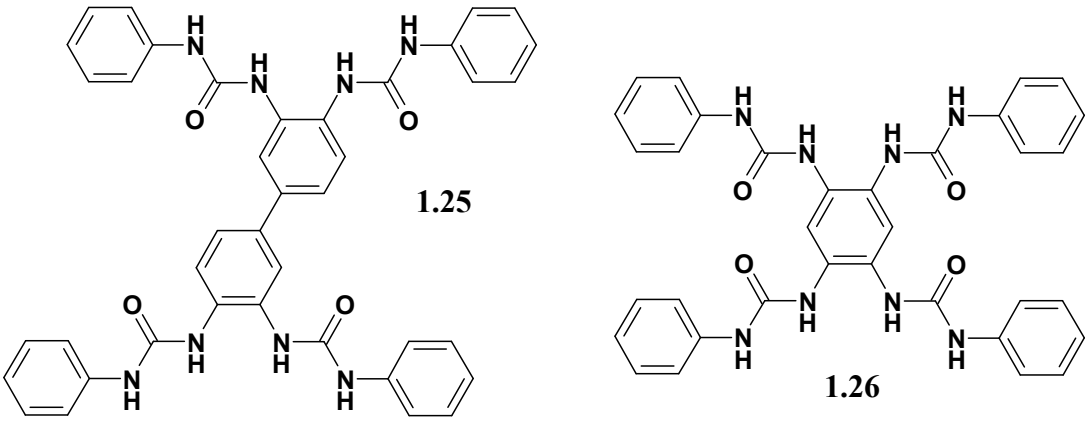

Figure 1.17 – Expanded tetrakis-urea receptors **1.25** and **1.26**.

Anion binding studies with these compounds revealed that complexation to dicarboxylate anions leads to the formation of hydrogen-bonded molecular tapes in the solid state.[46] This highlights another important property of amide-containing and particularly urea-containing compounds – their natural ability to self-associate. The polarity and often high degree of planarity of an amide or urea lend them the ability to effectively hydrogen-bond to a neighbouring amide or urea, leading to the formation of long hydrogen-bonded chains, or tapes. An excellent overview of the self-assembly properties of these functional groups was written by Chang *et al*, who explored in detail the extent of the interactions and assemblies that could be formed through such interaction by structural analysis.[47] It has been found that the formation of these one-dimensional intermolecular hydrogen bonds can lead to gelation of many amide and urea containing compounds,[48-51] and we have also reported that interference of such linear interactions through the use of sterically hindering groups in proximity to the urea can have interesting and unexpected consequences on the nature of the assembly produced.[52]

1.3 Anion Receptor Frameworks

Since we have detailed the types of anion receptor group, and already suggested that the inclusion of more binding groups leads to more effective anion receptors, it seems a logical progression to discuss some of the ways in which the functional groups can be incorporated into a receptor compound. Many of the examples already discussed rely on a pair of binding groups to enhance binding to a single anion in two dimensions, but it has also been shown that often three-dimensional receptors show even greater binding ability. As many of the common anions are spherical or tetrahedral, the ability of a receptor to surround such anions plays an important role in the binding process. There are two ways to construct a polytopic anion receptor – through the use of covalently-synthesised organic cores, or self-assembly around a metal centre.

1.3.1 Organic Frameworks

The formation of an anion receptor based around an organic core is perhaps the simplest to achieve synthetically. Often, functionalisation of an amine to a urea or amide is synthetically facile. Kim and coworkers sought to synthesise a series of anion receptor 'tweezers' based around the steroid chenodeoxycholic acid, making use of the high capability for functionalisation of the natural product.[53] Functionalisation of the alcohol groups with urea-containing alkyl chains gave a series of compounds of general form **1.27** (Figure 1.18).

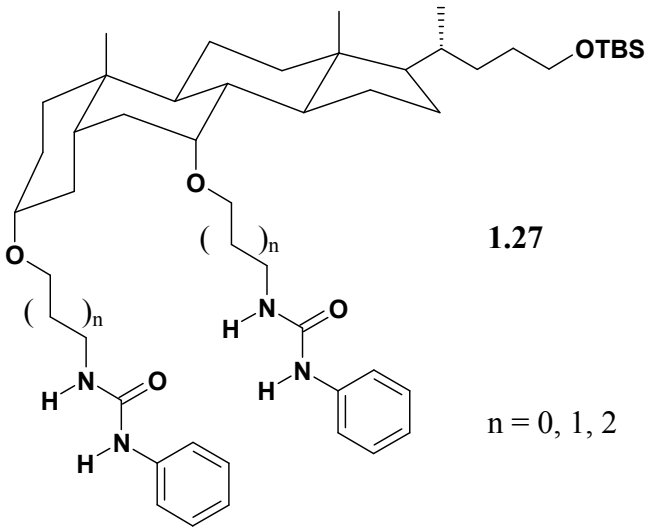

Figure 1.18 – Chenodeoxycholic acid-based receptors.

Anion binding studies showed consistent formation of a 1:1 host:guest complex with all of the common anions (halides, acetate, $H_2PO_4^-$), indicating that the arms of the receptor are close enough in space to successfully interact simultaneously with the same anion, yet are sufficiently flexible to bind in such a manner irrespective of the size of the anion. Binding to acetate was, for the most part, disfavoured over binding to chloride and $H_2PO_4^-$, suggesting that the acetate anion is a poor fit to the receptor site, being of a non-spherical shape and charge distribution. Binding to fluoride showed evidence of a 1:2 host:guest complex, again attributed to deprotonation of a urea.[53]

In a similar way, Davis and colleagues synthesised a number of tripodal receptor compounds based on the same steroid core (**1.28** and **1.29** – Figure 1.19).[54-55]

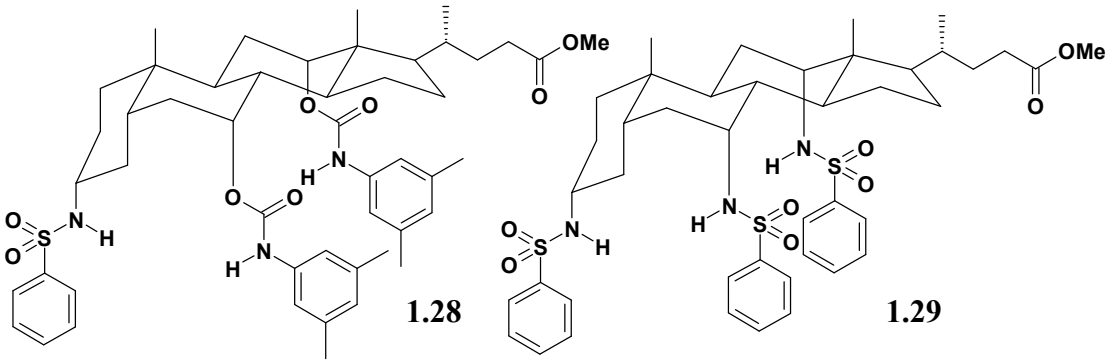

Figure 1.19 – Cholic acid-based receptors **1.28** and **1.29**.[54]

When carbamates were used as binding groups as in **1.28**, the group found that the receptor proved most effective at binding chloride and bromide, both giving similar binding constants, with larger anions such as iodide and tosylate being much more weakly bound. With **1.29**, containing three secondary amines with electron-withdrawing tosylate groups attached, the low binding for iodide and tosylate remains, but now the receptor shows a significant preference for chloride over bromide, with approximately a tenfold enhancement in binding to chloride over bromide. Indeed, the chloride-bound complex was found to be stable enough to be detectable by negative ion mass spectrometry, while the other complexes were not.

A particularly effective and more structurally simple core for a receptor is the tri-amine tris(2-aminoethyl)amine (abbreviated to 'tren'). This is a small yet flexible tripodal molecule that has already been featured as part of the earlier azacryptand receptors. Tren has more recently found extensive use as a frame for simple anion receptors. Early work by Reinhoudt and coworkers focussed on a series of tripodal tri-amides, based on the C_3 symmetric tren and the dipodal diethylenetriamine (DETA) (Figure 1.20).[56] Anion binding studies of the various hosts in $CDCl_3$ solution

gave consistent 1:1 host:guest complexation with chloride and hydrogen sulphate, but showed a 1:2 ratio with dihydrogen phosphate, an effect believed to be caused by a dimerisation of the $H_2PO_4^-$ ions through intermolecular hydrogen bonds.[57]

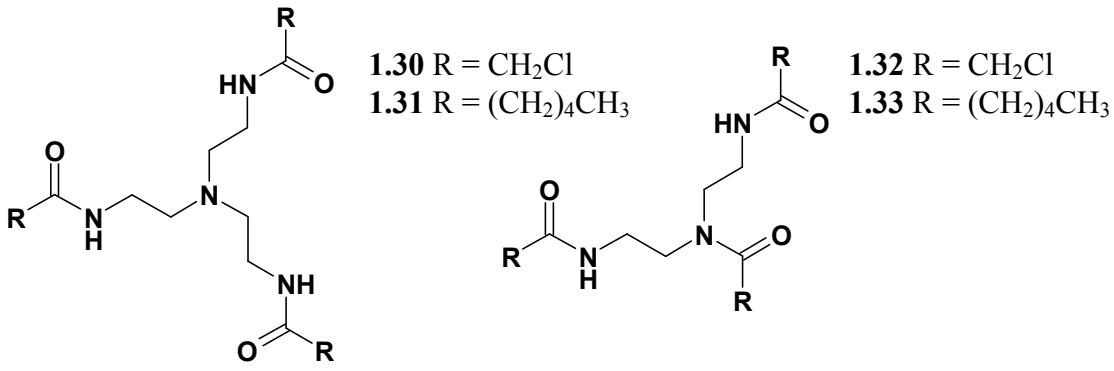

Figure 1.20 – Tren-based amide receptors **1.30** and **1.31**, and the corresponding DETA analogues **1.32** and **1.33**.[56]

In an attempt to design a better phosphate-selective receptor, Raposo and colleagues synthesised the tren-based urea **1.34** (Figure 1.21) as both the urea and thiourea analogue, as well as the cis-1,3,5-tris(aminomethyl)cyclohexane derived tripod **1.35**, which contains a lower degree of flexibility but does possess a similar-sized cavity to **1.34**.[58] The two urea tripods both showed a high affinity for phosphate binding, giving high association constants even in highly competitive DMSO solvent, although the more flexible **1.34**, in contrast to what was predicted, showed binding a factor of ten stronger than the less flexible **1.35**, suggesting that the flexibility of **1.34** allows it to more easily rearrange the binding groups to maximise binding interactions. The thiourea analogue of **1.34** showed a binding strength of similar strength to the cyclohexane-derived receptor, despite the higher acidity of the thiourea protons. Further functionalisation of **1.34** with *p*-carboxyphenyl groups reduced the binding affinity to phosphate, since the bound host-guest complex would then have six

negative charges. In contrast, functionalising the pendant arms with additional hydrogen-bond donor groups led to an increase in binding strength.

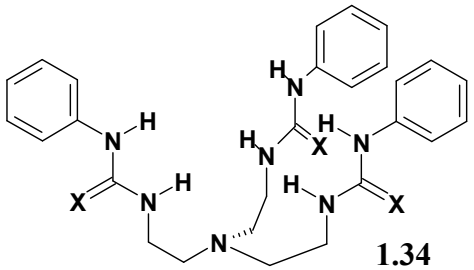

1.34
X = O, S

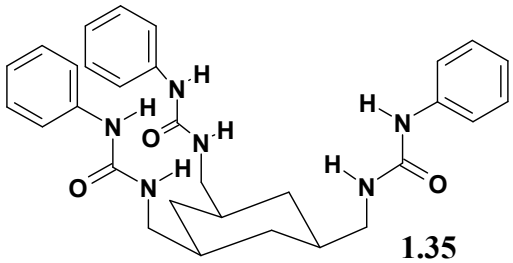

1.35

Figure 1.21 – Tren-based urea/thiourea **1.34** and cyclohexane-based **1.35**, showing the similarities between the receptor geometries and sizes.[58]

Some groups have taken the idea of tren-based anion receptors and combined them with known cation receptors to generate ion-pair detecting systems. Bowman-James and coworkers were interested in the ion extraction capabilities of these compounds, and synthesised a number of alkyl and aryl substituted amido-tren receptors to serve as the anion complexation agent, with a separate inclusion of a macrocyclic crown ether for the complexation of a cesium counter-ion.[59] Such an approach proved successful in accelerating the rate at which $CsNO_3$ salt is extracted from an aqueous phase to an organic phase, a process which is usually slow. Similar extraction was not found with simple monoamide control compounds, indicating that enclosure of the anion within the binding site of the receptor is necessary for solubility. Similar work by Beer *et al.* incorporated the metal-binding group into the anion receptor framework, leading to the synthesis of **1.36** (Figure 1.21).[60]

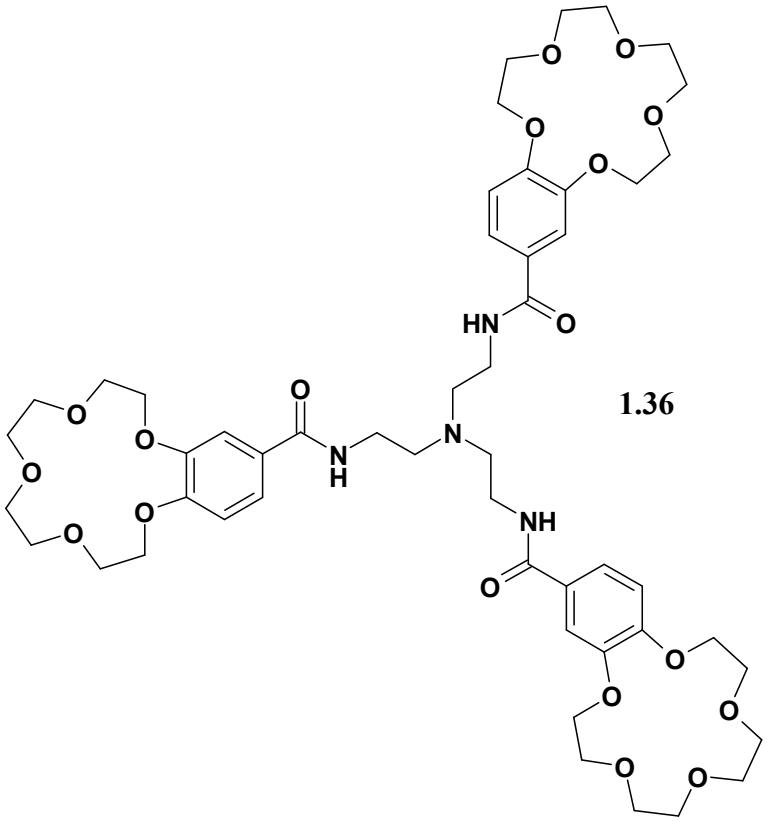

Figure 1.21 – Receptor **1.36**.[60]

This combination anion/cation receptor proved effective as an anion receptor, particularly when complexed with three sodium ions in the crown ether functionalities, with the binding strength of the anion being enhanced often tenfold when sodium cations are present. The receptor showed a particular affinity for the pertechnetate anion TcO_4^-, a radioactive byproduct of nuclear fuel processing, and proved successful as a transport agent in the extraction of the anion from a simulated nuclear waste solution.

More recently, it has been found that tren-based ureas also show a particularly high affinity for sulphate anions, as the shape and flexibility of the tren core allows a receptor to engage in multiple hydrogen bonds to the anion, and at moderate pH. Das

and colleagues synthesised **1.37** (Figure 1.22) and looked at its anion binding properties,[61] finding that sulphate bound to the receptor significantly more strongly than nitrate, acetate and even phosphate.

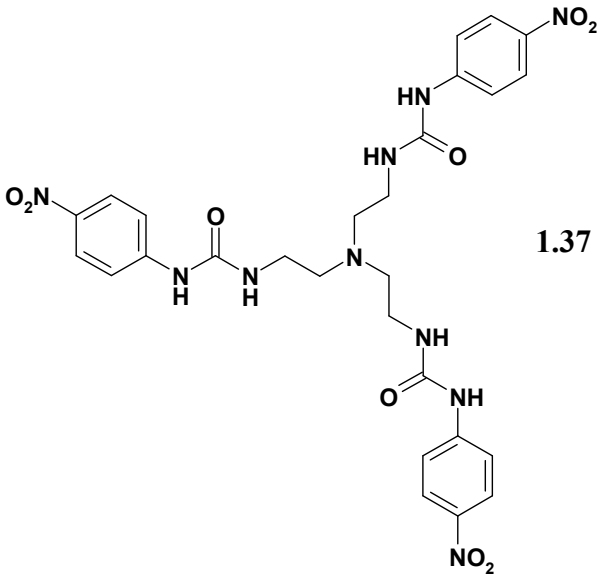

1.37

Figure 1.22 – Tripodal receptor **1.37**.[61]

The group were also able to crystallise the complex of **1.37** with sulphate, and found that in the solid state the system adopts a $[(\mathbf{1.37})_2(SO_4)_2]^{2-}$ complex, including a number of water molecules which hydrogen bond between the sulphates to create a 'rugby-ball' shaped adduct previously unknown.

Smith and colleagues synthesised a number of tren amides designed as HCl receptors.[62] The tren moiety is an effective starting point for an acid receptor, since the central nitrogen atom is still highly basic, and coordination of the proton to this atom can enhance binding ability by providing an extra hydrogen bond donor.[63] This group found that it was possible to tune the anion binding behaviour of the receptor by modification of the pendant arms of the binding site, with the bulky receptor **1.38** (Figure 1.23) providing the most interesting effect. Compound **1.38** reverses the

normal selectivity for phosphate over chloride typical of most receptor compounds, particularly tren-based receptors, and binds chloride strongest. This is identified as being due to the increased steric bulk of the side groups of the binding site, as phosphate is less able to enter the cavity to bind.[64]

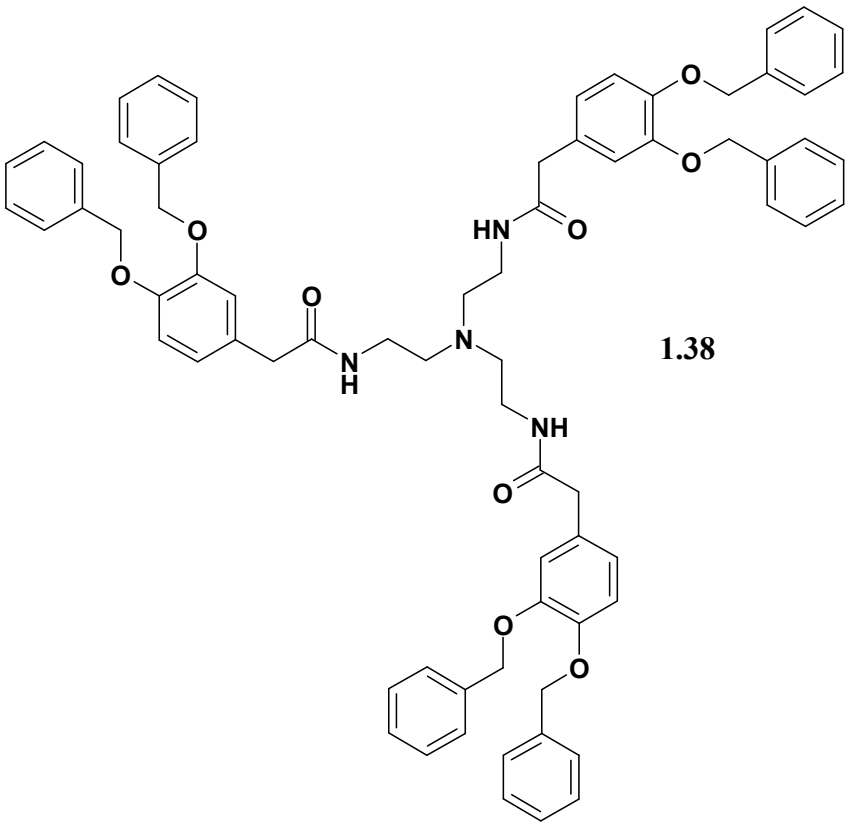

Figure 1.23 – Chloride-selective receptor **1.38**.[62]

Receptor **1.38** was then studied for its ability to bind to the ion pair of HCl, and it was found that in constrast to the expected 1:1 complex containing HCl bound within the receptor cavity, data suggested that the preferred stoichiometry was 1:2 host:guest, with one chloride bound inside the cavity with one acid proton coordinated to it, while the second chloride is bound outside of the cavity via a hydrogen bond to the core ammonium N-H groups. Studies into the transport properties of **1.38** showed promise, as the receptor was able to ferry HCl from an aqueous acid solution to a pH

neutral aqueous phase across a dichloromethane boundary. Compound **1.38** is able to solubilise the H^+ and Cl^- ions, forming a screen between the highly charged ions and the apolar medium, but it is also able to release them once again when transport is complete – an important factor to consider when designing an ion transport receptor.[65] Tren is not the only core structure of interest, and other methods of assembling receptor compounds exist. One method receiving increasing interest is to mount the binding groups onto a large macrocycle such as a calixarene. Such systems have well-defined core structures and the possibility of additional interactions with the aromatic walls of the interior of the core itself. As an example, Reinhoudt *et al.* synthesised a number of tri-functionalised calix[6]arene receptor compounds with urea or thiourea groups as the binding species.[66] While the same group had previously reported a series of anion receptors based on the calix[4]arene core,[67-68] calix[6]arenes had previously received little attention as anion receptors due to their greater difficulty in synthesis and poor controllability of conformation. The receptors they synthesised (**1.39** & **1.40**, Figure 1.24) had their conformations stabilised by C-H – arene π interactions.

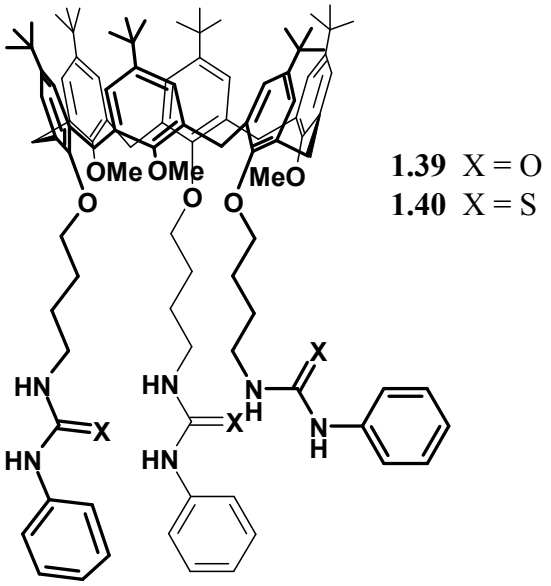

1.39 X = O
1.40 X = S

Figure 1.24 – Calix[6]arene receptors **1.39** and **1.40**.[66]

Both **1.39** and **1.40** showed weak binding to anions such as iodide, cyanide and thiocyanate, both showed much stronger anion to chloride and bromide. The urea receptor **1.39** showed stronger binding to both than the thiourea **1.40**, but somewhat unexpectedly, both **1.39** and **1.40** show higher binding to bromide than chloride, suggesting that the size of cavity formed by the three binding groups is of a better fit for bromide than the smaller chloride. In particular though, both **1.39** and **1.40** showed a significantly stronger binding response to a range of tricarboxylate anions, though this is partly due to the higher charge density. It was hoped that the C_3 symmetry of the receptor would match best to anions of similar symmetry, and indeed this was found to be the case, as from a range of mono, di, and tricarboxylates, the strongest binding with both receptors were the C_3 symmetric 1,3,5-benzenetricarboxylate (trimesylate) and *cis*,*cis*-1,3,5-cyclohexanetricarboxylate trianions. While **1.39** showed only a small difference in binding strength between these two anions, with the cyclohexanetricarboxylate binding marginally stronger, the

thiourea analogue **1.40** showed a significant difference between the two, with trimesylate being bound much more strongly due to the excellent size/shape complementarity backed up by the higher acidity of the thiourea groups.

Another increasingly common organic receptor series is that based around a tribromomethyl-substituted benzene ring.[69] Starting from this compound, it is possible to react with a series of pyridine compounds to generate a tris-pyridinium tripod of the general form shown in Figure 1.25, wherein the bromine atoms are replaced with the pyridine groups, and are instead treated as counter-ions. Metathesis allows these counter ions to be replaced with less coordinating anions such as hexafluorophosphate, in order to allow for an unobstructed analysis of the anion binding properties of the receptor.[70]

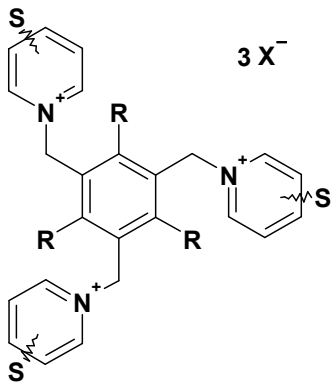

R = H, alkyl

S = Any functionality – e.g. amines, ureas etc.

X = anion – initially Br, metathesis to PF_6, BF_4, etc.

Figure 1.25 – General form of the tris-pyridinium receptors.[71]

While the positively charge nature of the basic receptor compound (R, S = H, X = PF_6) allows it to bind to anions,[70] further functionalisation of the receptor leads to far greater flexibility in binding and detection of anions. Work by Anslyn and colleagues reported the synthesis and characterisation of the related guanidinium-containing receptor **1.41** (Figure 1.26) based on the related triethylbenzene core.[72] Addition of ethyl groups to the core ring (R = ethyl) aids both in solubility of the host, as well as

encouraging an all-*cis* configuration of the three binding arms by steric interactions, as hexa-substituted benzene rings typically adopt an alternating up-down configuration.[73] This receptor was found to be highly selective for citrate, even in such highly competitive media such as water. The receptor was found to be extremely effective at binding citrate selectively in orange juice because of this selectivity.

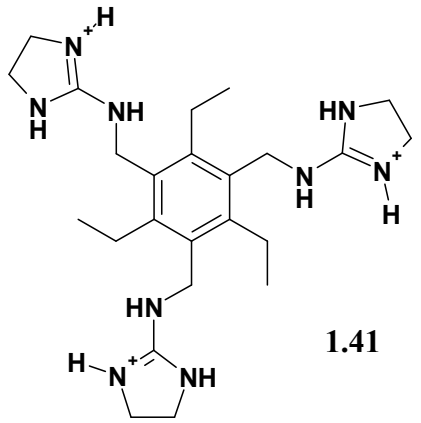

1.41

Figure 1.26 – Citrate-selective receptor **1.41**.[72]

Work by Steed and colleagues designed and synthesised a range of 'pinwheel' compounds based on the same triethylbenzene structure, with a few modifications from the basic receptor.[71] Functionalisation of the pyridinium groups with secondary amines substituted with reporter groups such as anthracene – providing a fluorescent response to binding – or ferrocene – providing an electrochemical response – allows for a detectable change upon binding of the receptor to an anion. Interestingly, anion binding data of the amine-substituted receptors suggested that in addition to the amine binding to the anion, an additional hydrogen bond is present between the anion and the C-H nearest to the pyridinium centre. This effect is also observed in the simple unsubstituted pyridinium-based receptor, with this C-H—anion hydrogen bond being the only non-electrostatic complexation interaction, although binding to this receptor

is understandably much weaker than for the amine-appended receptors. Evidence of this was found crystallographically (Figure 1.27) and showed complexation of bromide to the receptor within the central cavity, coordinated to three pyridinium groups.[70]

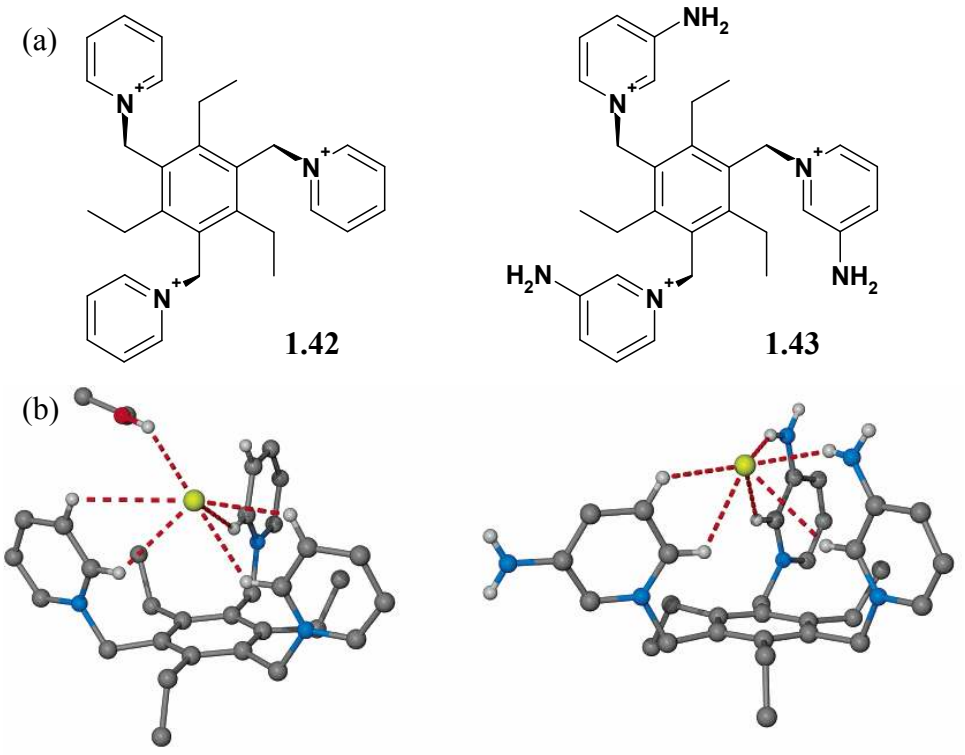

Figure 1.27 – (a) Tris(pyridinium) 'pinwheel' receptors **1.42** and **1.43** (counter ions are PF_6), with (b) X-ray molecular structures showing the complexes with bromide. Non hydrogen-bonding hydrogen atoms and extra PF_6 counter ions removed for clarity.[70]

Despite the appearance of some of the ethyl groups also aligned upward alongside the binding groups in the solid-state structure, solution studies indicated that all three exist in a 'down' configuration on the ^{1}H NMR timescale. Affinities for anions show fairly expected trends, with chloride being bound more strongly than bromide or iodide. Best results were found when the pyridinium groups were functionalised in

the *meta* (3) position, since this position gives rise to parallel N-H and *ortho* C-H bonds, and thus allows for the greatest interaction between host and guest. For receptors with larger functionalities the binding strength is reduced due to steric hindrance of the binding site. Interestingly, this effect was found to increase the binding affinity for acetate, particularly for the anthracenyl analougue **1.44** (Figure 1.28) which showed a dramatic increase in the binding to acetate by adopting a differing '2 up, 1 down' arrangement and thus was able to bind to two independent acetate anions.

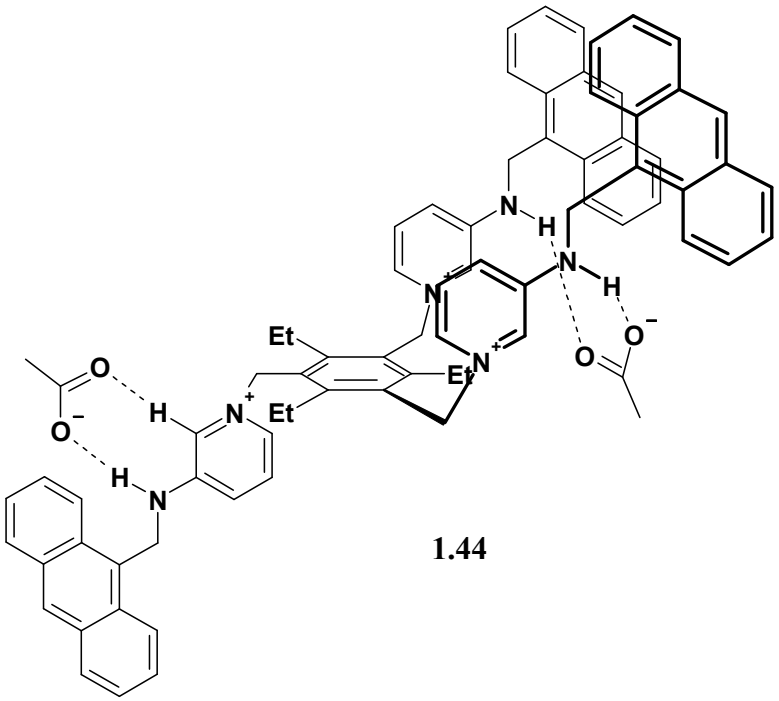

1.44

Figure 1.28 – Receptor compound **1.44** showing the 1:2 host:guest complexation mode with acetate. Additional counter ions not shown for clarity.

With its anthracenyl groups, **1.44** is a fluorescent compound, and it was hoped that binding to an anion could lead to a change in the fluorescent properties of the receptor, since the three groups are pulled into close proximity by binding to halides. While no significant effect besides quenching of the fluorescence of **1.44** was

observed upon binding to anions, it was found that upon exposure to UV radiation, the anthracyl groups in **1.44** undergo both intra- and inter-molecular cycloaddition reactions with other anthracenyl groups,[70] leading to an enhancement in fluorescence formed by the photodimerisation. This effect was also observed by others on related anthracene-containing receptors.[74]

Replacing the fluorescent anthracyl reporter group with the redox responsive ferrocenyl reporter group gave a receptor with excellent affinity for halides, again due to the high size/shape complementarity between the spherical anions and the binding cavity of the receptor, with a 1:1 binding mode again being observed.[75] A similar behaviour to **1.44** is observed when acetate is the anion, though the effect is less pronounced. Following the binding of anions by cyclic voltammetry, thus probing the change in the redox potential of the ferrocenyl groups, showed the greatest shift in the redox potential with chloride, while iodide caused only a negligible shift in the potential, confirming the ^{1}H NMR spectroscopy trends for binding strength.

More recently, receptors based on the triethylbenzene core have been designed with urea-based binding groups in place of the secondary amines. Reaction of the tribromomethyl triethylbenzene reactant with simple pyridyl ureas led to the synthesis of the receptor compounds **1.45** and **1.46** (Figure 1.29).[76]

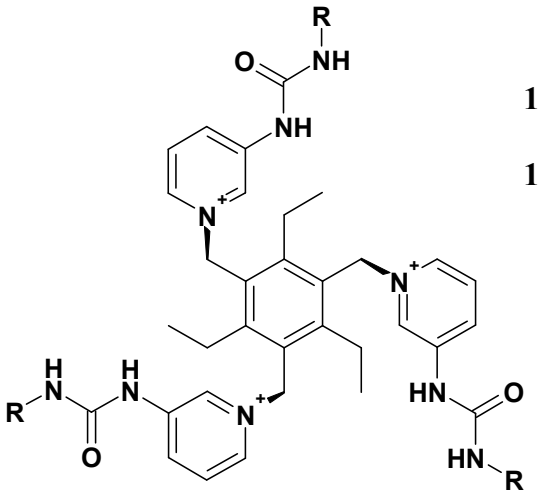

1.45 R = *p*-tolyl

1.46 R = *n*-octyl

Figure 1.29 – 'Pinwheel' receptors **1.45** and **1.46**.[76]

Anion binding studies on these two receptors revealed a similar binding mode to the earlier amide-based receptors, with hydrogen bonding between the pyridinium C-H and one of the urea N-H groups binding to the anion. This behaviour is atypical of ureas in general, and implies that the three positive charges of the pyridinium moieties is more directive of the binding site than the hydrogen bond donors. Also of interest was the difference in behaviour of the receptor arms with the change in pendant groups between **1.45** and **1.46**. While **1.45** was found to favour the 'three up' conformation of binding to chloride seen with other receptors, **1.46** adopted a 'two up, one down' geometry with the same anion, though both still show a 1:1 host:anion complexation ratio. The capsule nature of the **1.45**-chloride complex is generated by C-H—π interactions between *p*-tolyl groups, not present in **1.46** which has no aromatic end groups.[76] Because of this effect, binding of the receptors to different anions gave radically different behaviour – since bromide is larger than chloride, it cannot fit within the cavity generated by **1.45**, and so leads to formation of a 1:3

complex with the receptor instead. One bromide is held in the centre of the receptor by C-H—anion interactions and electrostatic attraction, as well as hydrogen bonding to one of the arms, while the other two urea groups each bind individually to other bromide anions, leading to the charge-neutral **1.45**.3Br complex.

Others have also designed anion receptors around the 'pinwheel' triethylbenzene core, following Anslyn in building functionalisation much closer to the core itself. Work by Schmuck and Heller used the triethylbenzene core to synthesise the biomimetic receptor **1.47** (Figure 1.30).[77] **1.47** contains multiple functionalities and is designed to bind to larger carbohydrate anions.

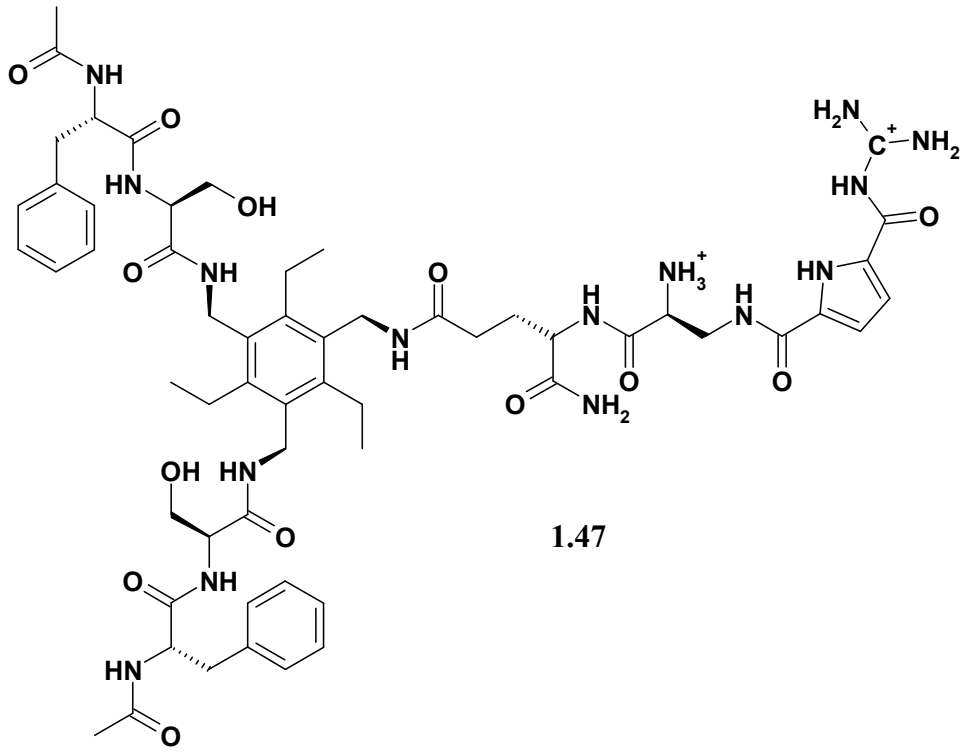

1.47

Figure 1.30 – Biomimetic receptor **1.47**.[77]

This receptor was found to be an excellent choice when binding larger biological anions, showing high affinity for AMP and a variety of glucophosphates in buffered, aqueous (20% water in DMSO) medium. As a comparison, the group also proved that

the receptor **1.47** was highly selective for such anions, as acetate gave no detectable binding under the same conditions.

1.3.2 Metal-templated Receptors

The alternative to designing a receptor around an organic framework is to assemble the binding groups around a metal core, typically a transition block metal, although lanthanides can also be used.[78] Metals are desirable as core structures because they can bring a number of interesting properties to the receptor. For one, metal complexes often have well-defined geometries, with octahedral, square planar, and linear being among the most common. Second, many metal fragments are redox-active, which as has already been mentioned[29] can be used as a method of detection of a bound anion.

A fine example of the use of metal complexes to preorganise a receptor was the work by Atwood and colleagues,[79] which reported the synthesis of a capsule formed between the simple bis-pyridyl ligand **1.48** and copper nitrate (Figure 1.31). While the complexation of organic ligands to metal ions is not new, the capsule shows how well-defined assemblies can be formed through the process of self-assembly. Nitrate anions are trapped within the capsule, held in place by the presence of a cluster of water molecules.

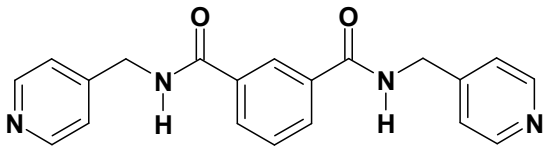

1.48

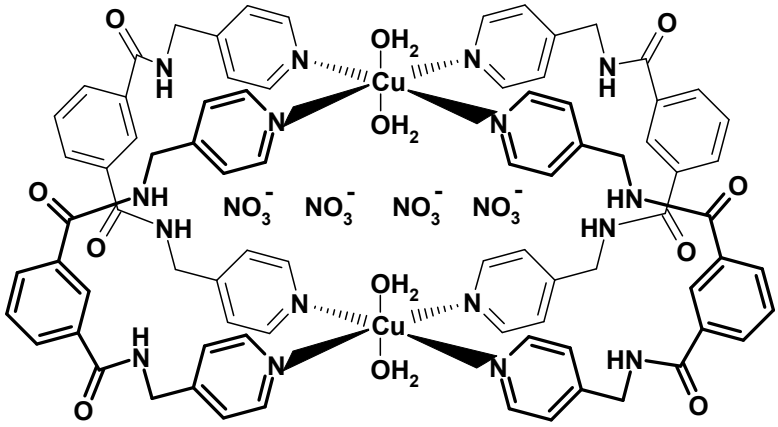

Figure 1.31 – Ligand **1.48**, and the capsule complex formed with $Cu(NO_3)_2$.[79]

This capsule makes use of the natural tendency of copper(II) salts to form Jahn-Teller distorted octahedral complexes, and is a prime example of the use of the well-defined structural geometry of many metal complexes. Along a similar line of thought, Mingos *et al.* synthesised a mixed-metal receptor cage based around the simple nickel-amidinothiourea complex **1.49**.[80] The nickel(II) complex adopts a square planar geometry, and by exploiting the higher affinity between palladium and sulphur, the capsule complex is formed (Figure 1.32). The resulting complex proved to be effective at encapsulating chloride, with the anion lying at the centre of an octahedral arrangement of the metal ions, and bound not only by the electrostatic interactions of these metals, but also by eight hydrogen bonds from the adjacent N-H groups of the amidinothiourea ligands.

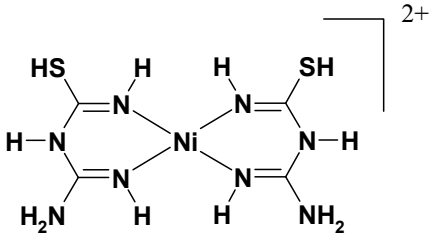

1.49

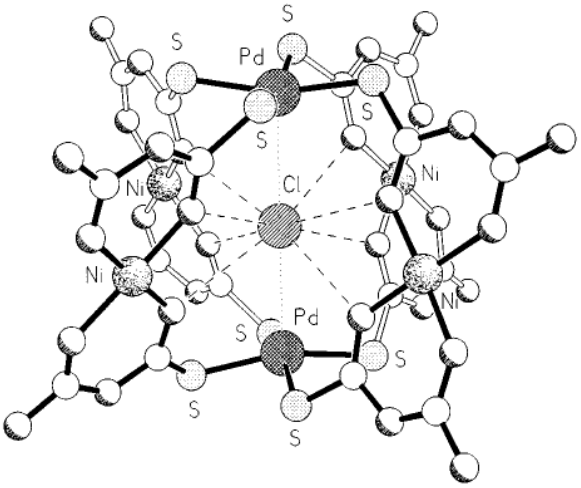

Figure 1.32 – Nickel (II) amidinothiourea complex **1.49** and a molecular structure of the mixed-metal capsule[80] – reproduced by permission of the Royal Society of Chemistry.

Loeb and colleagues reported the synthesis of a receptor similar in design to the triethylbenzene receptors, using meta-substituted pyridyl ligands as receptor groups, but this time complexed to a platinum core rather than a substituted aryl ring.[81] The receptor **1.50** (Figure 1.33) can exist in a number of rotational conformations, in a similar way to structurally related calix[4]arene receptors, due to easy rotation around the Pt-N bonds. In the solid-state structure of the parent complex **1.50**$[PF_6]_2$, the receptor adopts a 1,2-alternate conformation which places two pairs of amide groups on opposite sides of the Pt-N_4 plane. Interestingly, the PF_6 counter anions were not found to interact with the amide N-H groups in the solid structure, instead the N-H groups point to the outside of the complex and the amide C=O binds to coordinated dichloromethane solvent.

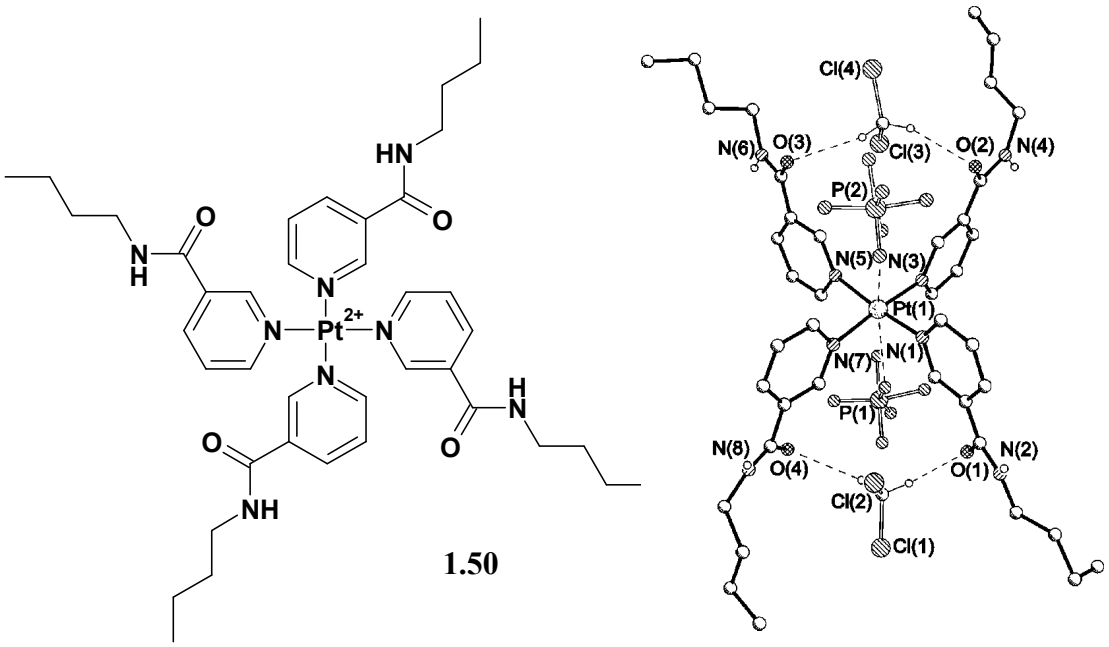

Figure 1.33 – Platinum (II)-templated receptor **1.50** and the X-ray molecular structure of **1.50**$[PF_6]_2.2CH_2Cl_2$.[81] – reproduced by permission of the Royal Society of Chemistry.

This 1,2-alternate arrangement seen in the crystal structure proved an ideal arrangement for binding to planar, bidentate anions, with acetate and nitrate both showing formation of a 1:2 host:guest species during anion binding studies, with binding to the second anion actually being made more favourable by binding to the first, indicating a positive allosteric effect. Other, tetrahedral oxoanions such as perrhenate bind to the receptor in a 1:1 stoichiometry, due to the larger size and lower directionality of charge leading to a distortion of the receptor geometry, causing binding to the second anion to be disfavoured.[81]

Similar work by Steed and colleagues considered a number of pyridyl ureas and their interactions with different metal salts, particularly silver(I).[82] Silver(I) salts typically adopt a linear geometry in complexes, and it was determined that pyridyl ureas such as **1.51** (Figure 1.34) were good ligands for the metal.

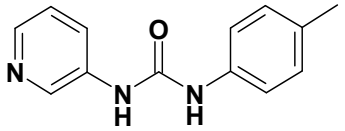

1.51

Figure 1.34 – Pyridyl urea **1.51**.[82]

The nature of the anion was found to be important in determining the overall structure of the receptor-anion complex. The general form of the complex was determined as $[ML_2]X$ for singly-charged anions, and $[ML_2]_2X$ for dianions. Differences in the structure, determined by X-ray crystallography, arose based on the nature of X – when the anion is trifluoromethanesulphonate ($CF_3SO_3^-$), **1.51** forms two-dimensional coordination polymers, with the anions bridging between pairs of $[ML_2]^+$ units. Similarly, coordination of the receptor to sulphate leads to formation of a two-dimensional array formed by similar interactions, with the anion surrounded by four of the $[ML_2]^+$ units and bonded by hydrogen bonding to the urea protons. The interesting result was found when the anion chosen was nitrate, as the complex $[Ag(\mathbf{1.51})_2]NO_3$ was found to form a discrete assembly with the nitrate coordinated to two urea groups coordinated to the same metal in a pincer-like arrangement (Figure 1.35). Most interestingly, the silver no longer adopts the typically linear geometry, as twisting of the complex generated by the binding to the nitrate forces the silver to adopt a more trigonal arrangement, with a third coordination site being filled by solvent (in this case methanol).

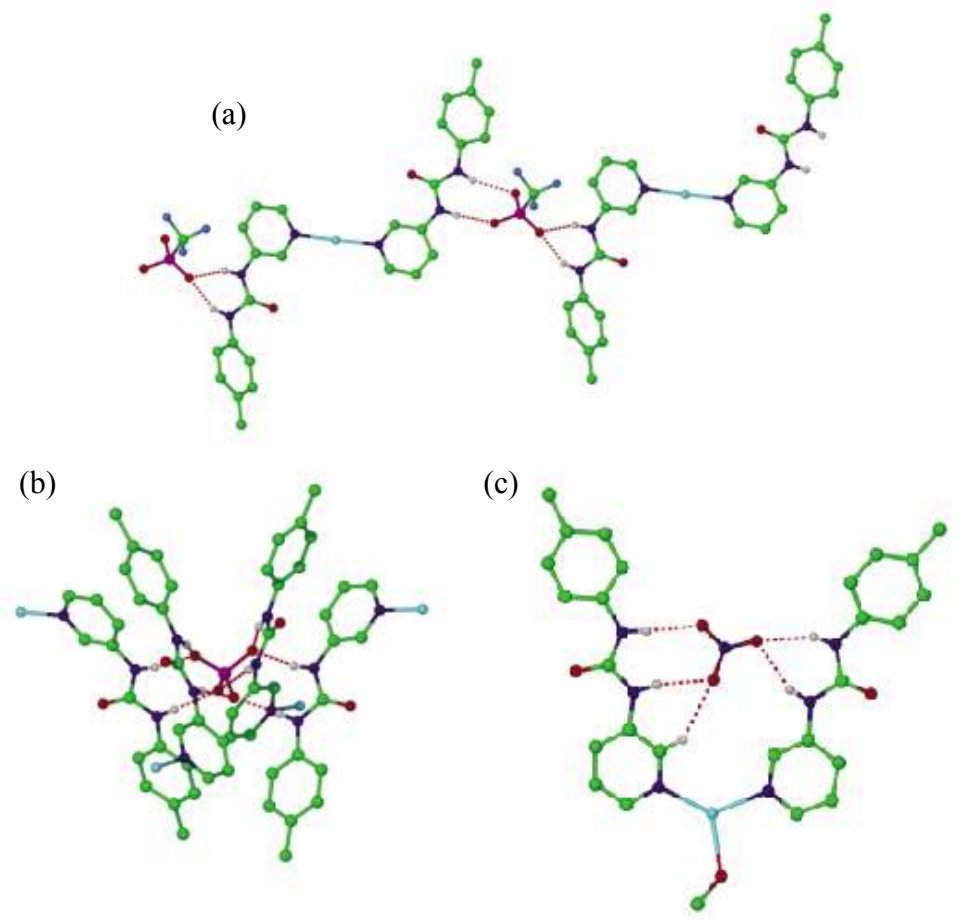

Figure 1.35 – X-ray structures of (a) [Ag(**1.51**)$_2$]CF_3SO_3, (b) [Ag(**1.51**)$_2$]$_2SO_4$, and (c) [Ag(**1.51**)$_2$]NO_3.MeOH. Only hydrogen bonding hydrogen atoms shown for clarity.[82] Reproduced by permission of the Royal Society of Chemistry.

Anion binding studies of **1.51** and the [Ag(**1.51**)$_2$]$^+$ complex showed that the free ligand binds anions in the manner expected for a simple urea molecule, with strong selectivity for acetate and weak binding to nitrate. When complexed to the silver, binding to acetate is still high, and shows evidence of a 1:3 host:guest binding mode consistent with breaking up of the Ag(**1.51**)$_2^+$ complex to two equivalents of the (**1.51**)OAc complex with formation of silver acetate. The Ag(**1.51**)$_2^+$ complex does show a remarkable increase in binding to nitrate over the free **1.51**, with a fairly significant 1:2 host:anion complex also being detected. This was determined as being

caused by coordination of the second nitrate anion to the silver in the third coordination site, replacing the coordinated solvent.[83]

Reaction of **1.51** with metal salts that typically adopt different geometries was found to generate a greater range of complexes. For example, treatment of **1.51** with cobalt(II) sulphate gives a cup-shaped complex (Figure 1.36), in which the cobalt adopts an octahedral geometry with four ligands in equatorial coordination sites, with the remaining two sites coordinating water. The basic structure is the same for all M(II) salts, although again the Cu(II) complex shows Jahn-Teller distortion.[84]

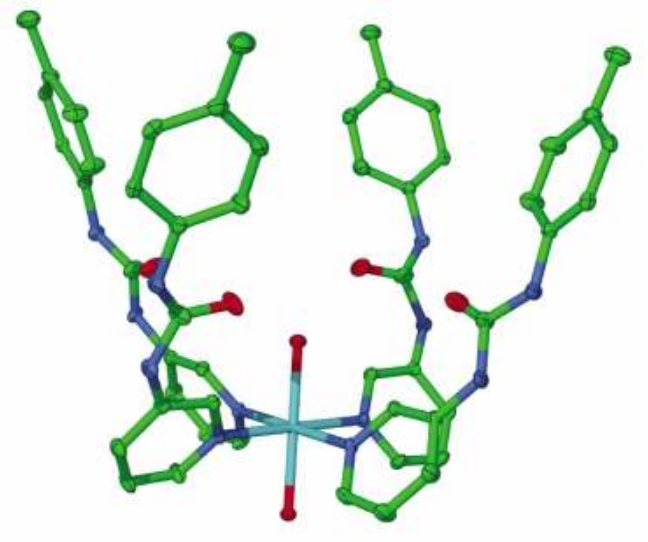

Figure 1.36 – Structure of the $[Co(\mathbf{1.51})_4(H_2O)_2]^{2+}$ unit. Hydrogen atoms removed for clarity.[84] – reproduced by permission of the Royal Society of Chemistry.

Of note is that the anion is not found within the cavity generated by the complex, at least in the solid-state structure – as can be seen in the figure, the urea protons point out of the bowl and bind to the anions between ML_4 units. Inside the cavity, a small water cluster is present and held in place by hydrogen bonding to the urea carbonyl groups, as well as the metal-coordinated water molecules.

In a similar study, Loeb and coworkers revisited earlier platinum-based receptor complexes[81] and synthesised a new tetrapodal complex using the urea-substituted isoquinoline **1.52** as the coordinated binding group (Figure 1.37).[85]

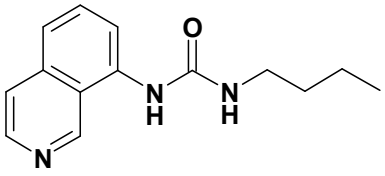

1.52

Figure 1.37 – Isoquinoline ligand **1.52**.[85]

Compound **1.52** was designed in the hopes of being a selective sulphate receptor – the isoquinoline groups create a larger cavity than pyridine-derived ligands and should therefore allow anions inside of the cavity. Spherical anions, such as halides, were found to bind in a 1:2 host:guest complexation mode with the binding arms in an alternate arrangement, with no evidence of any allosteric effect on binding the second anion, suggesting that at lower concentrations of anion a 1:1 host:guest complex in the cone conformation is present and rearrangement occurs to the alternate conformation at higher anion concentrations in order to accommodate the second anion and balance the 2+ charge of the platinum. As intended, tetrahedral anions, particularly the di-anion SO_4^{2-}, bound to the receptor very strongly and in a simple 1:1 host:guest cone complex.[85]

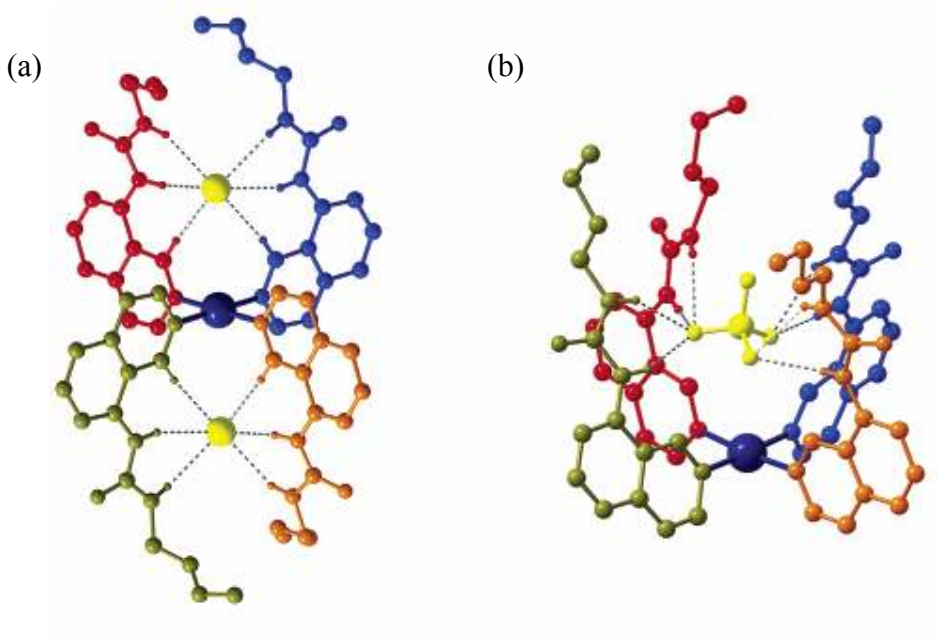

Figure 1.38 – Ball-and-stick representation of (a) [Pt(**1.52**)$_4$]Cl$_2$ and (b) [Pt(**1.52**)$_4$]SO$_4$ complexes, showing the four ligands in red, green, blue and orange, with the anions in yellow. Non hydrogen-bonding hydrogen atoms removed for clarity.[85]

The same group later synthesised a dipodal receptor based on **1.52**. Two ligands were coordinated to the platinum in a *trans* fashion, with the remaining coordination sites filled with simple pyridine ligands.[86] This receptor showed equally high binding to sulphate and phosphate, with the expected 1:1 ratio forming initially, however without the additional binding arms to fully encapsulate sulphate, formation of a 1:2 complex is also observed, in a similar manner to the halides. Binding constants were consistently lower, since with only half the number of bonding interactions possible, the anions are less well bound to the receptor.

1.4 Aims

We have detailed some of the many ways in which anion receptors may be constructed, particularly in the ways that the anion may be attracted to and held by the receptor, through the use of electrostatic interactions and neutral hydrogen bonding species. It is perfectly possible to design a receptor that contains one or the other separately, or even both together, and the best method is not always obvious. Electrostatic interactions rely on the natural tendency of opposite charges to attract, but they lack direction, and receptors utilising such interactions generally require more careful engineering to be truly effective. On the other hand, use of amides and ureas to hydrogen bond to anions can be a very powerful technique, as they contain high degrees of directionality and are often easy to prepare, but often other issues, such as poor solubility, can limit the options of neutral receptors. Combining the two is a fair choice, but often leads to more complex synthesis and is more difficult to predict.

Likewise, in the manner of selecting a framework to base an anion receptor on, there are several lines of thought, and each has their merits and weaknesses. Organic molecules are extremely wide ranging and give an almost endless list of possibilities, as well as often being more stable by offering no alternative reaction with an anion other than to bind, but can be unpredictable in the form and nature of their structure. Metal complexes are usually better defined structurally, but lability can lead to breakdown of a receptor when anions are added.

This work will look at a range of organic and metallic frames as anion receptors with a series of different binding groups. Of particular interest are receptors of a tripodal geometry, as these fit well with the natural shape of many common anions. A number of different tripodal cores will be considered, including studies on highly flexible organic hosts based on the increasingly common tren moiety; less-flexible organic hosts based on *para*-rosaniline, an aromatic tri-amine commonly used as a dye due to its deep red-purple colour; and a number of metallic cored tripods combining known pyridine-metal coordination methods with a specially selected, facially-capped octahedral ruthenium (II) moiety. Anion binding constants will typically be determined via ^{1}H-NMR spectroscopic titrations, though other techniques, such as UV/Visible spectroscopy and fluorometry may be used where appropriate.

1.5 References

1. P. B. Davis, M. Drumm and M. W. Konstan, *Am. J. Respir. Crit. Care Med.*, 1996, **154**, 1229-1256.
2. X. D. Lou, L. Qiang, J. G. Qin and Z. Li, *ACS Appl. Mater. Interfaces*, 2009, **1**, 2529-2535.
3. R. Huston, Y. C. Chan, T. Gardner, G. Shaw and H. Chapman, *Water Res.*, 2009, **43**, 1630-1640.
4. P. Sylvester, T. Moller and O. Boyd, in *Waste Management and the Environment Iv*, eds. M. Zamorano, C. A. Brebbia, A. Kungolos, V. Popov and H. Itoh, Wit Press, Southampton, 2008, vol. 109, pp. 719-727.
5. J. D. Roach and D. Tush, *Water Res.*, 2008, **42**, 1204-1210.
6. C. H. Park and H. E. Simmons, *J. Am. Chem. Soc.*, 1968, **90**, 2431-2432.
7. E. Garcia-España, P. Diaz, J. M. Llinares and A. Bianchi, *Coord. Chem. Rev.*, 2006, **250**, 2952-2986.
8. B. Dietrich, M. W. Hosseini, J.-M. Lehn and R. B. Sessions, *J. Am. Chem. Soc.*, 1981, **103**, 1282.
9. B. Dietrich, M. W. Hosseini, J. M. Lehn and R. B. Sessions, *Helv. Chim. Acta*, 1983, **66**, 1262-1278.
10. B. Dietrich, J. Guilhem, J.-M. Lehn, C. Pascard and E. Sonveaux, *Helv. Chim. Acta*, 1984, **67**, 91-104.
11. M. W. Hosseini and J.-M. Lehn, *Helv. Chim. Acta*, 1988, **71**, 749.
12. F. P. Schmidtchen, *Angew. Chem. Intl. Ed. Eng.*, 1977, **16**, 720-721.
13. F. P. Schmidtchen, *Chem. Ber.*, 1980, **113**, 864-874.
14. K. Ichikawa, M. A. Hossain, T. Tamura and N. Kamo, *Supramol. Chem.*, 1995, **5**, 219-224.
15. J. L. Sessler, D. Q. An, W. S. Cho and V. Lynch, *Angew. Chem. Intl. Ed.*, 2003, **42**, 2278-2281.
16. J. L. Sessler, P. Anzenbacher, K. Jursikova, H. Miyaji, J. W. Genge, N. A. Tvermoes, W. E. Allen, J. A. Shriver, P. A. Gale and V. Kral, *Pure Appl. Chem.*, 1998, **70**, 2401-2408.
17. J. L. Sessler, D. E. Gross, W.-S. Cho, V. M. Lynch, F. P. Schmidtchen, G. W. Bates, M. E. Light and P. A. Gale, *J. Am. Chem. Soc.*, 2006, **128**, 12281-12288.

18. J. L. Sessler, S. K. Kim, D. E. Gross, C.-H. Lee, J. S. Kim and V. M. Lynch, *J. Am. Chem. Soc.*, 2008, **130**, 13162-13166.
19. M. Shionoya, H. Furuta, V. Lynch, A. Harriman and J. L. Sessler, *J. Am. Chem. Soc.*, 1992, **114**, 5714-5722.
20. V. A. Russell and M. D. Ward, *New J. Chem.*, 1998, **22**, 149-153.
21. B. Dietrich, T. M. Fyles, J.-M. Lehn, L. G. Pease and D. L. Fyles, *J. Chem. Soc., Chem. Commun.*, 1978, 934.
22. B. Dietrich, D. L. Fyles, T. M. Fyles and J. M. Lehn, *Helv. Chim. Acta*, 1979, **62**, 2763-2787.
23. R. P. Dixon, S. J. Geib and A. D. Hamilton, *J. Am. Chem. Soc.*, 1992, **114**, 365-366.
24. M. W. Gobel, J. W. Bats and G. Durner, *Angew. Chem. Intl. Ed. Eng.*, 1992, **31**, 207-209.
25. V. Jubian, R. P. Dixon and A. D. Hamilton, *J. Am. Chem. Soc.*, 1992, **114**, 1120-1121.
26. R. Gross, J. W. Bats and M. W. Gobel, *Lieb. Annal. Der Chemie*, 1994, 205-210.
27. K. Ariga and E. V. Anslyn, *J. Org. Chem.*, 1992, **57**, 417-420.
28. R. J. Motekaitis, A. E. Martell, I. Murase, J. M. Lehn and M. W. Hosseini, *Inorg. Chem.*, 1988, **27**, 3630-3636.
29. P. D. Beer, C. Hazlewood, D. Hesek, J. Hodacova and S. E. Stokes, *J. Chem. Soc.-Dalton Trans.*, 1993, 1327-1332.
30. P. D. Beer, Z. Chen, A. J. Goulden, A. Grieve, D. Hesek, F. Szemes and T. Wear, *J. Chem. Soc.-Chem. Commun.*, 1994, 1269-1271.
31. K. T. Holman, M. M. Halihan, S. S. Jurisson, J. L. Atwood, R. S. Burkhalter, A. R. Mitchell and J. W. Steed, *J. Am. Chem. Soc.*, 1996, **118**, 9567-9576.
32. K. T. Holman, M. M. Halihan, J. W. Steed, S. S. Jurisson and J. L. Atwood, *J. Am. Chem. Soc.*, 1995, **117**, 7848-7849.
33. J. W. Steed, R. K. Juneja and J. L. Atwood, *Angew. Chem. Intl. Ed.*, 1994, **33**, 2456-2457.
34. Z. M. Yin, Y. H. Zhang, J. Q. He and J. P. Cheng, *Tetrahedron*, 2006, **62**, 765-770.
35. P. A. Gale, J. L. Sessler, V. Kral and V. Lynch, *J. Am. Chem. Soc.*, 1996, **118**, 5140-5141.

36. F. P. Schmidtchen, *Org. Lett.*, 2002, **4**, 431-434.
37. P. Gale, in *Encyclopedia of Supramolecular Chemistry*, eds. J. W. Steed and J. L. Atwood, Marcel Dekker, New York, 2004, pp. 31-41.
38. P. J. Smith, M. V. Reddington and Wilcox, Craig S., *Tetrahedron Lett.*, 1992, **33**, 6085-6088.
39. E. Fan, S. A. Vanarman, S. Kincaid and A. D. Hamilton, *J. Am. Chem. Soc.*, 1993, **115**, 369-370.
40. M. Boiocchi, L. Del Boca, D. E. Gomez, L. Fabbrizzi, M. Licchelli and E. Monzani, *J. Am. Chem. Soc.*, 2004, **126**, 16507-16514.
41. V. Amendola, D. Esteban-Gomez, L. Fabbrizzi and M. Licchelli, *Acc. Chem. Res.*, 2006, **39**, 343-353.
42. C. M. G. Dos Santos, T. McCabe and T. Gunnlaugsson, *Tetrahedron Lett.*, 2007, **48**, 3135-3139.
43. S. J. Brooks, P. A. Gale and M. E. Light, *Chem. Commun.*, 2005, 4696-4698.
44. B. H. M. Snellink-Ruel, M. M. G. Antonisse, J. F. J. Engbersen, P. Timmerman and D. N. Reinhoudt, *Eur. J. Org. Chem.*, 2000, 165-170.
45. S. J. Brooks, P. A. Gale and M. E. Light, *Cryst. Eng. Comm.*, 2005, **7**, 586-591.
46. M. E. Light, P. A. Gale and S. J. Brooks, *Acta. Cryst. E-Structure Reports Online*, 2006, **62**, O1905-O1907.
47. Y. L. Chang, M. A. West, F. W. Fowler and J. W. Lauher, *J. Am. Chem. Soc.*, 1993, **115**, 5991-6000.
48. D. J. Abdallah and R. G. Weiss, *Advanced Materials*, 2000, **12**, 1237-+.
49. M. de Loos, B. L. Feringa and J. H. van Esch, *Eur. J. Org. Chem.*, 2005, 3615-3631.
50. M. de Loos, A. G. J. Ligtenbarg, J. van Esch, H. Kooijman, A. L. Spek, R. Hage, R. M. Kellogg and B. L. Feringa, *Eur. J. Org. Chem.*, 2000, 3675-3678.
51. P. J. Flory, *Faraday Discuss. Chem. Soc.*, 1974, **57**, 7-18.
52. A. M. Todd, K. M. Anderson, P. Byrne, A. E. Goeta and J. W. Steed, *Cryst. Growth Des.*, 2006, **6**, 1750-1752.
53. K. S. Kim, H. S. Jang and H. S. Kim, *Bull. Korean Chem. Soc.*, 2006, **27**, 1445-1449.
54. A. P. Davis, J. J. Perry and R. P. Williams, *J. Am. Chem. Soc.*, 1997, **119**, 1793-1794.

55. A. J. Ayling, M. N. Perez-Payan and A. P. Davis, *J. Am. Chem. Soc.*, 2001, **123**, 12716-12717.
56. S. Valiyaveettil, J. F. J. Engbersen, W. Verboom and D. N. Reinhoudt, *Angew. Chem. Int. Ed.*, 1993, **32**, 900-901.
57. L. S. Flatt, V. Lynch and E. V. Anslyn, *Tetrahedron Lett.*, 1992, **33**, 2785-2788.
58. C. Raposo, M. Almaraz, M. Martin, V. Weinrich, L. Mussons, V. Alcazar, C. Caballero and J. R. Moran, *Chem. Lett.*, 1995, 759.
59. K. Kavallieratos, A. Danby, G. J. Van Berkel, M. A. Kelly, R. A. Sachleben, B. A. Moyer and K. Bowman-James, *Anal. Chem.*, 2000, **72**, 5258-5264.
60. P. D. Beer, P. K. Hopkins and J. D. McKinney, *Chem. Commun.*, 1999, 1253-1254.
61. D. A. Jose, D. K. Kumar, B. Ganguly and A. Das, *Inorg. Chem.*, 2007, **46**, 5817-5819.
62. K. J. Winstanley, S. J. Allen and D. K. Smith, *Chem. Commun.*, 2009, 4299-4301.
63. P. D. Beer, A. R. Graydon, A. O. M. Johnson and D. K. Smith, *Inorg. Chem.*, 1997, **36**, 2112-2118.
64. P. D. Beer, F. Szemes, V. Balzani, C. M. Sala, M. G. B. Drew, S. W. Dent and M. Maestri, *J. Am. Chem. Soc.*, 1997, **119**, 11864-11875.
65. A. P. Davis, D. N. Sheppard and B. D. Smith, *Chem. Soc. Rev.*, 2007, **36**, 348-357.
66. J. Scheerder, J. F. J. Engbersen, A. Casnati, R. Ungaro and D. N. Reinhoudt, *J. Org. Chem.*, 1995, **60**, 6448-6454.
67. Y. Morzherin, D. M. Rudkevich, W. Verboom and D. N. Reinhoudt, *J. Org. Chem.*, 1993, **58**, 7602.
68. J. Scheerder, F. Fochi, J. F. J. Engbersen and D. N. Reinhoudt, *J. Org. Chem.*, 1994, **59**, 7815-7820.
69. C. Walsdorff, W. Saak and S. Pohl, *J. Chem. Res. (S)*, 1996, 282 - 283.
70. K. J. Wallace, W. J. Belcher, D. R. Turner, K. F. Syed and J. W. Steed, *J. Am. Chem. Soc.*, 2003, **125**, 9699-9715.
71. L. O. Abouderbala, W. J. Belcher, M. G. Boutelle, P. J. Cragg, M. Fabre, J. Dhaliwal, J. W. Steed, D. R. Turner and K. J. Wallace, *Chem. Commun.*, 2002, 358-359.

72. A. Metzger, V. M. Lynch and E. V. Anslyn, *Angew. Chem., Int. Ed. Engl.*, 1997, **36**, 862-865.
73. G. Hennrich and E. V. Anslyn, *Chem. Eur. J.*, 2002, **8**, 2218-2224.
74. G. McSkimming, J. H. R. Tucker, H. Bouas-Laurent and J. P. Desvergne, *Angew. Chem. Int. Ed.*, 2000, **39**, 2167-2169.
75. L. O. Abouderbala, W. J. Belcher, M. G. Boutelle, P. J. Cragg, J. W. Steed, D. R. Turner and K. J. Wallace, *Proc. Nat. Acad. Sci. USA*, 2002, **99**, 5001-5006.
76. D. R. Turner, M. J. Paterson and J. W. Steed, *J. Org. Chem.*, 2006, **71**, 1598-1608.
77. C. Schmuck and M. Heller, *Org. Biomol. Chem.*, 2007, **5**, 787-791.
78. T. Gunnlaugsson, M. Glynn, G. M. Tocci, P. E. Kruger and F. M. Pfeffer, *Coord. Chem. Rev.*, 2006, **250**, 3094-3117.
79. L. J. Barbour, G. W. Orr and J. L. Atwood, *Nature*, 1998, **393**, 671-673.
80. R. Vilar, D. M. P. Mingos, A. J. P. White and D. J. Williams, *Chem. Commun.*, 1999, 229-230.
81. C. R. Bondy, P. A. Gale and S. J. Loeb, *Chem. Commun.*, 2001, 729-730.
82. D. R. Turner, E. C. Spencer, J. A. K. Howard, D. A. Tocher and J. W. Steed, *Chem. Commun.*, 2004, 1352-1353.
83. D. R. Turner, B. Smith, E. C. Spencer, A. E. Goeta, I. R. Evans, D. A. Tocher, J. A. K. Howard and J. W. Steed, *New J. Chem.*, 2005, **29**, 90-98.
84. D. R. Turner, M. B. Hursthouse, M. E. Light and J. W. Steed, *Chem. Commun.*, 2004, 1354-1355.
85. C. R. Bondy, P. A. Gale and S. J. Loeb, *J. Am. Chem. Soc.*, 2004, **126**, 5030-5031.
86. M. G. Fisher, P. A. Gale, M. E. Light and S. J. Loeb, *Chem. Commun.*, 2008, 5695-5697.

2. Flexible Tripodal Anion Receptors

2.1 Aims

In an attempt to develop a range of flexible receptor tripods, the starting tri-amine tris(2-aminoethyl)amine (tren) was selected as the structural core. Tren has a well-documented history for its use as a chelating ligand for various soft metals such as copper,[1-3] while protonated ammonium analogues[4] and secondary amine derivatives[5-6] have already been shown to serve as anion receptors. The functionalisation of tren with additional moieties is a fairly facile process, and tren-based amides,[7-9] and ureas[10-12] are receiving increasing attention as anion receptors, thanks to the flexibility of the tren core and the good size and shape complementarity of the receptor to many small anions that is found as a result. In addition, the high flexibility of the tren core, particularly when coupled with urea functionality, allows some of these receptor complexes to show gelation under the right conditions,[13-14] though this gelation ability seems highly dependent on the nature of the pendant group of the urea. None of the compounds detailed here were found to gel under any conditions they were subjected to over the course of any crystallisation, purification, or during analysis.

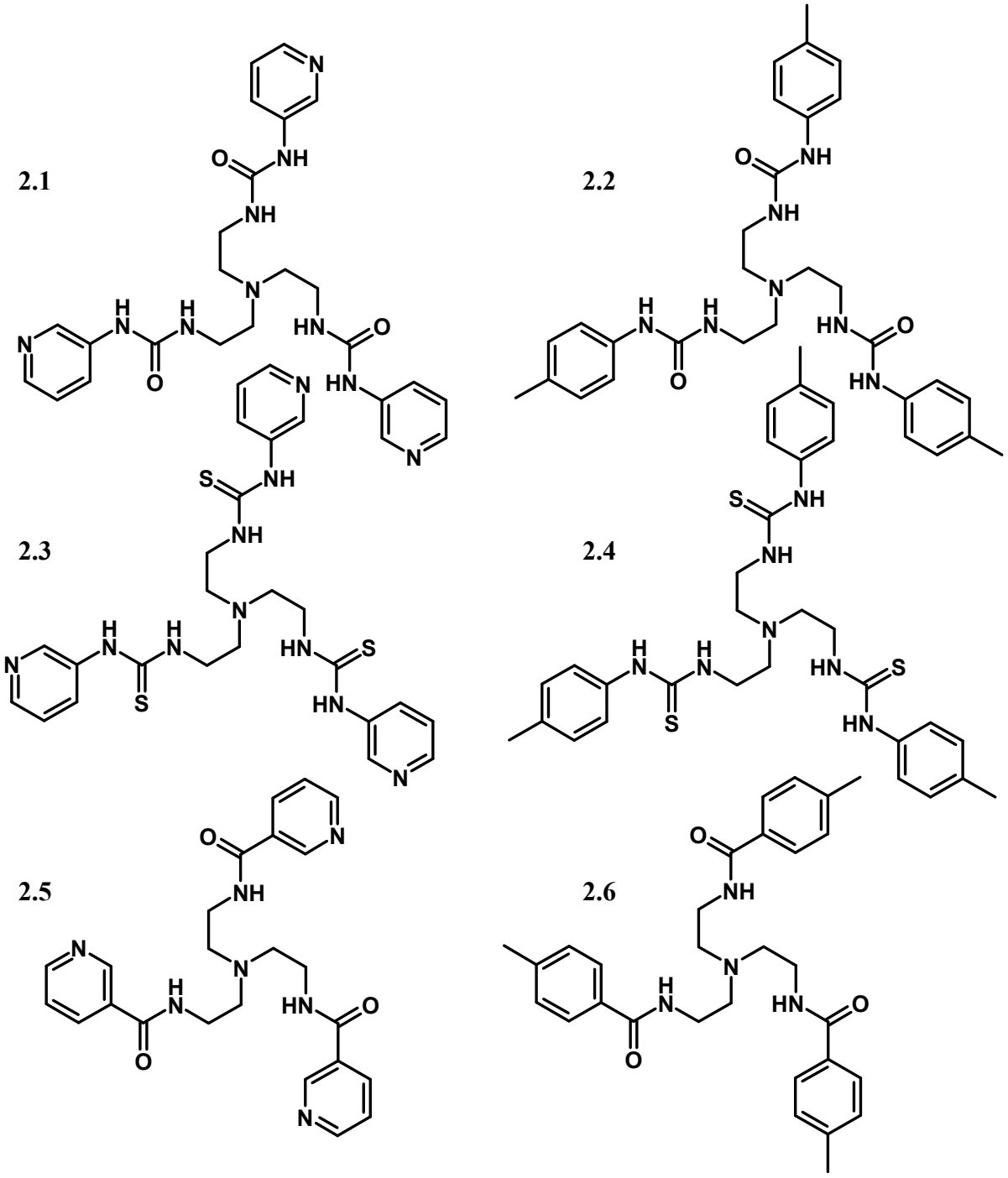

Figure 2.1 – Tren-based receptor compounds **2.1**-**2.6**

Initially, the tris(pyridylurea) compound (**2.1**) was a primary target compound, combining the anion binding properties of the urea with the cation binding capability of the pyridyl unit, especially since earlier work has shown that 3-pyridyl urea species could prove effective gelators.[15-16] Synthesis of this ligand proved difficult, and the chemistry of the compound has since been reported by others.[17-18]

The *p*-tolyl derived compounds (**2.2**, **2.4**, **2.6**) were synthesised as model compounds without the cation-binding properties, and also to look at the effect of the electron donation/withdrawal capability of the pendant groups.

The overall aim was to compare and contrast the anion binding capability of the urea, thiourea, and amide sub-units, keeping the framework and pendant structure the same, and to compare these tripods' anion binding properties against those similar systems reported in the literature. To achieve this, compounds **2.2-2.6** were synthesised (Figure 2.1) and their responses to the presence of various anions were analysed, typically by ^{1}H NMR spectroscopy. Synthesis of the urea **2.2** was achieved by reaction of tren with three equivalents of *p*-tolyl isocyanate. Similarly, synthesis of the thioureas **2.3** and **2.4** involved reaction of tren with three equivalents of the appropriate isothiocyanate. Synthesis of the amides was more complicated – **2.5** was synthesised serendipitously by reaction of tren with nicotinoyl azide during an attempt to synthesise **2.1**, while the *p*-tolyl-derived **2.6** was synthesised intentionally *via* a reaction involving *p*-toluic acid and boric acid to generate a reactive intermediate[19] which was then reacted with tren to give the product.

Crystals were grown of **2.2** and **2.5** from methanol/chloroform mixture (1:1) and pure chloroform respectively by slow evaporation of the solvent. Both show similarities in their conformations, with a repeating ABAB pattern of hydrogen bonding through the ureas/amides, in which two receptor arms hydrogen bond to each other in an intramolecular fashion and then bind to the third arm of a neighbouring compound in a repeating pattern, being the prevalent intermolecular interaction in both cases (see Figure 2.2). It has been found to be common for tren-based systems to adopt this binding pattern in the crystal structure,[13-14, 20] and seems to be mostly independent on the identity of the functional groups. Urea-urea hydrogen bonding distances are in the region of 1.9 – 2.2 Å ($H^{\cdots}O$ distances, 2.8 – 3.0 Å N-O distances), which are typical of compounds of this type.[13-14]

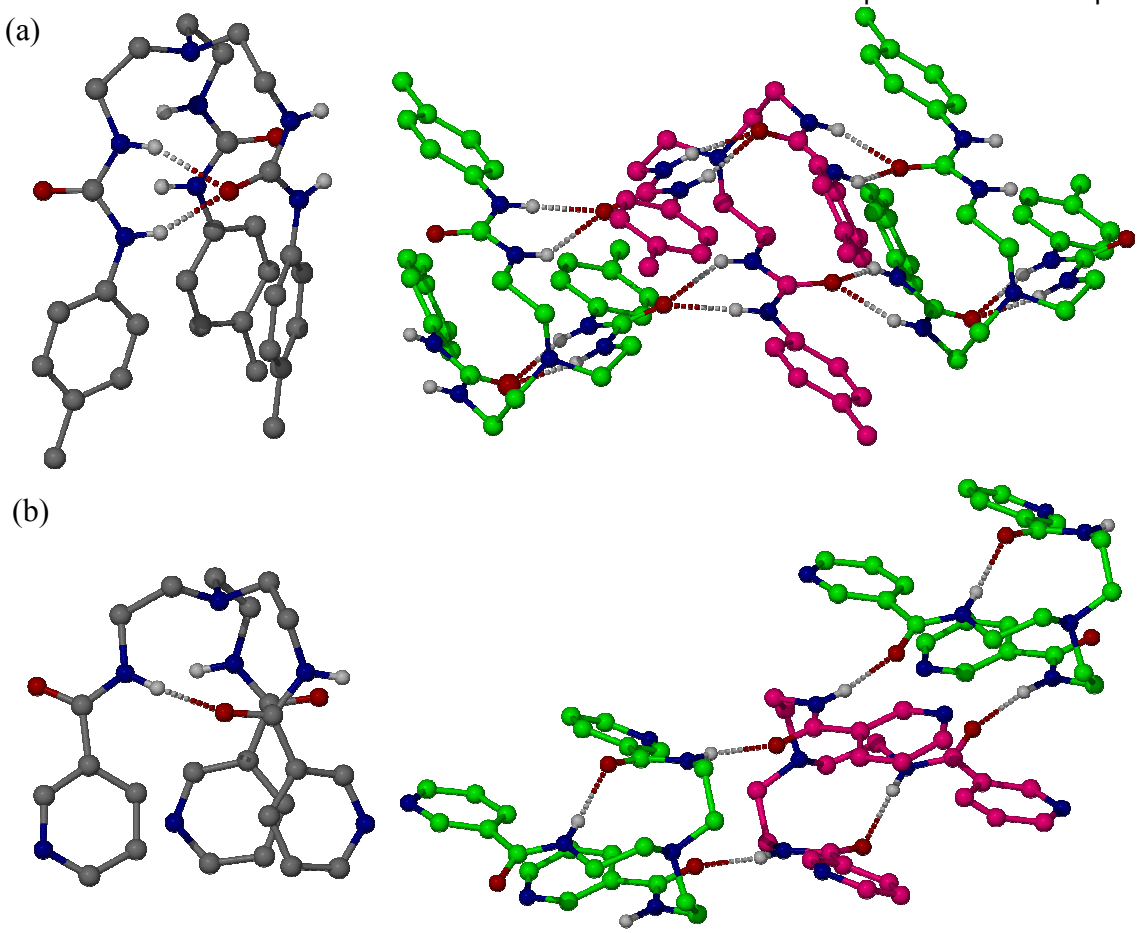

Figure 2.2 – X-ray molecular structures of (a) **2.2** and (b) **2.5**, along with the ABAB patterns exhibited by each, coloured green and red. Non-hydrogen-bonding hydrogen atoms removed for clarity.

2.2 Anion Binding Studies

The anion binding capabilities of the compounds **2.2**-**2.6** were studied using ^{1}H NMR spectroscopic titrations. Typically, 5 mg of the host compound was dissolved in 0.5 ml of 10% protic methanol in $CDCl_3$ (the methanol was required for solubility of the urea **2.2**, but was added to all of the experiments to allow for a direct comparison of the different receptors). Guest solutions, consisting of a tenfold excess over the host, were prepared by dissolving the appropriate amount of the anion (as the tetrabutylammonium salt) in 1 ml of $CDCl_3$. The guest solution was added to the host

solution in 10 μl (0.1 equiv.) aliquots until the chemical shift change between additions was sufficiently small (typically after 1.5 equivalents), at which point the additions were made in 50 μl (0.5 equiv.) increments to a maximum of 5 equivalents. Analysis of the curves generated (Figures 2.3 – 2.6) using the non-linear least squares fitting program HypNMR 2006[21] generated β values tabulated below (Tables 2.1 – 2.4) with appropriate sigma values – β_2 and β_3 are calculated from these by subtraction, and represent the second binding step, either of addition of a second host species or a second guest respectively. For the most part, monoanionic guests were chosen for a better comparison, although the trianionic trimesylate (1,3,5-benzenetricarboxylate, abbreviated to O_3Tm^{3-}) was included due to it being similar in size to the cavity within the receptor, its threefold symmetry, and its high degree of planarity. No data could be refined for **2.6**, as the amide N-H resonance was not detected in the solvent mixture for this compound. Attempts to follow the titration by observing the shift in the resonances assigned to the aromatic C-H groups proved difficult, since any shift was indistinguishable from error in the measurement.

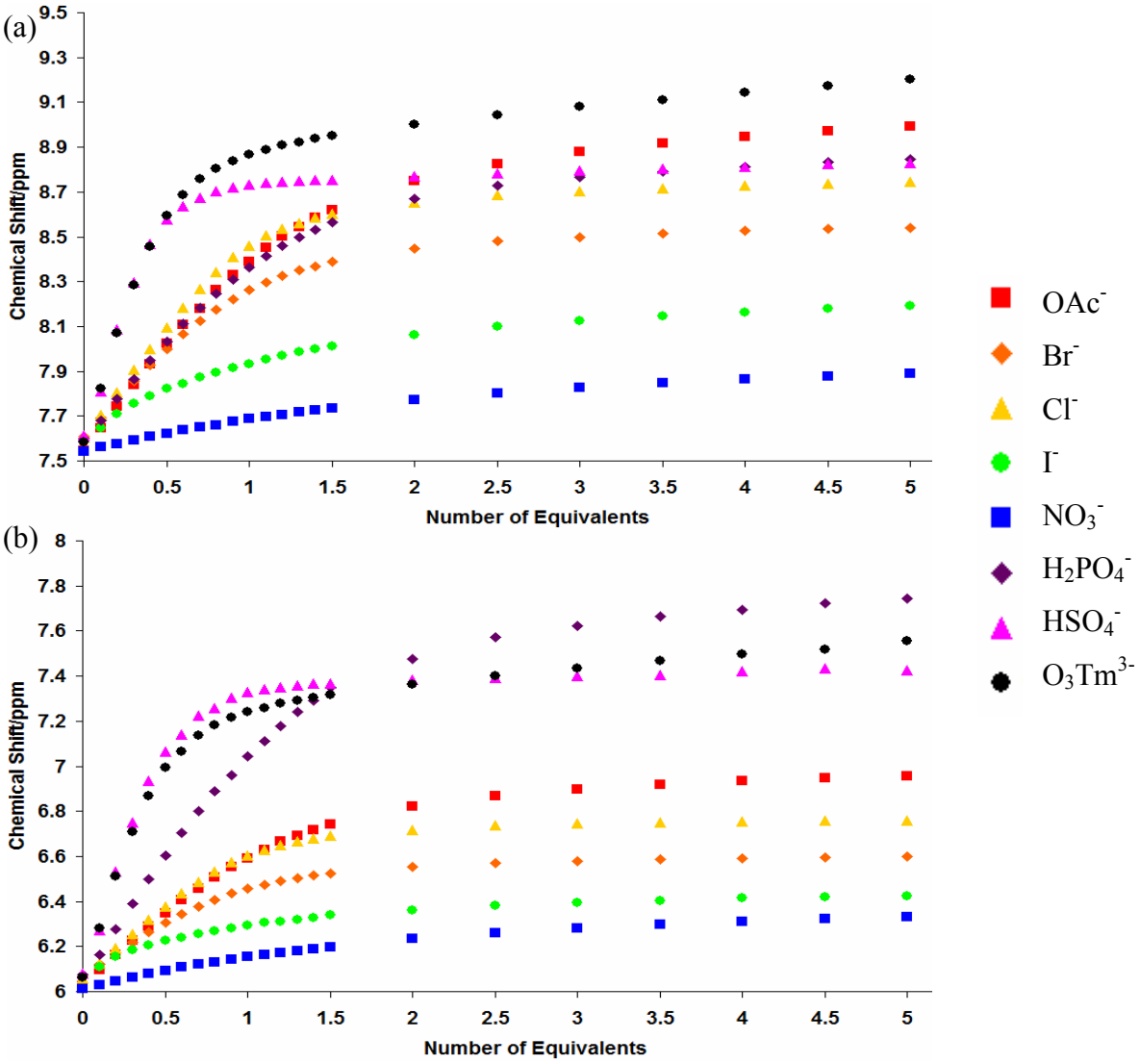

Guest	β_1	β_{21}	β_2	β_{12}	β_3
Chloride	2.78(1)	4.35(1)	1.57	N/A	N/A
Bromide	2.37(1)	3.55(3)	1.18	N/A	N/A
Iodide	1.23(8)	2.88(9)	1.65	N/A	N/A
Nitrate	0.92(2)	N/A	N/A	N/A	N/A
Acetate	2.19(1)	N/A	N/A	3.50(3)	1.31
Hydrogen Sulphate	2.93(6)	5.49(9)	2.56	N/A	N/A
Dihydrogen Phosphate	3.33(2)	N/A	N/A	5.04(1)	1.71
Trimesylate	1.92(4)	4.68(1)	2.76	N/A	N/A

Figure 2.3 – Chemical shift changes of resonances assigned to (a) aromatic NH and (b) aliphatic NH groups of **2.2** with addition of anions, and β values, derived from ^{1}H NMR titrations in 10% MeOH/$CDCl_3$ at 20°C. Anions at NBu_4^+ salts.

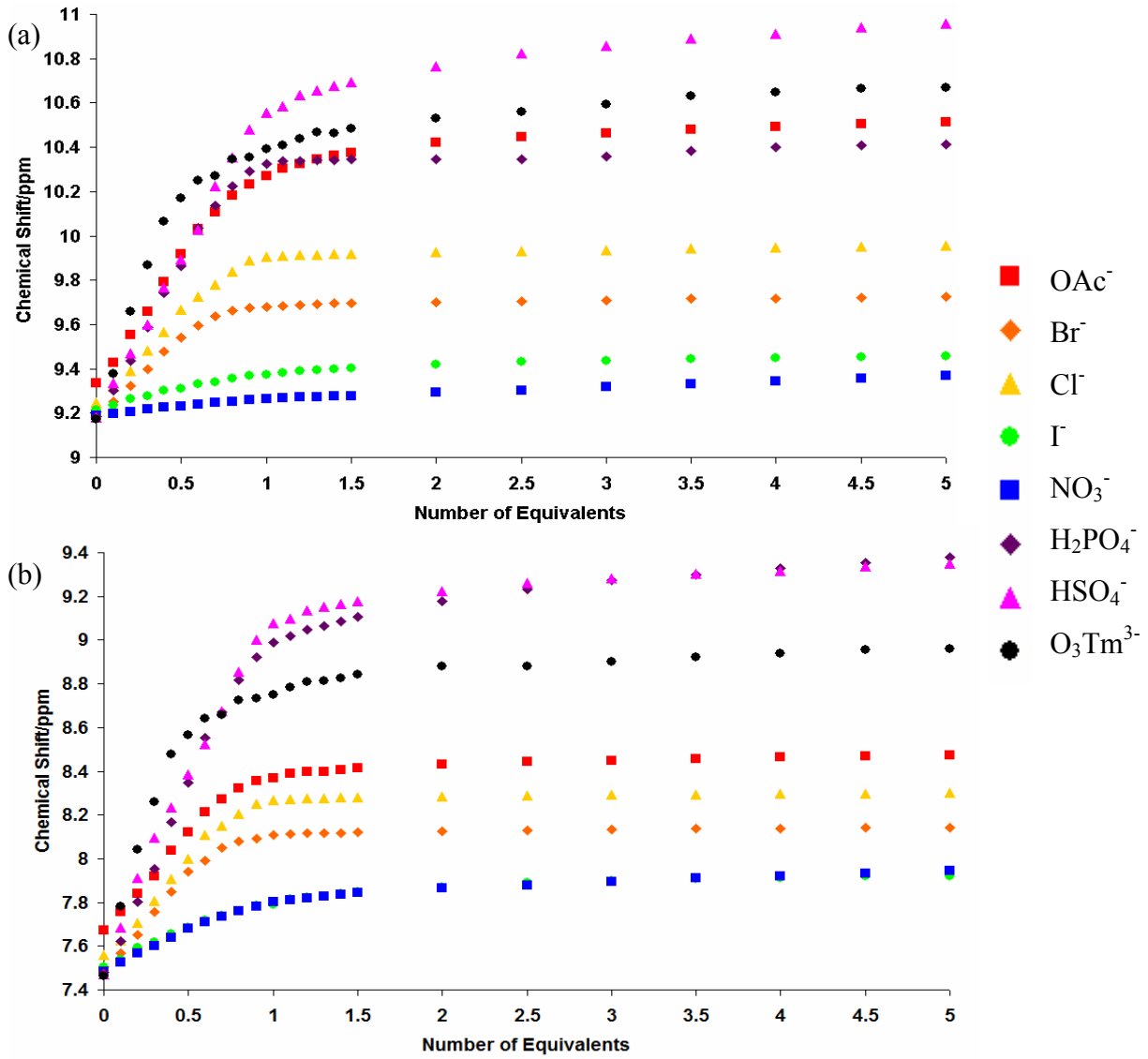

Guest	β_1	β_{21}	β_2	β_{12}	β_3
Chloride	4.34(2)	6.44(6)	2.1	N/A	N/A
Bromide	3.77(7)	6.07(3)	2.3	N/A	N/A
Iodide	2.51(2)	N/A	N/A	N/A	N/A
Nitrate	2.49(5)	N/A	N/A	N/A	N/A
Acetate	3.50(3)	6.02(6)	2.52	N/A	N/A
Hydrogen Sulphate	3.65(3)	6.10(8)	2.45	N/A	N/A
Dihydrogen Phosphate	3.58(5)	6.1(1)	2.52	N/A	N/A
Trimesylate	3.34(1)	6.89(3)	3.55	N/A	N/A

Figure 2.4 – Chemical shift changes of resonances assigned to (a) aromatic NH and (b) aliphatic NH groups of **2.3** with addition of anions, and β values, derived from ^{1}H NMR titrations in 10% MeOH/$CDCl_3$ at 20°C. Anions at NBu_4^+ salts.

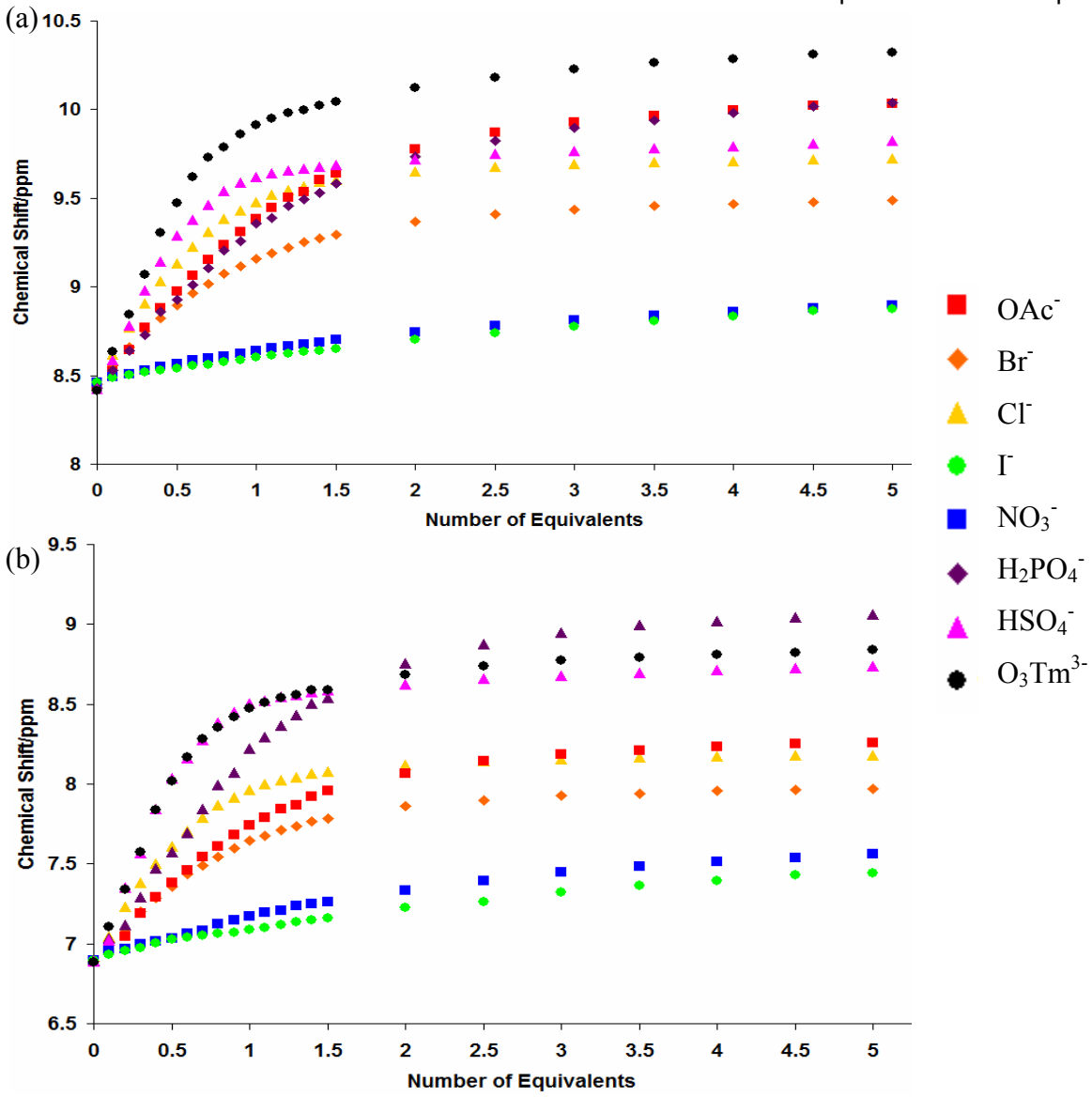

Guest	β_1	β_{21}	β_2	β_{12}	β_3
Chloride	2.74(2)	4.32(6)	1.58	N/A	N/A
Bromide	2.27(2)	3.58(9)	1.31	N/A	N/A
Iodide	1.21(1)	N/A	N/A	1.53(1)	0.32
Nitrate	2.00(1)	N/A	N/A	3.06(9)	1.06
Acetate	2.52(6)	N/A	N/A	3.97(9)	1.45
Hydrogen Sulphate	3.21(1)	5.48(4)	2.27	N/A	N/A
Dihydrogen Phosphate	3.71(6)	N/A	N/A	5.70(7)	1.99
Trimesylate	3.87(2)	7.33(3)	3.46	N/A	N/A

Figure 2.5 - Chemical shift changes of resonances assigned to (a) aromatic NH and (b) aliphatic NH groups of **2.4** with addition of anions, and β values, derived from ^{1}H NMR titrations in 10% MeOH/$CDCl_3$ at 20°C. Anions at NBu_4^+ salts.

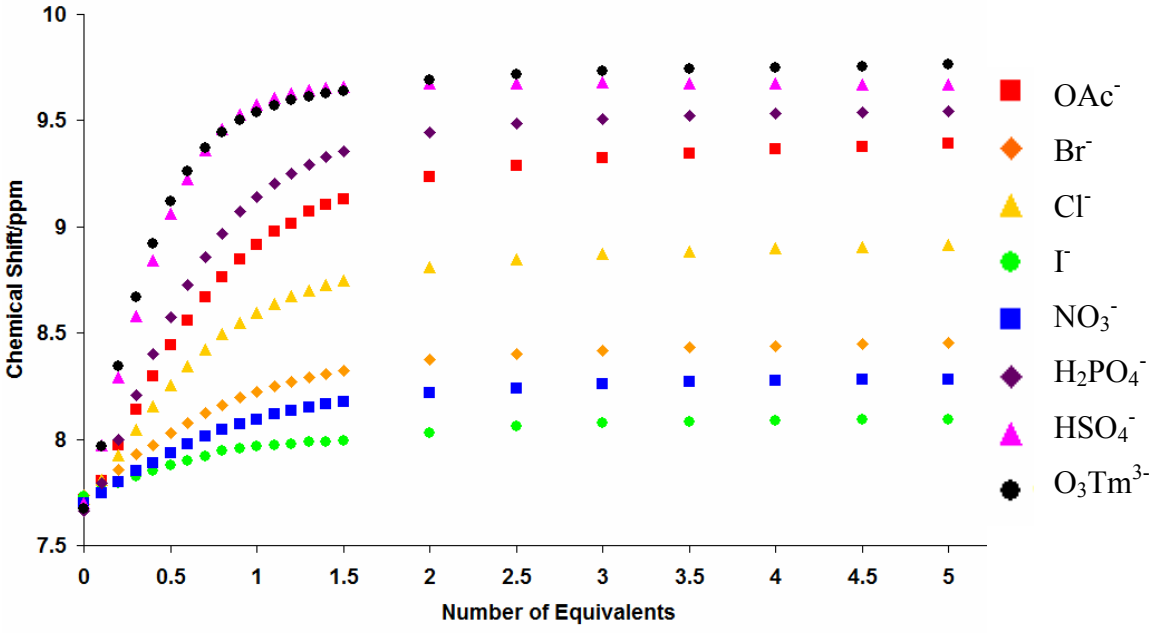

Guest	β_1	β_{21}	β_2	β_{12}	β_3
Chloride	2.90(2)	4.95(6)	2.05	N/A	N/A
Bromide	2.49(1)	3.97(6)	1.48	N/A	N/A
Iodide	2.3(1)	N/A	N/A	N/A	N/A
Nitrate	2.39(4)	N/A	N/A	N/A	N/A
Acetate	2.57(2)	N/A	N/A	N/A	N/A
Sulphate	4.06(1)	6.54(5)	2.48	N/A	N/A
Phosphate	2.86(3)	N/A	N/A	N/A	N/A
Trimesylate	3.38(3)	6.05(6)	2.67	N/A	N/A

Figure 2.6 - Chemical shift changes of resonance assigned amide NH group of **2.5** with increasing concentration of anions, with log β values for, derived from ^{1}H NMR titrations in 10% MeOH/$CDCl_3$ at 20°C. Anions at NBu_4^+ salts.

The behaviour of the hosts was found to vary with the nature of the anion. Spherical mono-anions such as chloride, bromide and hydrogen sulphate are able to interact with two host molecules simultaneously, as is evidenced by the presence of a fairly high 2:1 host:guest equilibrium constant, assigned due to the titrations showing maximum chemical shift change well before one equivalent is added. This is in agreement with crystallographic evidence found elsewhere[17-18] for tren-based receptor compounds with sulphate. Also, the titration data suggests that this effect is not observed when acetate is chosen as the guest. This is perhaps not surprising, as the charge on acetate is much more directional than the charge on halides or pseudo-spherical oxo-anions, as the methyl group of acetate is uncharged. In this case the high binding affinity for acetate is manifested with multiple acetate anions binding to the same receptor. Interestingly, dihydrogen phosphate is found to bind in a similar fashion to acetate, whereas it may be expected it would follow the same trend as hydrogen sulphate and the halides due to the similarity in size and shape between phosphate and sulphate. This difference may be attributable to the formation of a larger capsule, in a similar manner to the pentafluorophenyl urea receptor synthesised by others,[22] in which phosphate forms a 2:2 host:guest complex capsule, with a larger central cavity able to contain a phosphate dimer formed *in situ*.

For the most part, the refined binding constants obey the expected trend $\beta_1 > \beta_2$ (or β_3, in those cases where 1:2 host:guest binding occurs), signifying that binding of the second equivalent of host or guest to the complex is typically weaker than the first. However, it is important to draw attention to the rare cases where this is not the case, particularly in the interactions of receptors **2.2** and **2.3** with the trimesylate anion, where binding of the second host to generate the 2:1 host:guest complex is actually enhanced by the first binding step. Thus, the host-guest complex is actually a more

favourable environment for a host molecule to bind to than the free guest, a process which likely involves effective interdigitation of the receptor arms such that the binding takes place through additional interactions beyond simple host-to-guest hydrogen bonds. Such assemblies may perhaps involve π-π and C-H-π interactions between pendant groups. A similar effect is observed for receptor **2.2** with iodide, and reinforces the idea that such a process is encouraged when the guest is slightly too large, or perhaps not an ideal shape match for the receptor cavity.

Job plot analyses confirm the presence of 2:1 host:guest species with chloride and sulphate and the presence of 1:2 host:guest species with acetate and phosphate (Figure 2.7) with the urea/thiourea receptors, while the same treatment with the amide receptors instead suggests that the primary binding mode is 1:1 (Figure 2.8) in all cases, though this does disagree with the titration data, which was found not to refine as simply with chloride, bromide, sulphate and trimesylate. It is possible that this apparent 1:1 binding mode is caused by this speciation being the most likely at the concentrations used in the experiment, or it may be the case that the curve shows an average of a combination of 1:1, 1:2 and 2:1 binding modes. Likewise, the apparent 2:3 binding mode observed in the case of the receptors with e.g. acetate (Figure 2.7b) is attributed to a combination of a 1:1 and 1:2 binding style, as is consistent with the observed binding constants.

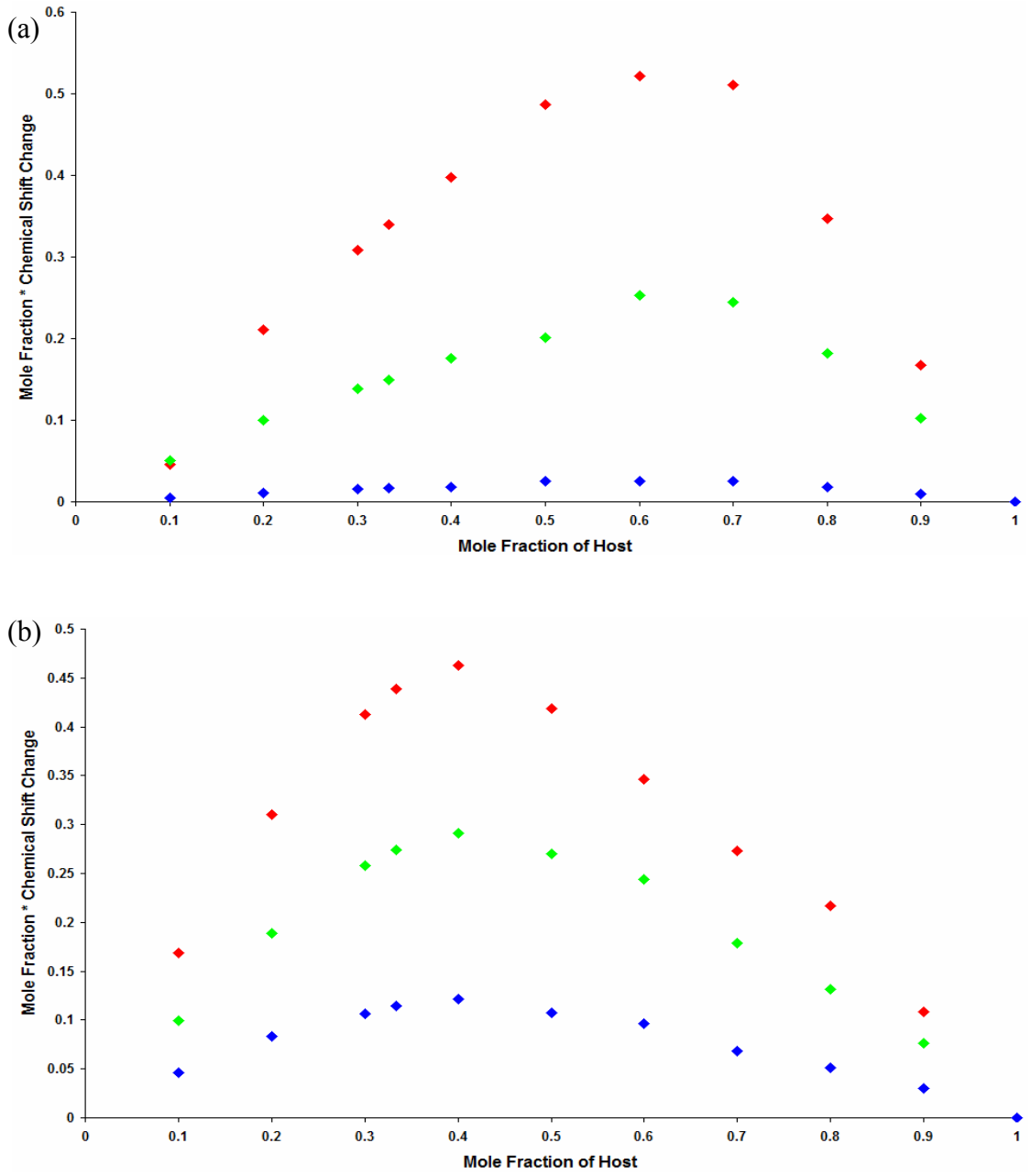

Figure 2.7 – Typical Job's Method plots for *p*-tolyl ureas/thioureas with (a) chloride or sulphate, and (b) acetate or phosphate. Red symbols mark aromatic NH, green symbols mark aliphatic NH, and blue symbols mark the nearest aromatic CH to the urea.

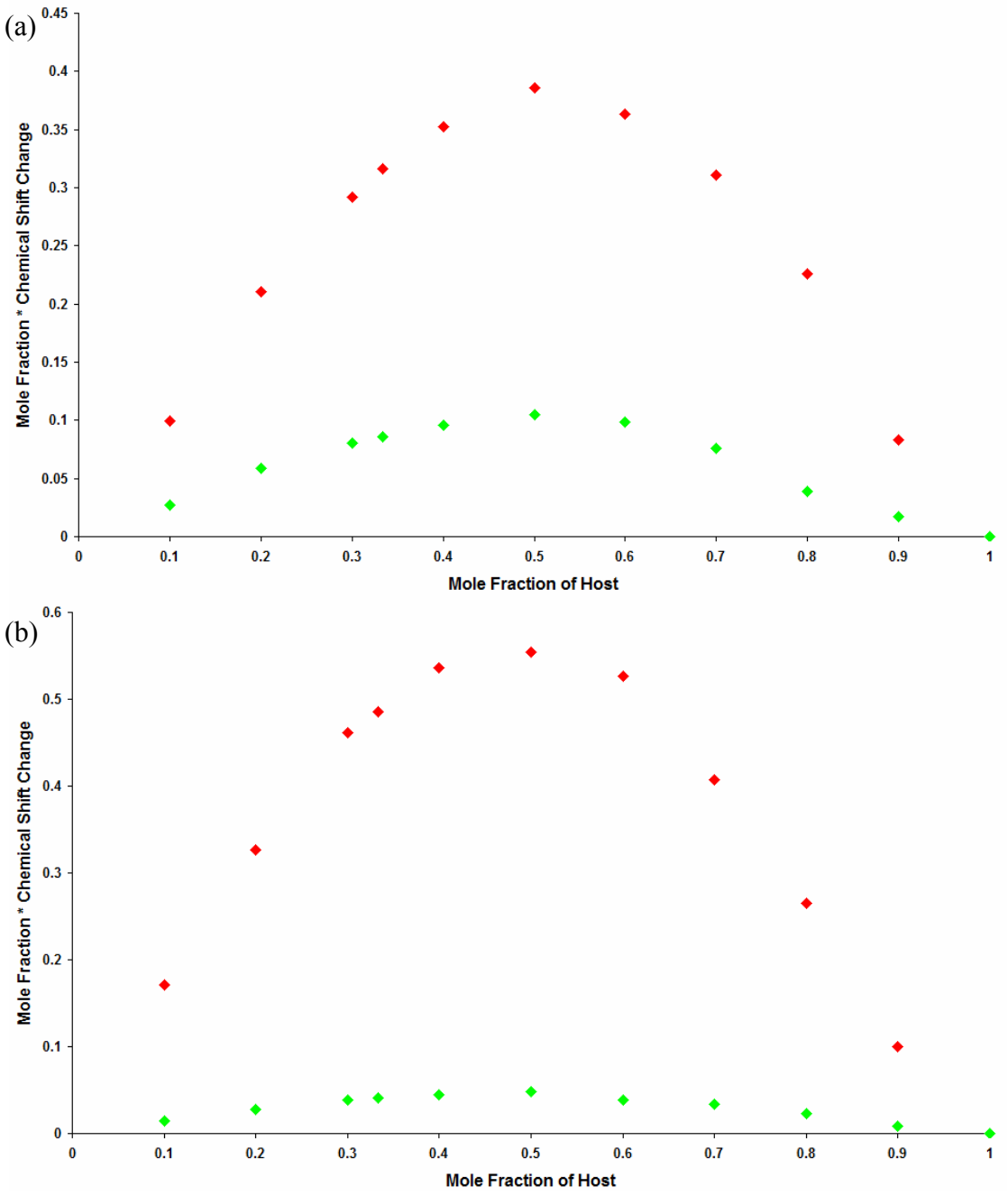

Figure 2.8 – Job plot data for amide receptor **2.5** with (a) chloride and (b) acetate. Red symbols represent amide N-H shift, green symbols represent pyridyl C-H shift. Other anions give consistent, matching data and were omitted.

Previous work into related alkyl-substituated tren amides[23] seems to suggest that a 1:1 receptor:anion complex is most favoured for the amide receptors, with a second anion being able to bind via protonation of the central tren nitrogen atom, yielding a complex of the form $[Host+H]^+[Guest]^-_2$. While this is a possible explanation for the inclusion of 1:2 receptor:anion binding constants with some of the systems studied here, no additional signal corresponding to this protonation was detected during the NMR titrations of any of the receptors. Although it is possible that this signal is not detected due to potential broadening of the peak, it would be expected for such a resonance to be visible throughout the range of receptors studied, especially as most NBu_4^+ salts are inherently acidic.

Changing the nature of the binding group has an often large effect on the binding affinity with the anions. With the *p*-tolyl-based receptors, changing from a urea to a thiourea causes only a small change in the binding to chloride, bromide and sulphate, suggesting that these anions are an excellent fit no matter how acidic the NH groups may be. A significant difference is observed for more basic anions such as nitrate, acetate and phosphate, which are bound far more strongly (in the region of ten times higher binding constants observed). Trimesylate, as the most basic anion studied, shows approximately a 100 fold increase in binding to the thiourea compared to the urea. The behaviour of the *p*-tolyl urea and thiourea and their binding to phosphate in particular is contrary to what has been reported previously. In a study of tren-based receptors as phosphate receptors, Raposo and colleagues[24] determined that the thiourea of a phenyl-appended receptor bound significantly weaker to phosphate than the urea due to the higher strength of intramolecular hydrogen bonds. In our systems, the interactions between thiourea arms (either in one receptor alone, or between a pair of receptors) are present, as evidenced by the slight sigmoidal nature of the curves,

but are more easily overcome by particularly favourably bound anions such as phosphate. Since little change is observed between the urea and the thiourea with regards to the halides, but greater change is found for the oxoanions, it seems likely that the acidity of the receptor group is more important for binding of oxoanions, while the strength of binding with halides is mostly independent of the acidity of the receptor.

As others have reported,[17, 24] tren-based receptors show a particular affinity for sulphate anions, particularly in competitive solvents, though of the compounds studied here, only **2.5** shows significant selectivity for sulphate, with a binding constant approximately a factor of ten higher than for any other anion. In fact, the *p*-tolyl-derived receptors generally show a higher affinity for phosphate, at least in the solvent system used. The trend of log β values found here is in good agreement with those found using simple amine-based tren receptors[5] which showed markedly higher association constants with sulphate and phosphate than chloride or bromide in $CDCl_3$ solvent.

The choice of trimesylate as an anion arose due to it being a confirmationally inflexible, well-defined trianion, hoped to be of an acceptable size for the receptor binding site. Considering the high degree of complementarity between acetate anions and urea receptors, it was hoped that the C_3 symmetric tricarboxylate would prove an excellent anion for combination with the tripodal receptors. Work by Fan and coworkers[25] detailed a naphthalene-containing urea receptor based on tren and its interactions with trimesylate and terephthalate anions, and showed that even in the highly competitive medium of DMSO, a log β value of >4 was found for the aromatic di- and tri-anions, though their data refined to a 1:1 binding mode, likely due to the increased competition with the solvent faced by the anion in DMSO. Our data

suggests that in less-competitive media, formation of the 2:1 receptor:guest capsule is more favourable due to the increased strength of interactions between receptor binding groups and the guest species.

2.3 Cation-receptor interactions

It was hoped that the pyridyl appended receptors would show the ability to coordinate to a metal centre, in a similar manner to the studies on mono and dipodal receptors with various silver and copper salts.[26-27] Custelcean's work on the pyridyl-urea tripod **2.1**[17] suggested that the 2:1 sulphate capsule was stabilised by the presence of M^{2+} species such as zinc or magnesium, and they were able to successfully crystallise the $Mg(receptor)_2SO_4$ complex. In the hopes that our own pyridyl derived amide and thiourea tripods would show related behaviour, we attempted to crystallise **2.3** and **2.5** in the presence of 0.5 equivalents of $ZnSO_4$ and $CuSO_4$, from both water and methanol, though no crystals were formed for either receptor in any case. Elemental analysis of the dried powders from these crystallisations were consistent with the formation of $M(L)_2SO_4$, though this is hardly conclusive as removal of the solvent from the crystallisation gives only the solid products initially added. No structural confirmation could be collected to compare with the urea receptor.

Work by Smith and coworkers[23] concerned with amide-derived receptors attempted to probe the ability of these receptors as transport materials, making use of the combined anion binding site and the basic nitrogen to transport HCl across a membrane. They found that the longer alkyl chain substituted receptors were effective at transporting the ion pair from an acidic aqueous solution in one side of a U-tube to distilled water on the other side through a membrane of chloroform. We attempted a similar experiment using our amide receptors, with less success. The *p*-tolyl based amide

proved insoluble in chloroform, but soluble in water once protonated by the acid, and so it remained dissolved in the aqueous HCl fraction and no transport took place. The pyridyl amide, on the other hand, was found to be soluble in both the chloroform and aqueous layers, but became insoluble in chloroform upon acidification, and again no transport of acid was observed.

Evidence of interactions between all receptor compounds and cationic metals is found from mass spectrometry data, wherein all of the receptors show the presence of a signal corresponding to twice their molecular ion plus 23, the mass of one sodium ion. It is not uncommon to see the presence of an $[M + Na]^+$ peak by MS, but our tren-based receptors are able to form an enlarged $[2\ M + Na]^+$ complex with sodium, even under the relatively harsh ionisation conditions. It is unclear as to whether the sodium is coordinated in the centre of a capsule of two receptor compounds, or whether the dimer is formed with sodium coordinated to the outside.

2.4 Summary

In summary, a range of previously unreported tris(2-aminoethyl)amine based anion receptors have been synthesised and studied, and have been found to share several traits in common with related literature-reported receptors, particularly in the solid-state structures and general trends of anion affinity. The similarities and differences between the amide, urea and thiourea as receptor binding groups have been investigated, and it has been shown that the receptor's ability to bind to a variety of anions and its selectivity towards different anions is influenced by the nature of the pendant arms as well as by the binding group itself, with the electron density around the binding site playing an important part in the affinity for various anions. The difference between ureas and thioureas has been determined to be far greater for oxoanions than for halides, with affinities between the oxoanions and thioureas being consistently higher for all of the oxoanions studied, while the halides bind to both ureas and thioureas with equal strength, all other factors being equal. Also, we have determined that 2:1 receptor:guest capsule formation of tren-based receptor species, found for others primarily with sulphate, and to a lesser extent phosphate, is potentially much more prevalent than first thought, with most spherical and pseudo-spherical anions displaying a similar capability in less competitive media. Solubilities generally range from amides being the most soluble, particularly in aqueous media, through thioureas – soluble in most chlorinated solvents – with ureas being the least soluble generally, with **2.2** possessing extremely poor solubility compared to the other receptors. Structurally, those receptors which were found to crystallise agree well with reported literature structures.[13-14]

2.5 Experimental Details

Synthesis of receptors:

Tris(2-(*p*-tolylureido)ethyl)amine (2.2):

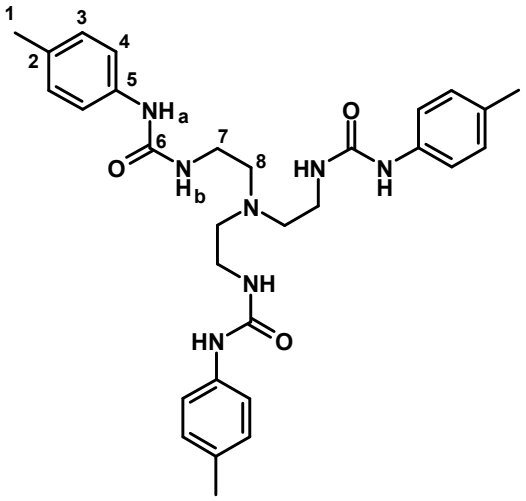

Tris(2-aminoethyl)amine (0.50 g, 4.00 mmol) was mixed with *p*-tolyl isocyanate (1.50 g, 12.0 mmol) in 50 ml CH_2Cl_2. The mixture was refluxed at 60°C for 6 hours and then left to cool overnight with stirring. The resulting precipitate was filtered and washed with acetone to give a clean white powder. Yield: 2.14 g, 3.92 mmol, 98%. ^{1}H NMR (DMSO-d_6, J/Hz, δ/ppm): 2.16 (s, 9H, H1); 2.50-2.55 (br m, 6H, H8); 3.10-3.15 (br m, 6H, H7); 6.00-6.10 (br m, 3H, NH_b); 6.90-7.00 (m, 6H, H3); 7.15-7.25 (m, 6H, H4); 8.34 (s, 3H, NH_a). ^{13}C{^{1}H} NMR (DMSO-d_6, δ/ppm): 20.72 (C1); 37.99 (C8); 54.47 (C7); 118.34 (C2); 129.42 (C3); 130.17 (C4); 138.32 (C5); 155.84 (C6). ESI$^+$-MS: m/z 546 $[M+H]^+$, 568 $[M+Na]^+$, 1113 $[2M+Na]^+$. Anal. Calc. for $C_{30}H_{39}N_7O_3$: C, 66.03; H, 7.20; N, 17.97. Found: C, 65.85; H, 7.14; N, 18.12. IR (cm^{-1}): 2860, 2813 (ν(N-H)), 1643 (ν(C=O)).

Tris(2-(3-pyridylthioureido)ethyl)amine (2.3):

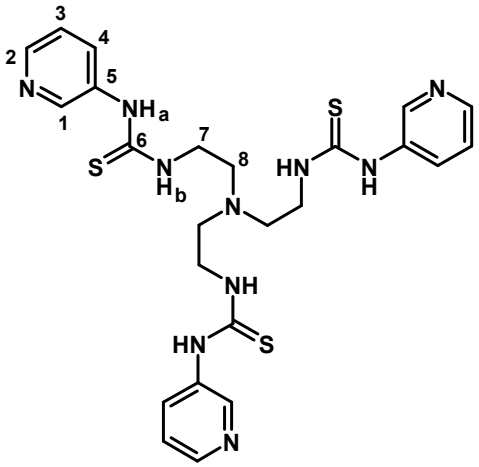

Tris(2-aminoethyl)amine (0.09 g, 0.60 mmol) was mixed with 3-pyridyl isothiocyanate (0.25 g, 1.80 mmol) in 20 ml CH_2Cl_2. The mixture was refluxed at 60^{o}C for 4 hours, resulting in the formation of a pale, lemon yellow precipitate which was filtered and washed with further CH_2Cl_2. Yield: 0.31 g, 0.55 mmol, 92%. ^{1}H NMR (DMSO-d_6, J/Hz, δ/ppm): 2.76 (t, 5.5, 6H, H8), 3.55-3.65 (br m, 6H, H7), 7.33 (ddd, 0.5, 4.6, 8.2, 3H, H3), 7.80-7.95 (br m, 3H, NH_b), 7.91 (br d, 8.2, 3H, H2), 8.28 (dd, 1.4, 4.6, 3H, H4), 8.54 (d, 2.5, 3H, H1), 9.74 (s, 3H, NH_a). $^{13}C\{^{1}H\}$ NMR (DMSO-d_6, δ/ppm): 40.13 (CH_2, C8), 51.99 (CH_2, C7), 123.16 (CH, C4), 130.45 (CH, C3), 131.53 (CH, C2), 136.02 (C5), 144.84 (CH, C1), 180.91 (C6). ESI^{+}-MS: m/z 555 $[M+H]^{+}$, 577 $[M+Na]^{+}$, 1131 $[2M+Na]^{+}$. Anal. Calc. for $C_{24}H_{30}N_{10}S_3$: C, 51.95; H, 5.45; N, 25.25. Found: C, 51.22; H, 5.42; N, 24.93. IR (cm^{-1}): 2924 (N-H stretch), 1508 (C=S stretch).

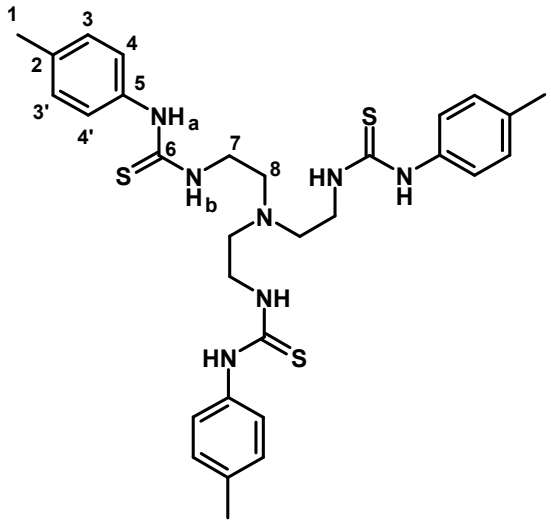

Tris(2-(*p*-tolylthioureido)ethyl)amine (2.4):

Tris(2-aminoethyl)amine (0.15 g, 1.00 mmol) was mixed with *p*-tolyl isothiocyanate (0.45 g, 3.00 mmol) in 20 ml CH_2Cl_2. The mixture was refluxed for 6 hours, forming a pale yellow precipitate after removal of the solvent, which was filtered and washed with diethyl ether. Yield: 0.55 g, 0.93 mmol, 94%. ^{1}H NMR ($CDCl_3$, J/Hz, δ/ppm): 2.30 (s, 9H, H1), 2.69 (br t, 4.7, 6H, H8), 3.65-3.80 (br m, 6H, H7), 6.73 (br s, 3H, NH_b), 7.00-7.20 (br m, 12H, H3/H4), 8.06 (br s, 3H, NH_a). $^{13}C\{^1H\}$ NMR (DMSO-d_6, δ/ppm): 20.46 (CH_3, C1), 41.84 (CH_2, C8), 52.16 (CH_2, C7), 123.63 (CH, C3), 125.71 (CH, C3'), 129.16 (CH, C4), 130.31 (CH, C4'), 133.61 (C2), 136.25 (C5), 180.25 (C6). ESI^+-MS: m/z 594 $[M+H]^+$, 616 $[M+Na]^+$, 1208 $[2M+Na]^+$. Anal. Calc. for $C_{30}H_{39}N_7S_3$: C, 60.67; H, 6.62; N, 16.51. Found: C, 60.22; H, 6.59; N, 15.51. (Reason for difference unknown). IR (cm^{-1}): 2921 (N-H stretch), 1511 (C=S stretch).

Tris(2-(3-pyridylamido)ethyl)amine (2.5):

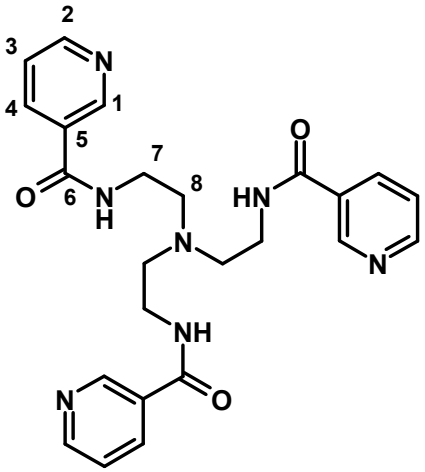

Nicotinoyl azide (1.50 g, 10.1 mmol) and Tris(2-aminoethyl)amine (0.50 g, 3.30 mmol) were dissolved in 25 ml acetonitrile and refluxed for 2 hours. The resulting solution was cooled and the solvent removed under vacuum to give a pale yellow precipitate. Washing this precipitate with diethyl ether removed the yellow colour and left a clean white powder as the final product. Yield: 0.70 g, 1.68 mmol, 50%. ^{1}H NMR (DMSO-d_6, J/Hz, δ/ppm): 2.73 (t, 6.5, 6H, H8), 3.30-3.50 (m, 6H, H7), 7.43 (dd, 4.8, 7.9, 3H, H3), 8.10 (d, 7.9, 3H, H4), 8.58 (t, 5.2, 3H, NH), 8.66 (dd, 1.0, 4.8, 3H, H2), 8.94 (d, 1.8, 3H, H1). ^{13}C{^{1}H} NMR (DMSO-d_6, δ/ppm): 38.40 (C8), 53.89 (C7), 123.9, 130.6, 135.4, 149.0, 152.37, 165.62 (C6). ESI^{+}-MS: m/z 462 $[M+H]^{+}$, 484 $[M+Na]^{+}$, 945 $[2M+Na]^{+}$. Anal. Calc. for $C_{24}H_{27}N_7O_3$: C, 62.46; H, 5.90; N, 21.24. Found: C, 62.81; H, 5.95; N, 20.86. IR (cm^{-1}): 2805 (N-H stretch), 1634 (C=O stretch).

Tris(2-(*p*-tolylamido)ethyl)amine (2.6):

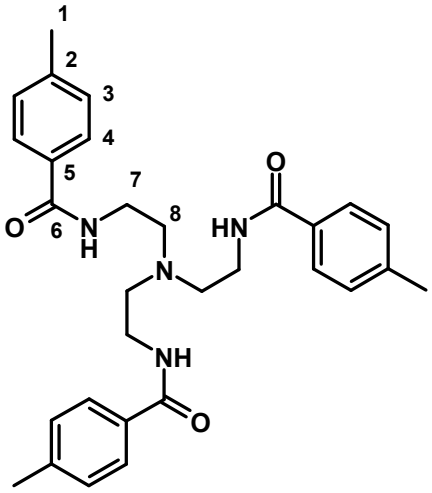

p-Toluic acid (0.82 g, 6.0 mmol) is suspended in toluene (30ml) in a round-bottomed flask. Boric acid (0.04 g, 0.6 mmol) is added and the mixture stirred for 30 mins. Tris(2-aminoethyl)amine (0.27 ml, 2 mmol) is added and the reaction mixture heated to reflux for 16h. The resulting precipitate is filtered, and washed with fresh toluene. Recrystallisation of the product with methanol gave the desired product as a white powder. Yield 0.84 g, 1.7 mmol, 84 %.

^{1}H NMR (DMSO-d_6, J/Hz, δ/ppm): 2.28 (s, 9H, H1), 2.55-2.75 (m, 6H, H8), 2.85-3.05 (m, 6H, H7), 4.5-6.5 (br m, NH/H_2O interactions), 7.09 (d, 7.8, 6H, H3), 7.76 (d, 7.8, 6H, H4). ^{13}C{^{1}H} NMR (DMSO-d_6, δ/ppm): 21.38 (C1); 37.04 (C8); 52.38 (C7); 128.50 (C2); 129.57 (C3); 135.83 (C4); 139.49 (C5); 170.77 (C6). ESI^{+}-MS: m/z 501.4 $[M+H]^{+}$, 523.5 $[M+Na]^{+}$, 1023.9 $[2M+Na]^{+}$. Anal. Calc. for $C_{30}H_{36}N_4O_3$: C, 71.97; H, 7.25; N, 11.19. Found: C, 70.85; H, 8.21; N, 11.01. (Reason for difference unknown). IR (cm^{-1}): 2848 (N-H stretch), 1588 (C=O stretch).

Crystal Data:

Crystals were grown from ligand **2.2** (0.05 g, 0.092 mmol) in Methanol/Chloroform (2 ml) by slow evaporation of the solvent.

Crystal data for **2.2**: $C_{30}H_{39}N_7O_3$, M = 545.68, colourless plate, 0.20 × 0.20 × 0.02 mm^3, triclinic, space group $P\bar{1}$ (No. 2), a = 9.2813(10), b = 12.9191(15), c = 13.7615 (16) Å, α = 83.41°, β = 70.86°, γ = 70.10°, V = 1465.7(3) Å^3, Z = 2, D_c = 1.236 g/cm^3, F_{000} = 584, SMART 1k, MoKα radiation, λ = 0.71073 Å, T = 120(2)K, $2\theta_{max}$ = 26.11º, 26614 reflections collected, 9007 unique (R_{int} = 0.0975). Final *GooF* = 0.852, *R1* = 0.0531, *wR2* = 0.1175, *R* indices based on 5039 reflections with I >2σ(I) (refinement on F^2), 361 parameters, 0 restraints. Lp and absorption corrections applied, μ = 0.082 mm^{-1}.

Crystals were grown from ligand **2.5** (0.05 g, 0.108 mmol) in chloroform (2 ml) by slow evaporation of the solvent.

Crystal data for **2.5**: $C_{24}H_{27}N_7O_3$, M = 461.53, colourless block, 0.31 × 0.15 × 0.09 mm^3, monoclinic, space group $P2_1/n$ (No. 14), a = 7.5140(4), b = 20.8875(12), c = 14.5608(9) Å, β = 97.596(2)°, V = 2265.2(2) Å^3, Z = 4, D_c = 1.353 g/cm^3, F_{000} = 976, Smart-6K, MoKα radiation, λ = 0.71073 Å, T = 120(2)K, $2\theta_{max}$ = 60.0º, 22941 reflections collected, 6611 unique (R_{int} = 0.0677). Final *GooF* = 0.891, *R1* = 0.0422, *wR2* = 0.0913, *R* indices based on 4114 reflections with I >2σ(I) (refinement on F^2), 307 parameters, 0 restraints. Lp and absorption corrections applied, μ = 0.093 mm^{-1}.

2.6 References

1. P. Scott and P. B. Hitchcock, *J. Chem. Soc.-Dalton Trans.*, 1995, 603-609.
2. A. M. DittlerKlingemann and F. E. Hahn, *Inorg. Chem.*, 1996, **35**, 1996-1999.
3. M. T. Albelda, E. Garcia-Espana, H. R. Jimenez, J. M. Llinares, C. Soriano, A. Sornosa-Ten and B. Verdejo, *Dalton Trans.*, 2006, 4474-4481.
4. C. Bazzicalupi, A. Bencini, A. Bianchi, A. Danesi, C. Giorgi and B. Valtancoli, *Inorg. Chem.*, 2009, **48**, 2391-2398.
5. A. Hossain, J. A. Liljegren, D. Powell and K. Bowman-James, *Inorg. Chem.*, 2004, **43**, 3751-3755.
6. P. S. Lakshminarayanan, I. Ravikumar, E. Suresh and P. Ghosh, *Inorg. Chem.*, 2007, **46**, 4769-4771.
7. P. D. Beer, P. K. Hopkins and J. D. McKinney, *Chem. Commun.*, 1999, 1253-1254.
8. J. M. Boon, T. N. Lambert, B. D. Smith, A. M. Beatty, V. Ugrinova and S. N. Brown, *J. Org. Chem.*, 2002, **67**, 2168-2174.
9. J. Kwak, A. D. Capua, E. Locardi and M. Goodman, *J. Am. Chem. Soc.*, 2002, **124**, 14085-14091.
10. H. Xie, S. Yi, X. Yang and S. Wu, *New J. Chem.*, 1999, **23**, 1105-1110.
11. R. Custelcean, B. A. Moyer and B. P. Hay, *Chem. Commun.*, 2005, 5971-5973.
12. D. A. Jose, D. K. Kumar, B. Ganguly and A. Das, *Inorg. Chem.*, 2007, **46**, 5817-5819.
13. M. de Loos, A. G. J. Ligtenbarg, J. van Esch, H. Kooijman, A. L. Spek, R. Hage, R. M. Kellogg and B. L. Feringa, *Eur. J. Org. Chem.*, 2000, 3675-3678.
14. C. E. Stanley, N. Clarke, K. M. Anderson, J. P. Lenthall and J. W. Steed, *Chem. Commun.*, 2006, 3199-3201.
15. D. K. Kumar, D. A. Jose, A. Das and P. Dastidar, *Chem. Commun.*, 2005, 4059-4061.
16. L. Applegarth, N. Clark, A. C. Richardson, A. D. M. Parker, I. Radosavljevic-Evans, A. E. Goeta, J. A. K. Howard and J. W. Steed, *Chem. Commun.*, 2005, 5423-5425.
17. R. Custelcean, P. Remy, P. V. Bonnesen, D. E. Jiang and B. A. Moyer, *Angew. Chem. Intl. Ed.*, 2008, **47**, 1866-1870.

18. B. Wu, J. J. Liang, J. Yang, C. D. Jia, X. J. Yang, H. R. Zhang, N. Tang and C. Janiak, *Chem. Commun.*, 2008, 1762-1764.
19. R. K. Mylavarapu, G. C. M. Kondaiah, N. Kolla, R. Veeramalla, P. Koilkonda, A. Bhattacharya and R. Bandichhor, *Org. Proc. Res. Dev.*, 2007, **11**, 1065-1068.
20. P. S. Lakshminarayanan, E. Suresh and P. Ghosh, *Inorg. Chem.*, 2006, **45**, 4372-4380.
21. P. Gans, *HypNMR 2006*, (2006) University of Leeds, Leeds.
22. P. S. Lakshminarayanan, I. Ravikumar, E. Suresh and P. Ghosh, *Chem. Commun.*, 2007, 5214-5216.
23. K. J. Winstanley, S. J. Allen and D. K. Smith, *Chem. Commun.*, 2009, 4299-4301.
24. C. Raposo, M. Almaraz, M. Martin, V. Weinrich, L. Mussons, V. Alcazar, C. Caballero and J. R. Moran, *Chem. Lett.*, 1995, 759.
25. A. Fan, H. K. Hong, S. Valiyaveettil and J. Vittal, *J. Supramol. Chem.*, 2002, **2**, 247-254.
26. D. R. Turner, B. Smith, A. E. Goeta, I. R. Evans, D. A. Tocher, J. A. K. Howard and J. W. Steed, *Cryst. Eng. Comm.*, 2004, **6**, 633-641.
27. C. L. Schauer, E. Matwey, F. W. Fowler and J. W. Lauher, *Mater. Res. Bull.*, 1998, 213-223.

3. Rigid Tripodal Anion Receptors

3.1 Aims

Pararosaniline, or Tris(4-aminophenyl)methanol, is a tripodal triamine that has seen use as a dye and biological staining agent.[1] thanks to its ability to form a highly coloured compound. Pararosaniline exists in a natural equilibrium between two forms (Figure 3.1), one a colourless neutral molecule possessing tetrahedral geometry, the other a highly coloured cationic form found at low pH. The colour arises from the high degree of conjugation present in the planar cation form.[2]

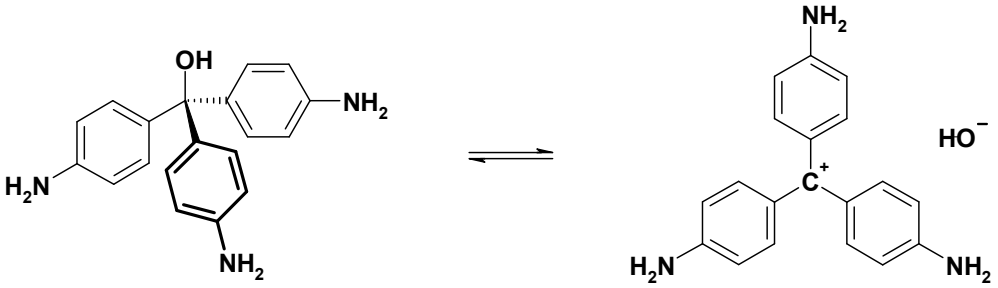

Figure 3.1 – The equilibrium between pararosaniline-OH and cationic form.

Ordinarily, this equilibrium lies strongly in favour of the colourless form, as evidenced by the presence of only the alcohol by ^{1}H-NMR spectroscopy. The observed pink colour of a solution of pararosaniline in a neutral medium are therefore likely due to minute quantities of the cationic form in the solution. Indeed addition of acid to a solution of pararosaniline significantly enhances the intensity of the colour, as detected by UV-Vis spectroscopy.[3]

Work on pararosaniline and related triphenylmethane has focussed on the phototropic behaviour of these dye compounds,[4] though as yet nothing has been reported on the use of pararosaniline as the basis for an anion receptor. It was therefore decided to incorporate pararosaniline as the core for a series of anion receptors, with the intent of utilising the high rigidity of the core to form a larger cavity binding site than earlier receptors, while simultaneously allowing for a visible response to the binding of anions with the innate colour of such receptors. A range of tripodal urea and thiourea tripods were synthesised from pararosaniline (Figure 3.2) by reaction of the triamine with the appropriate isocyanate or isothiocyanate. For the synthesis of **3.2**, the pyridine isocyanate was prepared in situ from reaction of nicotinic acid with diphenylphosphoryl azide, as described in chapter 2.

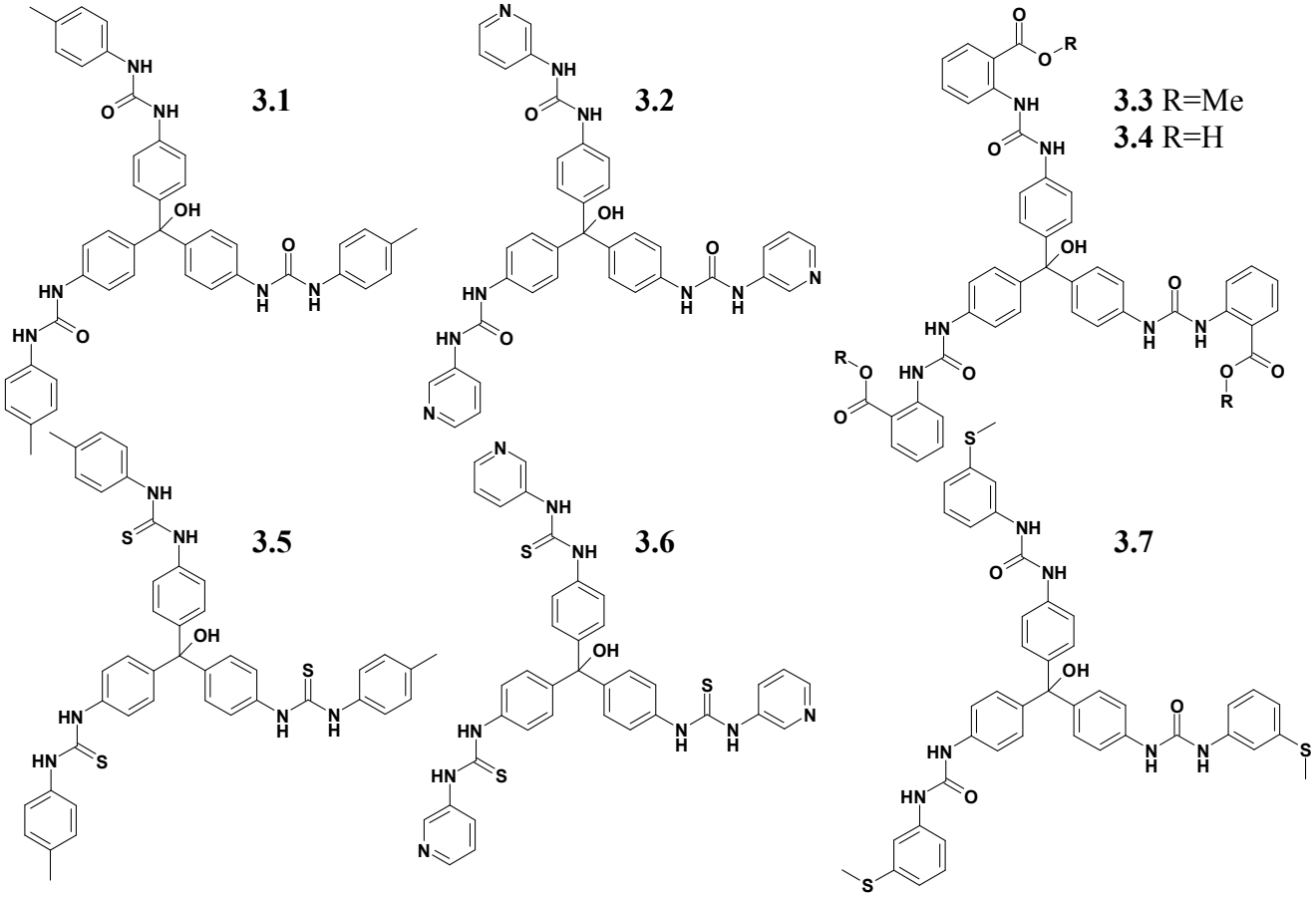

Figure 3.2 – Pararosaniline-based receptors prepared in this project.

Compound **3.1** was designed as a reference standard, in the same manner as the tren-based receptors, with **3.5** as the thiourea analogue. The others were designed with inbuilt metal-binding functionality, in the hopes that metal templation would occur. Considering that **3.2** is structurally related to the tolylureidopyridines studied by Turner and coworkers,[5] it was hoped that this receptor and its thiourea analogue **3.6** would behave in a similar manner to this simple pyridyl urea receptor compound. Receptor **3.3** can be converted to **3.4**, wherein the ester groups are hydrolysed to give carboxylic acid moieties, and it was intended that these carboxylic acid functionalities would also be able to complex to metals. Receptors such as **3.7**, containing methylsulphanyl moieties have proven to be effective at binding silver(I) cations,[6] thanks to the high affinity between sulphur and silver(I), so it was hoped that this receptor would provide a similar binding affinity and perhaps form expanded metal-templated assemblies.

Analysis of these tripods is fairly easy by ^{1}H NMR spectroscopy, as the core protons all show similar chemical shift values to each other when in the same solvent. The urea N-H resonances show some interesting trends depending on the nature of the end groups and the solvent present. For compound **3.1** in acetone, both occur at a shift of approximately 8 ppm, and are difficult to formally distinguish, since their environments are extremely similar. The same is true for **3.2**, although the chemical shift is higher (around 8.9 ppm), likely due to the solvent (DMSO) being more competitive than acetone and thus binding to the N-Hs groups. The N-H resonances in **3.5** are shifted even further ($\delta \sim 9.7$ ppm), due to the higher acidity of thiourea protons compared to urea protons. In only one of the above cases case do the urea N-Hs show greatly different shifts: **3.3** shows a difference of over one ppm between the N-H resonances. This is likely due to hydrogen bonding between the ester group and

the neighbouring N-H (b) which are well positioned to interact with one another (Figure 3.3). This will cause significant deshielding of the proton and give a much larger shift than the inner N-H (a), which does not engage in any intramolecular hydrogen bonding.

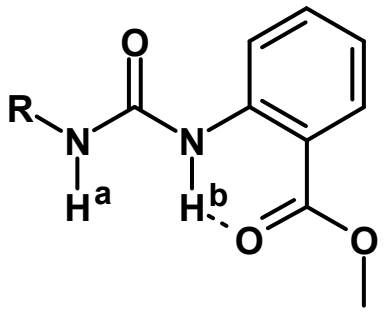

Figure 3.3 – Intramolecular hydrogen bonding between ester and urea N-H(b) in receptor **3.3**.

The intensity of the colour seems to be greatest in those tripods with *p*-tolyl endgroups. This may be due to the electron donating effects of the *p*-tolyl urea to the core chromophore, and the change in colour from the initial pink to blue/purple is likely caused by a decrease in the HOMO/LUMO transition energy - instead of absorbing blue light and giving a red colour, the ligand now absorbs lower energy red light to leave a blue colour. This suggests that **3.1**, **3.2**, and **3.5** are more able to cause a twist of the core away from its original conformation and thus break the conjugation pathway to an extent. By contrast, the aforementioned intramolecular hydrogen bonding interactions in **3.3/3.4** likely lead to an increase in the conjugation pathway and red-shift the colour observed.

(a)

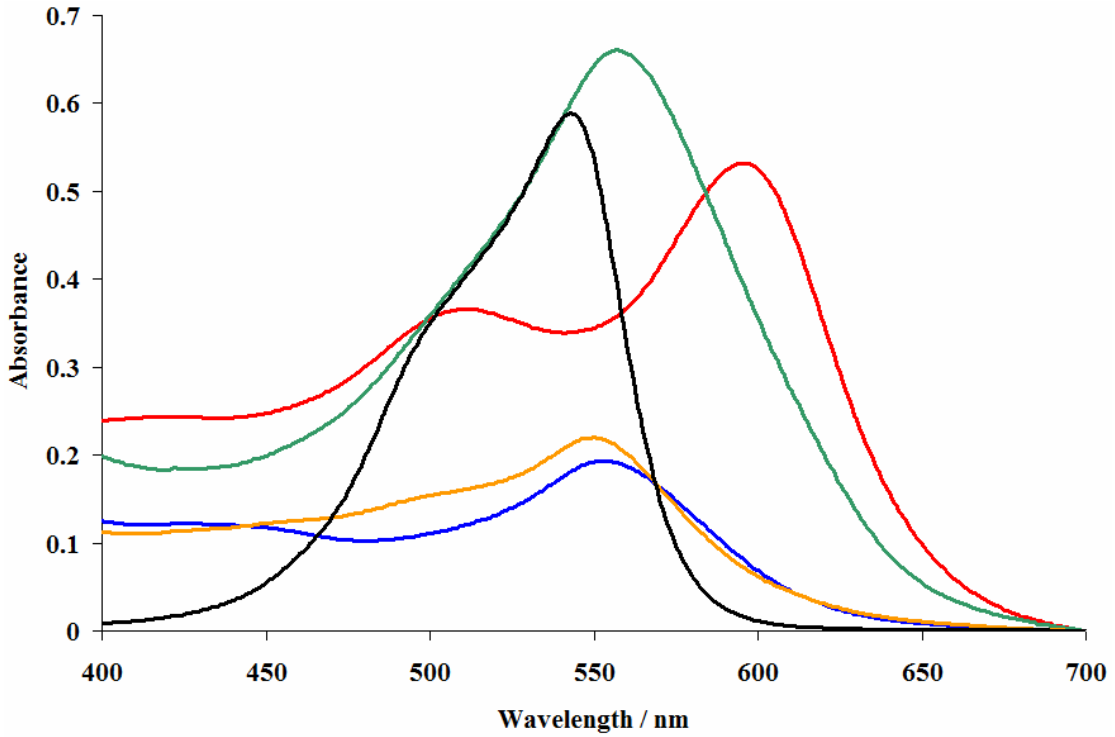

(b)

Figure 3.4 – (a) UV/Visible light absorption profiles of 5 x 10^{-4} moldm^{-3} solutions in DMSO of receptors **3.1** (red), **3.2** (green), **3.3** (blue), **3.7** (orange) and pararosaniline (black); (b) Vials containing (left to right) **3.1**, **3.2**, **3.5**, **3.6**, **3.7**, and **3.3** at the same concentration and solvent system.

It was noted that solutions of **3.1** gradually change in colour over a period of time, changing from the deep blue to a purpler colour. Following this change by UV/Visible spectroscopy revealed a significant change in the absorption profile

(Figure 3.5). The major absorbance at 595 nm, attributed to $\pi \rightarrow \pi^*$ transfer, initially remains fairly constant, with the second band at 511 nm growing along with a new absorbance band at 544 nm becoming increasingly significant over the first day. After this time, the absorbances at both 595 and 511 nm are found to decrease, leaving the new 544 nm band as the strongest absorption.

(a)

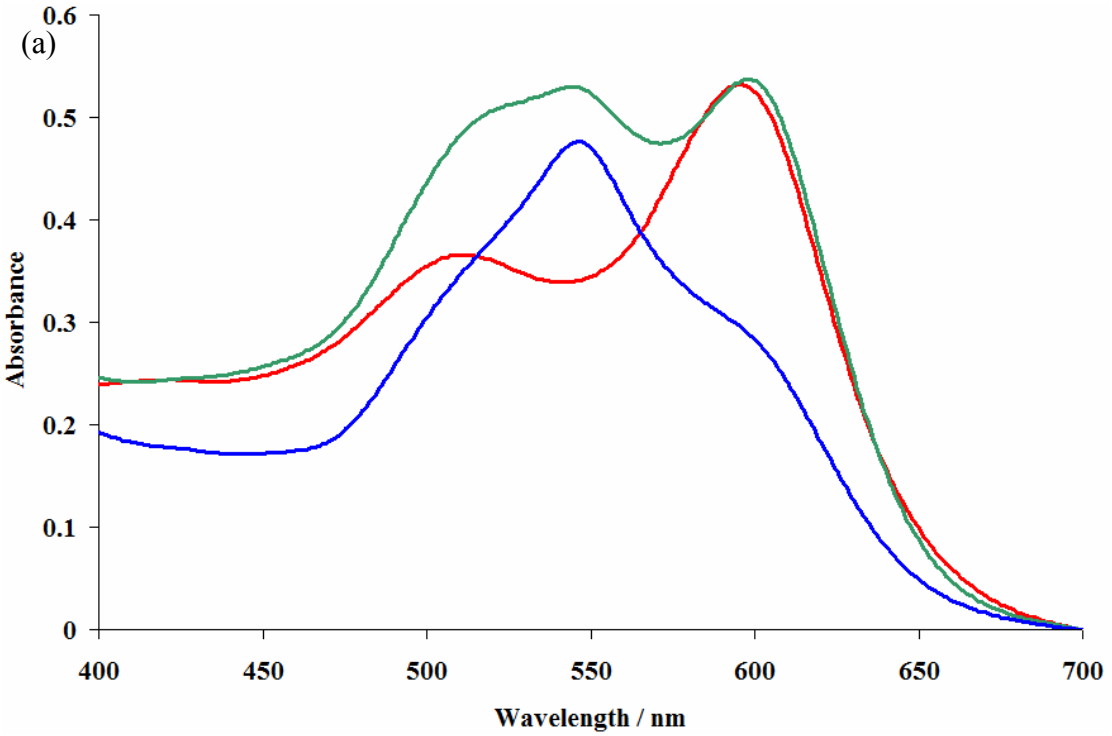

(b)

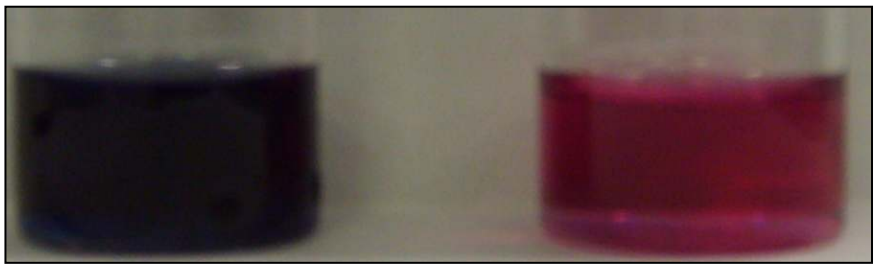

Figure 3.5 – (a) UV/Visible absorbance spectra of **3.1** at t = 0 (red), t = 1 day (green), and t = 7 days (blue) at 5 x 10^{-4} moldm^{-3} concentration in 10% DMSO in acetone. (b) vials containing the solutions t = 0 (left) and t = 7 days (right).

The cause for this change is not fully understood – evidence exists that pararosaniline undergoes a photochemically induced change upon absorption of UV radiation,[3] leading to formation of an increased quantity of the ionic form in solution, but this process is reversible by the exclusion of light and converts between colourless and coloured forms. No change in the absorbance wavelength is observed, only the intensity of the absorbance. By contrast, solutions of **3.1** undergo a permanent change in colour that is not reversed or even slowed by keeping the solution in the dark. It has also been suggested that pararosaniline undergoes photochemical degradation,[7] although this process irreversibly destroys the dye compound. No change in the ^{1}H-NMR spectrum is observed between the blue and purple solutions, suggesting that it is an effect purely associated with the cationic form, present in small amounts, and is probably not due to a degradation of the compound. Inclusion of anions such as chloride, sulphate or tosylate to the solution, particularly in the presence of acid is found to increase the rate of the change significantly with the change taking place over a matter of minutes rather than days, although removing the anion/acid does not reverse the colour change.

3.2 Anion Binding (Alcohol) by ^{1}H-NMR Spectroscopic Methods

Initially, the anion binding properties of the alcohol forms were assessed. Since the cationic forms of all of the receptors were not detectable in the ^{1}H-NMR spectra due to the equilibrium lying far to the alcohol form at neutral pH, it was determined that use of ^{1}H-NMR spectroscopic titrations was a valid technique to use for the determination of binding constants, since even at excess the presence of anions did not lead to the generation of any detectable quantity of the cation form. Titrations were carried out using a similar manner to those detailed in the previous chapter, and acetone-d_6 was chosen as the solvent. Considering the relatively high concentrations used in these experiments, the very low solubility of receptor **3.2**, and the thiourea receptors **3.5** and **3.6** precluded them from this study. Titration curves and refined binding constants are shown below (Figures 3.6 – 3.8, Tables 3.1 – 3.3).

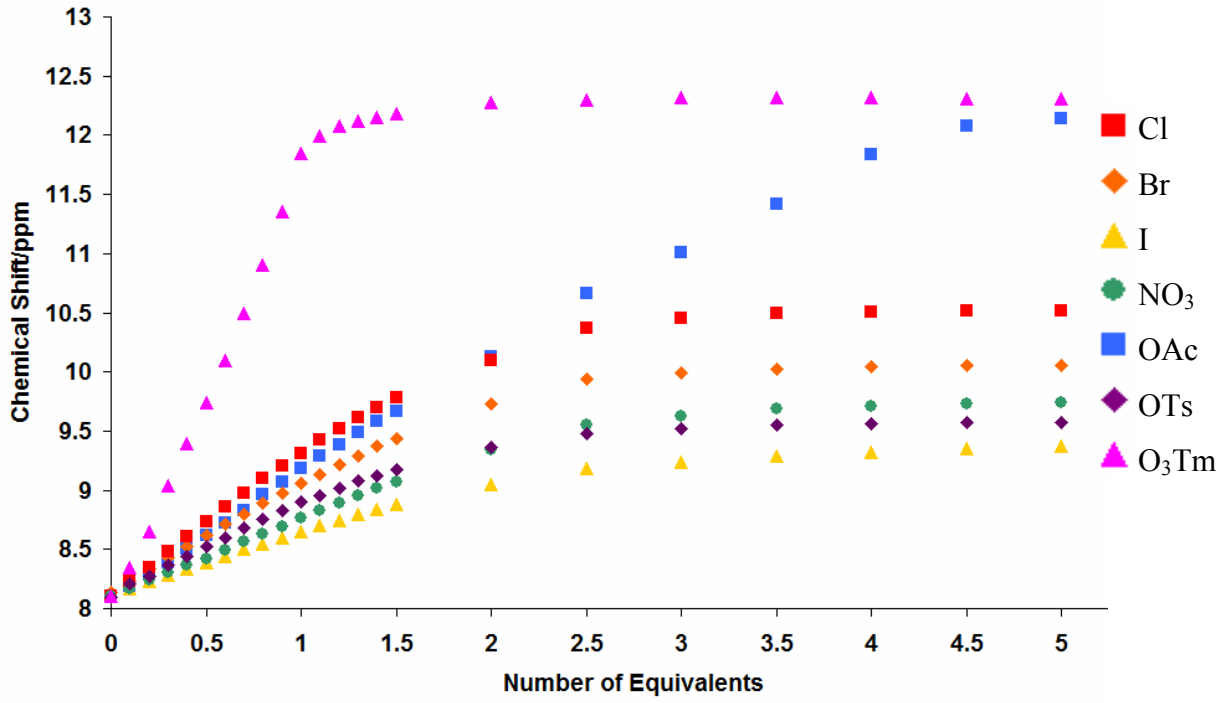

Figure 3.6 – ^{1}H-NMR titration curves for urea protons in **3.1** with a variety of anions. Both isotherms display similar shifts and curvature.

Guest	β_1	β_{12}	β_2	β_{13}	β_3
Chloride	3.61(1)	6.37(5)	2.76	9.01(5)	2.64
Bromide	2.77(1)	5.56(6)	2.79	7.60(8)	2.04
Iodide	1.76(1)	3.98(3)	2.22	N/A	N/A
Nitrate	2.91(6)	4.96(4)	2.05	N/A	N/A
Acetate*	4.07(1)	6.72(1)	2.65	8.66(3)	1.94
Tosylate	2.57(1)	4.89(1)	2.32	N/A	N/A
Trimesylate	4.2(1)**	N/A	N/A	N/A	N/A

Table 3.1 – β values for receptor **3.1**.

(* Also refined a 1:4 constant with β = 12.75(1) (β_4 = 4.09); **Requires inclusion of a 2:1 complex with β_{21} determined as 6.2(1) (β = 2.0).)

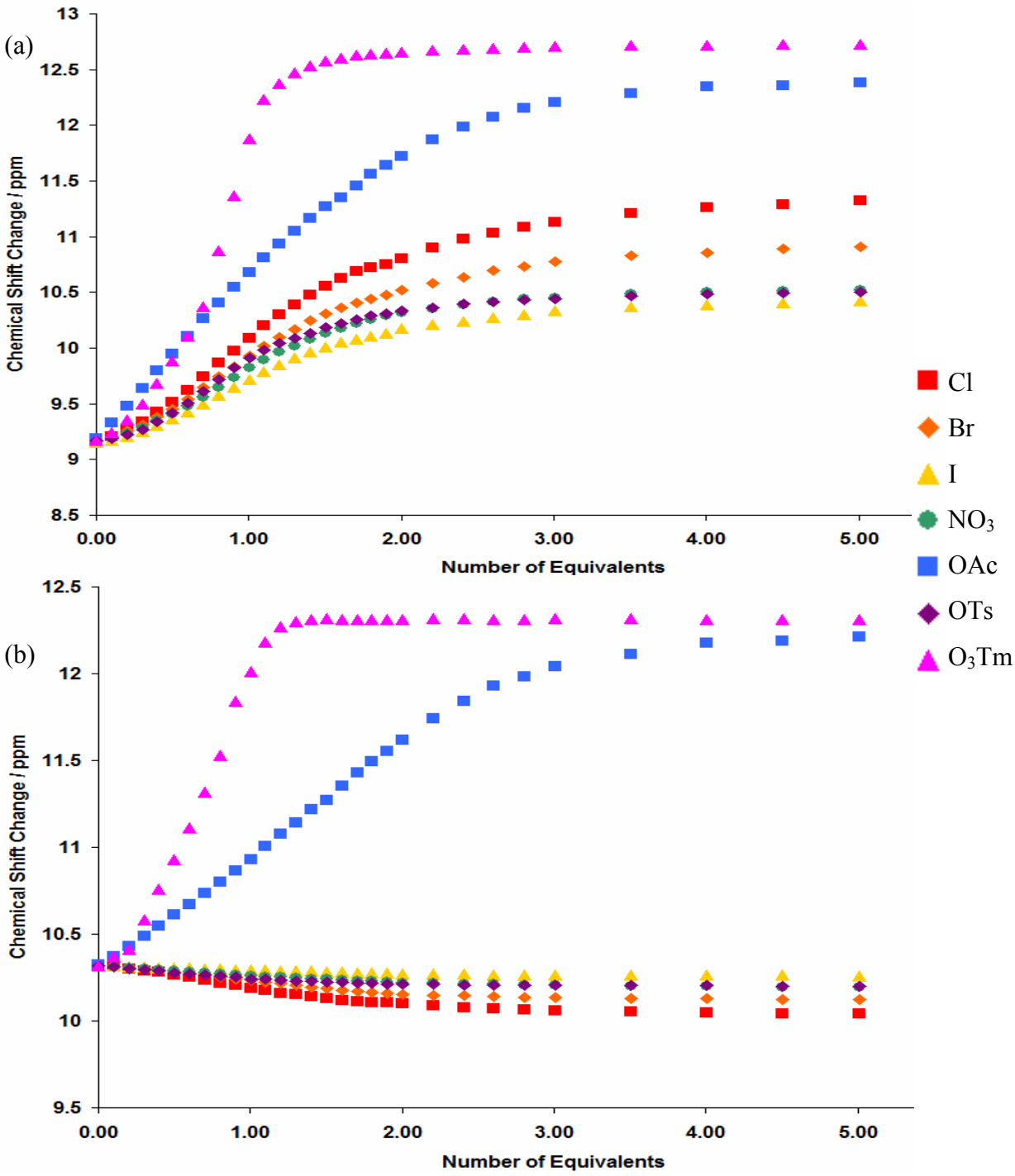

Figure 3.7 – ^{1}H-NMR titration curves for NH(a) and NH(b) (Figure 3.3) protons in **3.3** with a variety of anions.

Guest	β_1	β_{12}	β_2	β_{13}	β_3
Chloride	3.31(1)	5.34(1)	2.03	7.01(4)	1.67
Bromide	3.03(1)	4.90(1)	1.87	N/A	N/A
Iodide	2.58(4)	4.20(9)	1.62	N/A	N/A
Nitrate	2.99(1)	5.15(1)	2.16	N/A	N/A
Acetate	3.66(1)	6.65(4)	2.99	9.04(4)	2.39
Tosylate	3.16(3)	5.00(2)	1.84	N/A	N/A
Trimesylate	3.46(6)	N/A	N/A	N/A	N/A

Table 3.2 – β values for receptor **3.3**. All experiments refined with a self-association of $\beta_{20} = 1.5$, to model intramolecular binding, thus all values of β in the above table include this additional value. The inclusion of this additional constant was determined by dilution studies of the receptor following the appropriate resonance.

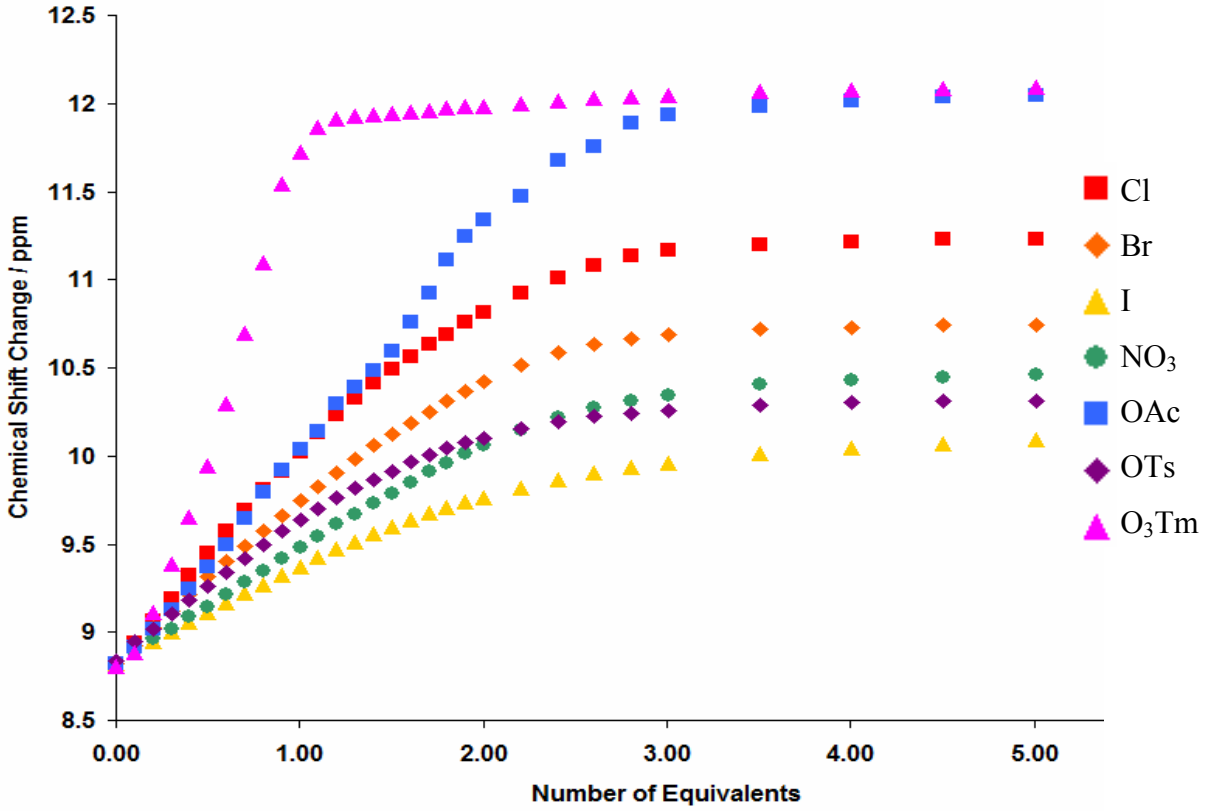

Figure 3.8 – ^{1}H-NMR titration curves for urea protons in **3.7** with a variety of anions. Both isotherms display similar shifts and curvature.

Guest	β_1	β_{12}	β_2	β_{13}	β_3
Chloride	3.70(3)	6.41(5)	2.71	9.00(6)	2.59
Bromide	1.69(1)	4.85(5)	3.16	6.09(5)	1.24
Iodide	1.86(1)	3.96(5)	2.1	N/A	N/A
Nitrate	2.97(8)	4.96(6)	1.99	N/A	N/A
Acetate	2.95(2)	6.44(3)	3.49	9.2(1)	2.76
Tosylate	3.77(8)	5.96(7)	2.19	N/A	N/A
Trimesylate	4.50(7)*	N/A	N/A	N/A	N/A

Table 3.3 – β values for receptor **3.7**.

(*Requires inclusion of a 2:1 complex with β_{21} calculated at 6.7(1) (β = 2.2).)

Binding with the receptors seems to confirm that the core is too rigid to allow for the folding around an anion observed with tren-based receptors, as binding occurs as if the receptor were three independent binding groups. Binding to most anions shows evidence of a 1:1, 1:2 and 1:3 host:guest species, as evidenced by the steady shift to higher ppm of the urea protons up to three equivalents of anion added. Strangely, bromide (and in some cases iodide) actually show a second binding event is more likely after the first has taken place, with the second binding constant being higher than the first. Perhaps binding to a larger, more weakly interacting anion causes a rearrangement of the receptor that favours binding to a second anion. In contrast to this, binding to the smaller chloride anion seems to suggest that there is no interaction between binding sites in this case, with the three binding constants being fairly similar in magnitude, although they are lower than the anion affinities for similar monodentate receptors.[8]

Interesting results were found for acetate, sulphate and trimesylate. With acetate, **3.1** shows strong evidence of a further complex, as the urea protons continue to experience shifting even after 3 equivalents of guest are added, with no curvature evident until after four equivalents have been added, whereupon the shift levels off suddenly. This presence of a 1:4 host:guest complex is accompanied by a change in colour of the solution being observed beyond three equivalents (Figure 3.9), and a corresponding disappearance of the alcohol OH, suggesting some interaction between the OH and the additional acetate, possibly deprotonation of the OH proton by basic acetate or perhaps loss of the OH to give a coloured $[\mathbf{3.1}(OAc)_4]^{3-}$ complex of the cation of **3.1**. This fourth acetate complexation appears to be strongly favoured by addition of the first three equivalents, as the fourth β value is significantly higher, and may reinforce the idea that the receptor is being deprotonated.

Figure 3.9 – 5 x 10^{-4} $moldm^{-3}$ solutions of **3.1** with increasing quantities of acetate (TBA salt) added – left to right: 1.0 equiv.; 2.0 equiv.; 3.0 equiv.; 4.0 equiv.; 5.0 equiv.

Interestingly, this effect is not observed for **3.3** or **3.7**, and seems to be specific to **3.1**. Both **3.3** and **3.7** show evidence of only three equivalents of acetate binding to the receptors. Job plot analysis of the receptor:acetate complexation process suggests that the favoured complexation mode is 1:2 (Figure 3.10) for all of the receptors, though again it may be the case that this is simply the most likely binding mode at the concentration of the experiment, or possibly a combination of 1:1, 1:2 and 1:3 complexation averaging out.

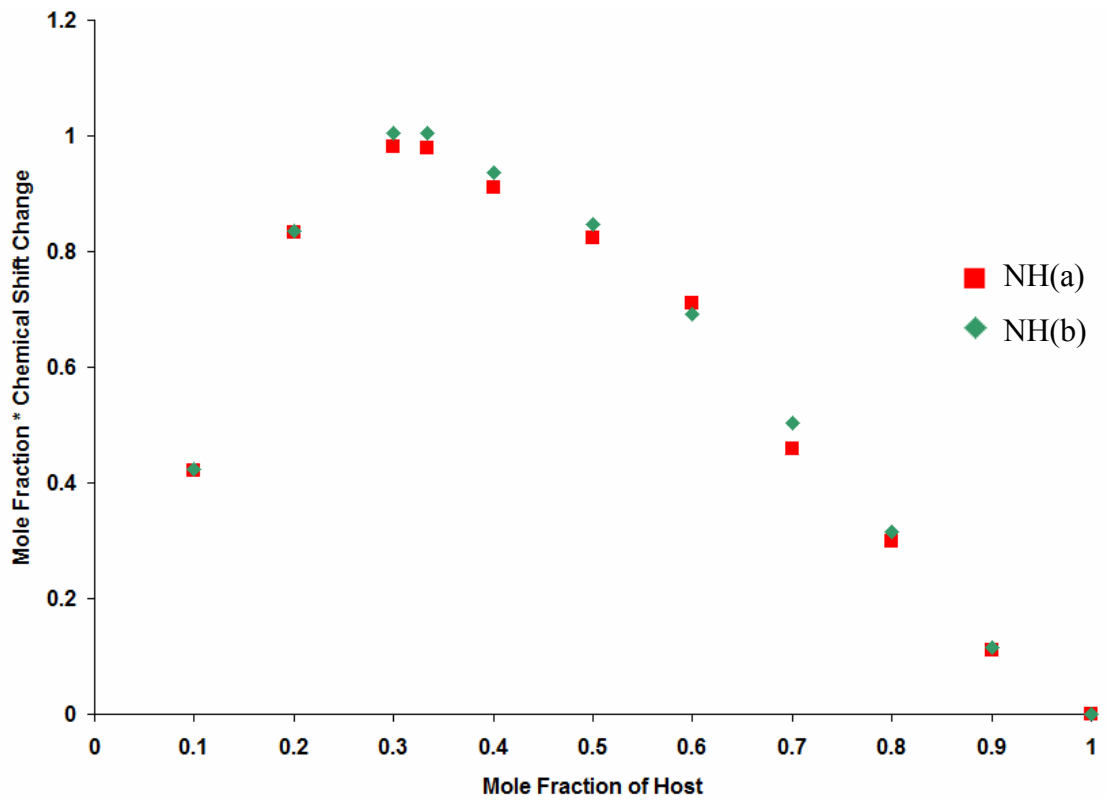

Figure 3.10 – Typical Job plot for receptors **3.1**, **3.3** and **3.7** with acetate.

Trimesylate (1,3,5-benzenetricarboxylate, abbreviated to O_3Tm^{3-}) shows evidence pointing to a large 1:1 interaction between host and guest. It was hoped that the larger size and similar C_3 symmetry of the trianion would make for a good match with the host, and indeed this seems to be the case. Binding to trimesylate brings a dramatic change in the ^{1}H-NMR spectrum of the host, with saturation of the receptor occurring after 1 equivalent of guest has been added, showing the excellent affinity and selectivity of all of the receptors for trimesylate. Signals corresponding to urea protons were observed to broaden over the course of the titration due to the increased exchange rate of the N-H protons caused by strong binding to the anion.

Sulphate and phosphate were found to cause precipitation of the receptor from solution almost immediately upon addition. After addition of only 0.3 equivalents, it

became almost impossible to distinguish the receptor peaks in the NMR spectrum, as a significant quantity was no longer in solution. This suggested that binding to these anions was occurring, and perhaps in a different manner to other anions.

During the Job plot analysis of receptor **3.1**, it was suggested that the favoured binding mode of **3.1** with chloride was not the expected 1:3 complex, but rather formation of a 2:3 host:guest species is preferred (Figure 3.11).

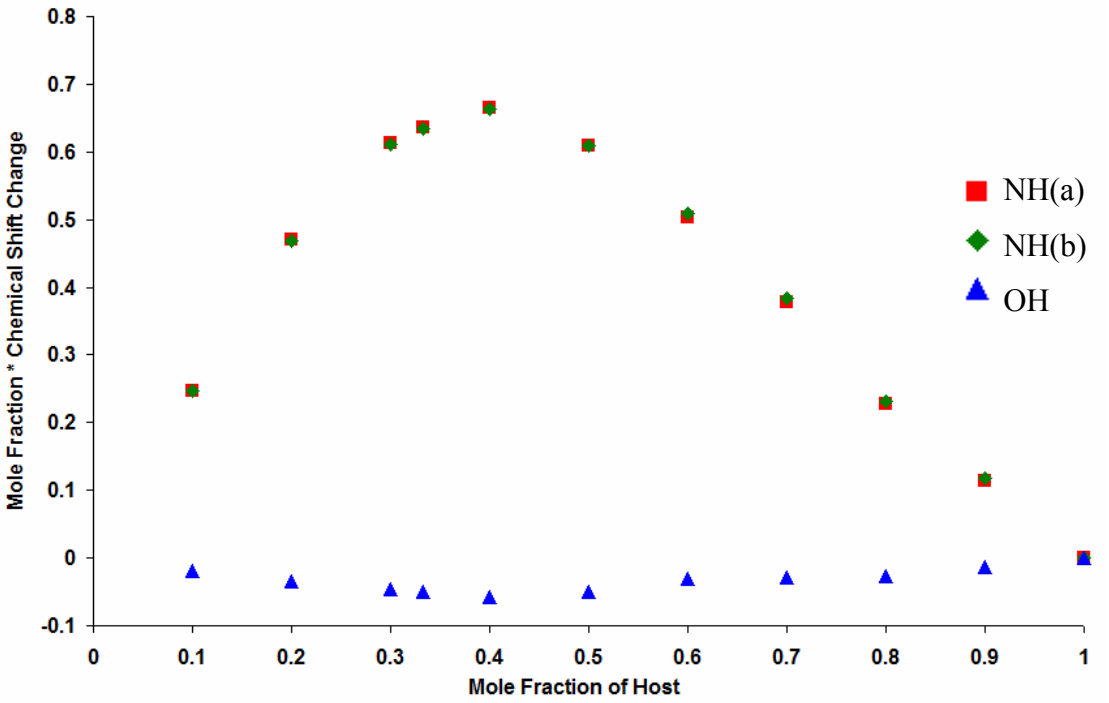

Figure 3.11 – Job plot for **3.1** with chloride.

Considering the rigid, tripodal shape of the receptor, combined with the tetrahedral geometry around the central carbon atom, it is attractive to consider the formation of a self-assembled capsule, with two receptor molecules bound together by three bridging chlorides, bound via hydrogen bonding through the urea groups. Proving the existence of such a capsule is difficult however – the Job plot may be showing a favoured binding mode between 1:1 and 1:2, and the titration data is found to fit equally well with or without inclusion of a 2:3 binding mode, although a small signal

(~25% abundance) in the negative-ion MS at m/z 505.3 corresponding to a possible $[(\mathbf{3.1})_2Cl_3]^{3-}$ complex is present. Attempts to prove the presence of a larger capsule by diffusion spectroscopy (DOSY) proved inconclusive. Computational modelling of such a complex (Figure 3.12) suggests that it is physically possible, with the two receptor molecules stacking in a staggered manner due to the twist in the arms. With the lack of deeper evidence it is not yet possible to definitively prove the existence of such a species.

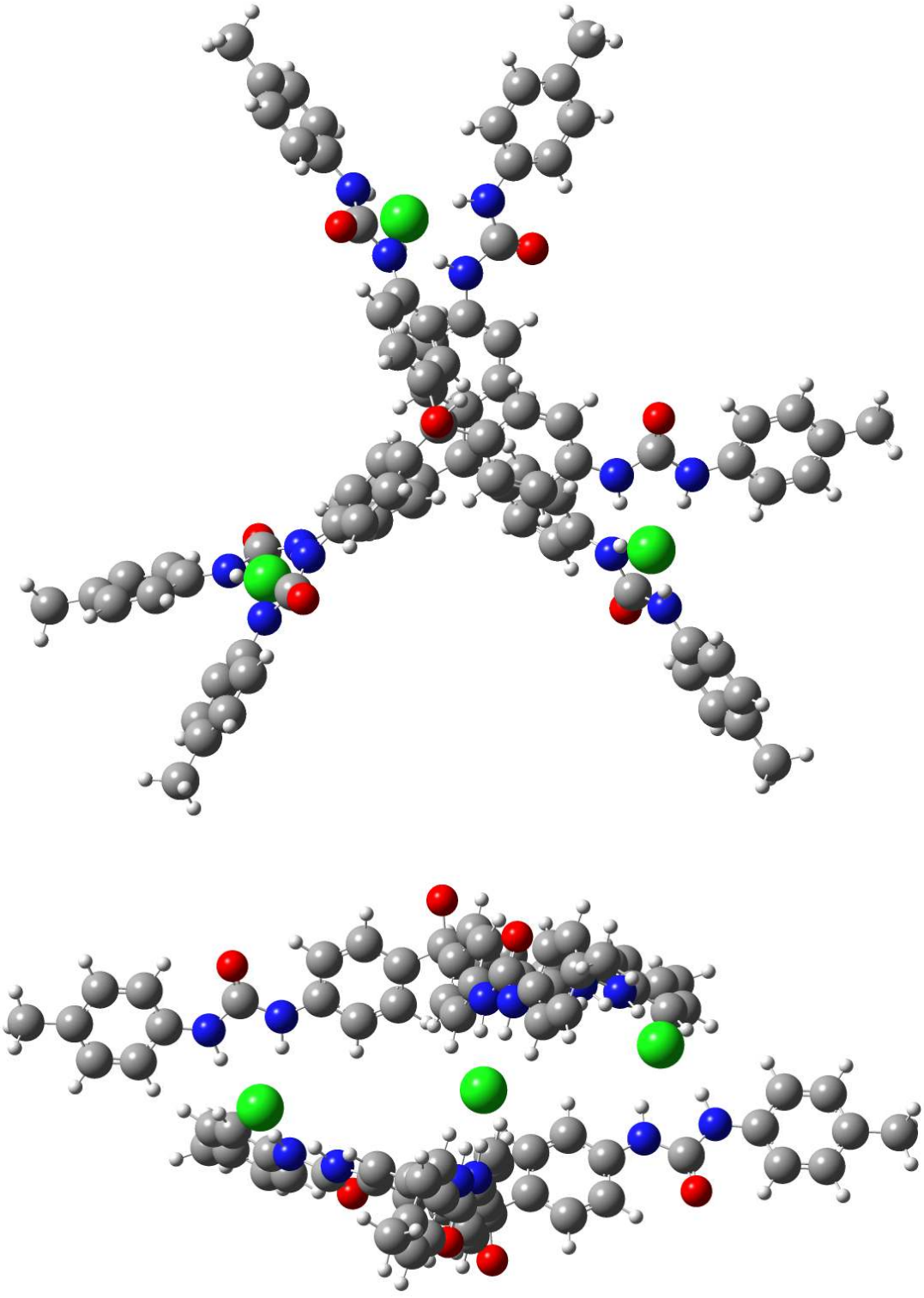

Figure 3.12 – Energetically minimised computational model of the $[(\mathbf{3.1})_2Cl_3]^{3-}$ complex (top view and side view), calculated using HF/STO3G level of theory.

3.3 pH Equilibrium Studies

Concentrations of 5 x 10^{-4} moldm^{-3} of solutions of the receptors are required to provide a suitable visible colour to the solutions, but this is due to the high tendency of pararosaniline compounds to remain in the alcohol form at neutral pH. As discussed is section 3.1, addition of H^+ species leads to loss of the alcohol OH and shifts the equilibrium towards the coloured cationic form. Addition of H^+ to a 5 x 10^{-4} moldm^{-3} solution of any of the receptors gives a dramatic increase in the colour intensity, leading rapidly to saturation of the spectrophotometer. In order to test the actual response to acid addition, much lower concentrations of receptor were used (1 x 10^{-5} moldm^{-3}). At this concentration, no visible colour is observed initially for any receptor. In order to minimise interference from counter ions, HBF_4 was used as the acid, generating the receptor$^+BF_4^-$ salt which could be used for anion binding studies. Initially, titration of a solution of HBF_4 in acetone into the solution of ligand was monitored by UV/Visible spectroscopy and after each addition of acid the pH of the solution was checked. The result showed that at around 10 equivalents (found to be pH 1.0) the colour is switched on drastically (Figure 3.13).

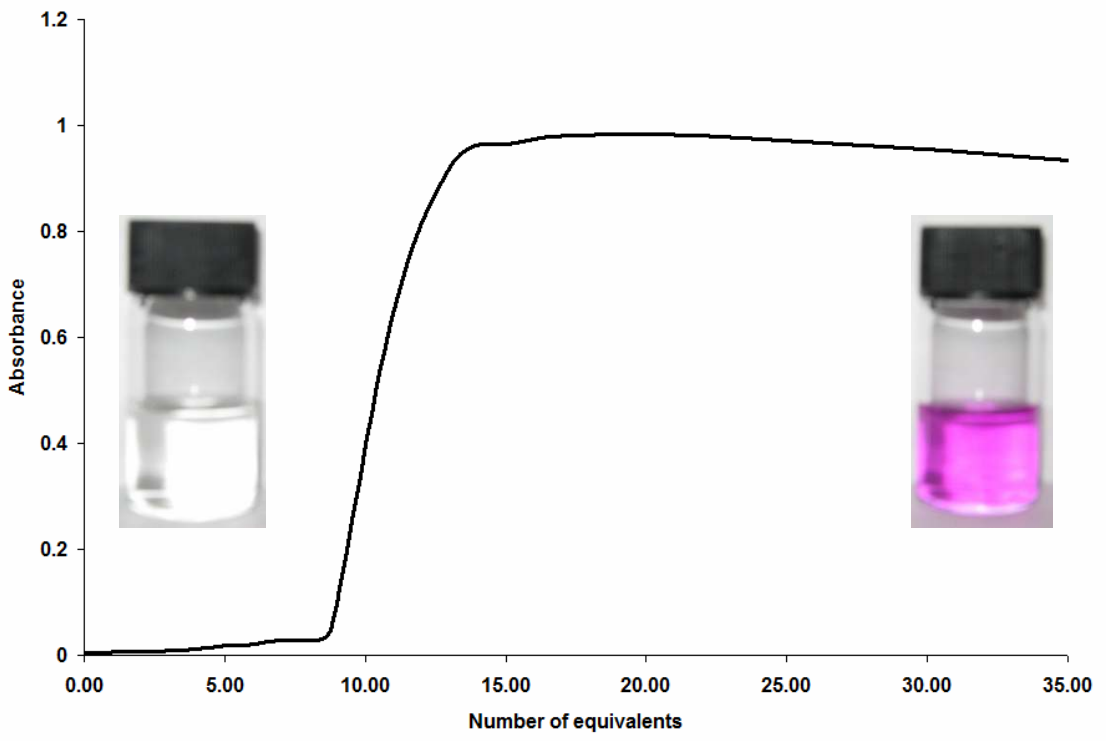

Figure 3.13 – Absorption profile of **3.1** at 556 nm wavelength with addition of HBF_4 solution with vials containing the solutions to show the colour difference.

It is interesting to note that the rate of change from colourless to coloured form is quite slow. Adding 9-10 equivalent measures to the solution causes a very gradual darkening of the colour, taking approximately 10-20 seconds from initial addition of the acid. Adding more equivalents of acid (15+) causes the change to occur more rapidly.

This colour change is reversible, and adding base to increase the pH back above 1 switches off the colour once again. This on-off change with pH is repeatably reversible, with continual additions of acid and base switching on and off the colour repeatedly, as shown in Figure 3.14.

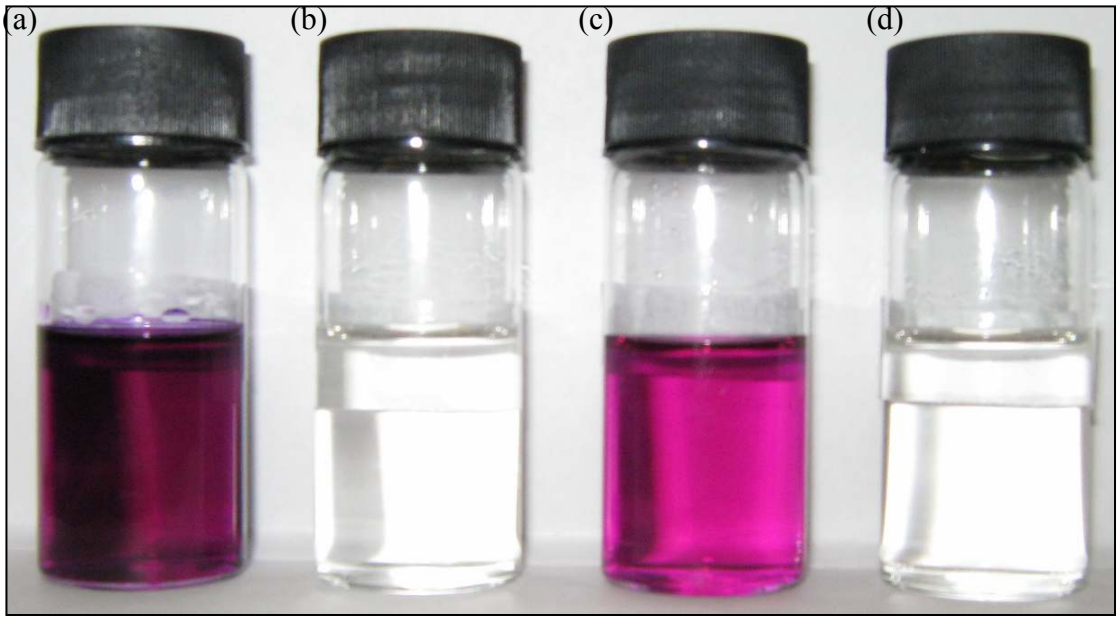

Figure 3.14 – (a) **3.1** acidified to pH 1 with HBF_4; (b) Solution (a) basified to pH 7 with NEt_3; (c) Solution (b) reacidified to pH 1 with additional HBF_4; (d) Solution (c) rebasified to pH 7 with additional NEt_3. Differences in intensity between (a) and (c) due to lower overall concentration of receptor.

Changing the acid from the weakly-coordinating tetrafluoroboric acid to the more strongly coordinating hydrochloric acid shows a detectable difference in the UV/Visible absorbance of the resulting solution (Figure 3.15), showing that coordination of an anion has an effect on the cation of the receptor as well as the neutral alcohol form.

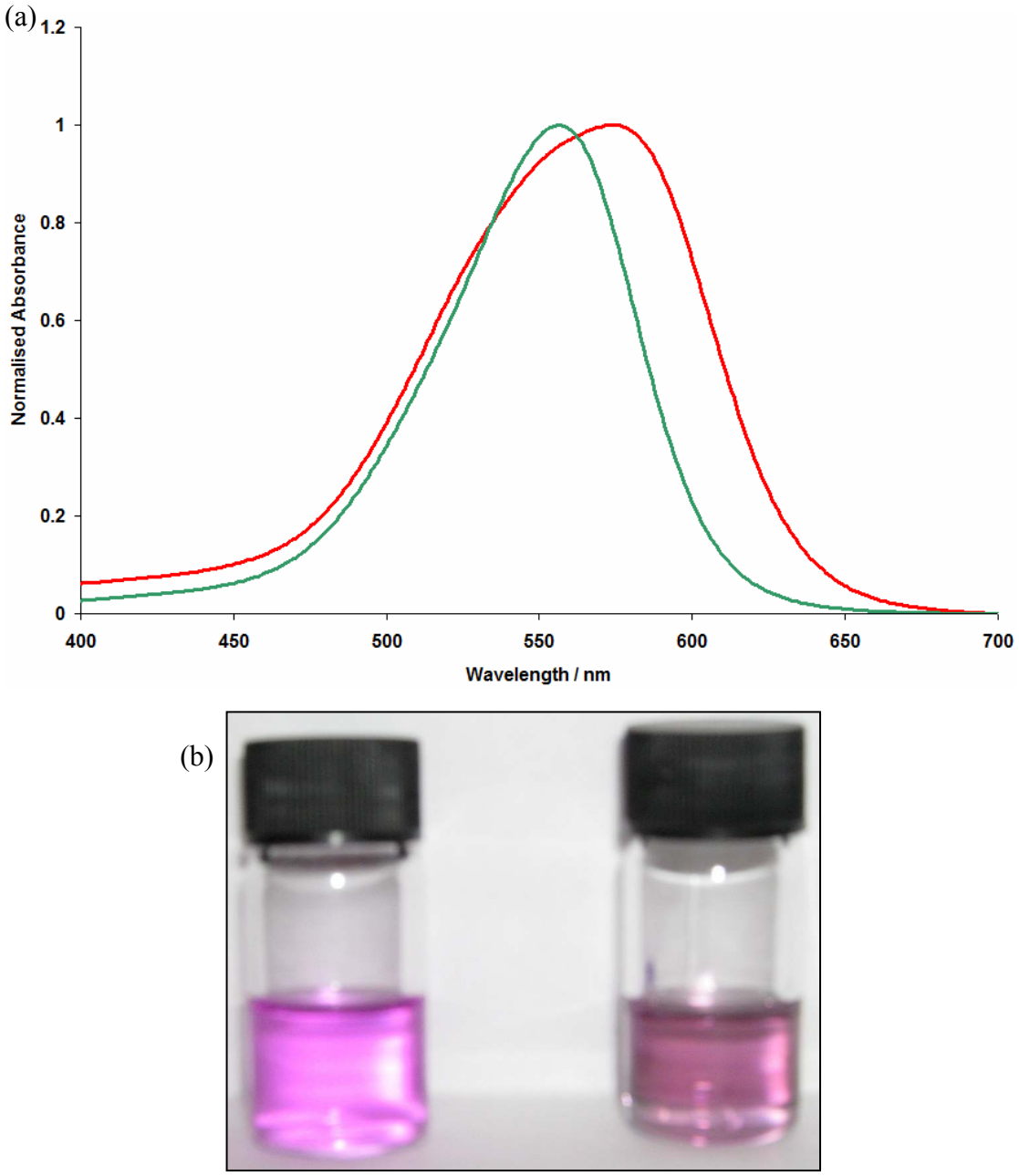

Figure 3.15 – (a) Normalised UV/Visible absorbance spectra for **3.1** in the presence of a 35-fold excess of HBF_4 (green line) and HCl (red line), and (b) vials containing the solutions – **3.1** + HBF_4 (left) and **3.1** + HCl (right).

Addition of a range of anions to the acidified solution has a noticeable effect on the presence and intensity of the colour, as shown in Figure 3.16. More basic anions, such as acetate, are more effective at increasing the pH by gathering up excess protons and so can switch the colour back off, while less basic anions are more likely to interact with the receptor instead of the acid and so are seen to shift the colour of the solution. Similarly, weakly coordinating anions such as iodide and nitrate, which do not interact strongly with the receptor, are seen to behave in a manner similar to acetate and switch off the colour.

Figure 3.16 – 1 x 10^{-5} moldm^{-3} solutions of **3.1** at pH 1 in presence of (left to right): Cl^-; Br^-; I^-; NO_3^-; OAc^-; OTf^-; OTs^-; HSO_4^-.

A number of interesting effects are observed on shifting the equilibrium from the neutral alcoholic form to the cationic form. Generally, solubility improves for the cationic form, with most of the urea receptors dissolving more completely in acetone. Most impressive in the solubility change is the pyridyl-appended **3.2**, which changes from having one of the lowest solubilities of the range of receptors to being fully soluble in aqueous media upon acidification, as shown in Figure 3.17.

Figure 3.17 – 1 x 10^{-5} $moldm^{-3}$ solutions of **3.2** in H_2O at pH 1 (left) containing HBF_4 and pH 7 (right) containing HBF_4 and NEt_3.

This dramatic change is attributed to protonation of the pyridyl groups in addition to loss of the alcohol OH, generating an easily-solvated tetracation. This dissolution is reversible, again by addition of base to increase the pH, although regeneration of the colourless alcohol form in water is impossible, as removal of the more acidic pyridinium protons causes precipitation of the $[receptor\text{-}OH]^+$ species as the salt of whichever acid was used initially (BF_4 in the case above).

3.4 Anion Binding (Cation) by UV/Visible Spectroscopic Methods

In order to compare the anion binding capabilities of the cationic form of the receptors with the neutral forms, separate studies were carried out. NMR spectroscopic studies proved difficult due to the higher concentration demanding much more acid present, leading to a poorly defined spectrum, with broad signals and noise. Due to the colour, UV/Visible spectroscopy was deemed a better method, though because of this it is important to make the distinction that the differences in concentration is likely to make direct comparison of binding constants meaningless. Instead, comparison of trends between binding modes and relative strengths of binding will be considered.

Typically, the binding experiments were carried out at a receptor concentration of 1 x 10^{-5} moldm^{-3} using acetone as a solvent. In each titration experiment, 3 ml of a stock solution of each receptor was pipetted into a UV cuvette using a 1 ml accurate syringe. A stock solution of HBF_4 in acetone was made such that 5 µl of acid solution was equal to 15 equivalents of acid and this amount was added to the cuvette for each experiment. Titration of a guest solution into the cuvette followed by collection of a UV/Visible profile for each addition showed the change in the absorbance of the receptor upon binding. Titration plots were collected and are summarised below (Figures 3.18 – 3.20). Binding constant data was refined using the SpecFit32 software[9] where possible.

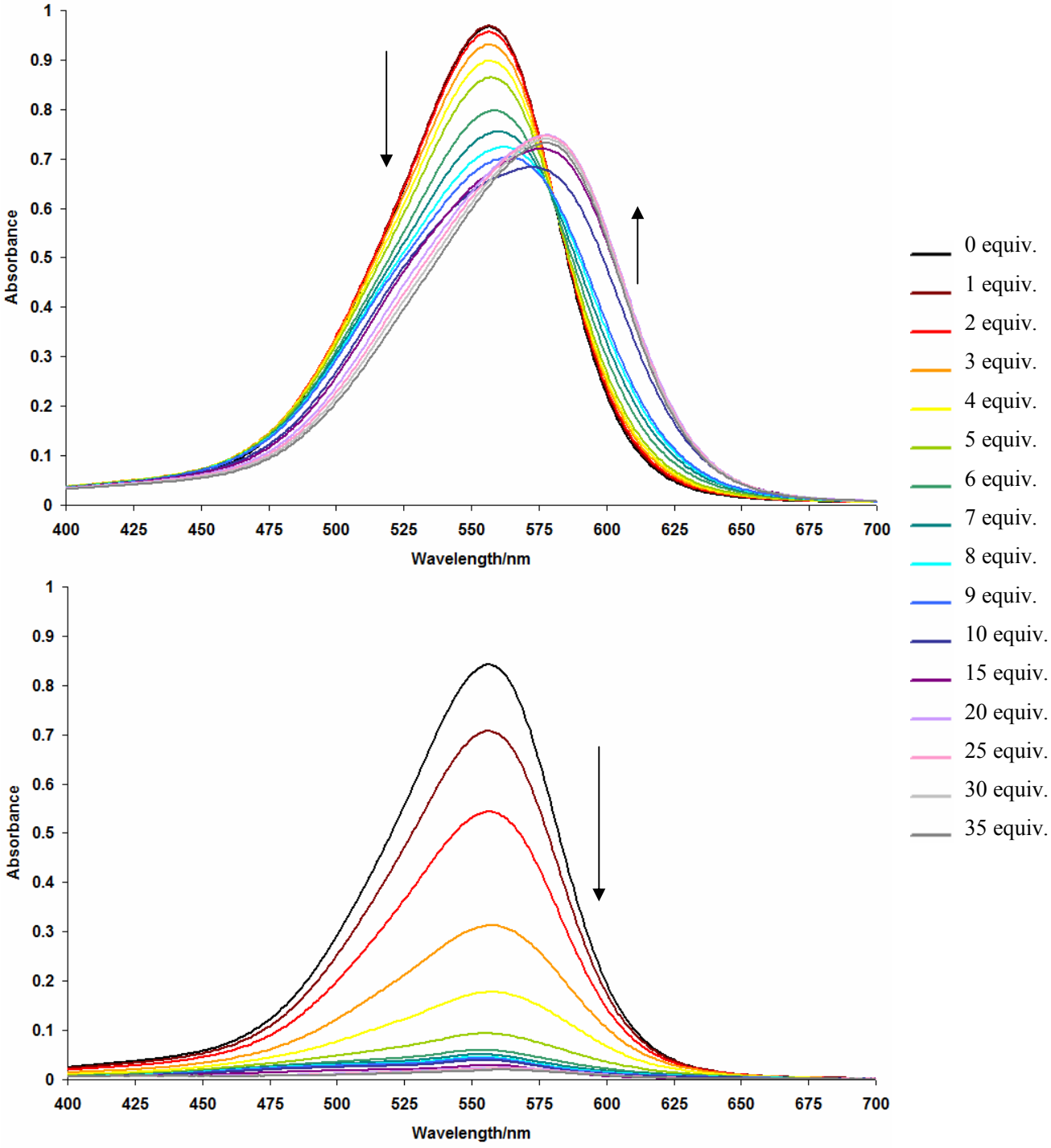

Figure 3.18 – UV/Vis spectroscopic titration plots for 1 x 10^{-5} moldm^{-3} solutions of **3.1** with (top) chloride and (bottom) acetate in acetone, initial pH of 1.

Addition of anions to acidified solutions of **3.1** typically followed one of the two trends shown above (Figure 3.17). Either the receptor absorbance shows a red shift to a higher wavelength, or it shows a drop in intensity as the equilibrium shifts back to the neutral alcohol form. Chloride shows the greatest red shift at 20 nm, followed by bromide at 15 nm. Of those anions that reduce the intensity of the absorbance, acetate and nitrate both show a strong effect, almost completely eliminating the coloured form after addition of only five equivalents. This is the point of the acidity curve at which the pH rises above 1, determined by recording the pH at and around this point, and is thus due to the anion preferentially interacting with acid protons over the receptor. Trifluoromethane sulphonate (Triflate, OTf) shows no binding to the receptor or the acid, and simply exhibits a linear decrease in absorbance intensity due to dilution. Iodide exhibits a similar behaviour to other halides, showing a small red shift (7 nm) in the absorbance, while also reducing the intensity of the band in a similar manner to triflate. This suggests that iodide is able to bind to the receptor, but does not help to stabilise the cationic form in the same way as the smaller and better bound chloride and bromide. Hydrogen sulphate interacts similarly, but exhibits a larger red shift (13 nm) and seems able to stabilise the cation to a degree, since dilution effects on the absorbance band are almost negated. Most interesting is the interaction between the receptor and *p*-tolyl sulphonate (tosylate, OTs), which despite being ordinarily a poorly bound anion shows a remarkable effect on the receptor colour, with a strong increase in intensity and a modest (14 nm) red shift observed (Figure 3.19). The intensity increase is attributed to the likely presence of trace quantities of *p*-tolyl sulphonic acid in the TBA salt, perhaps combined with the fairly high complementarity between the *p*-tolyl groups of both the host and anion making complexation favourable.

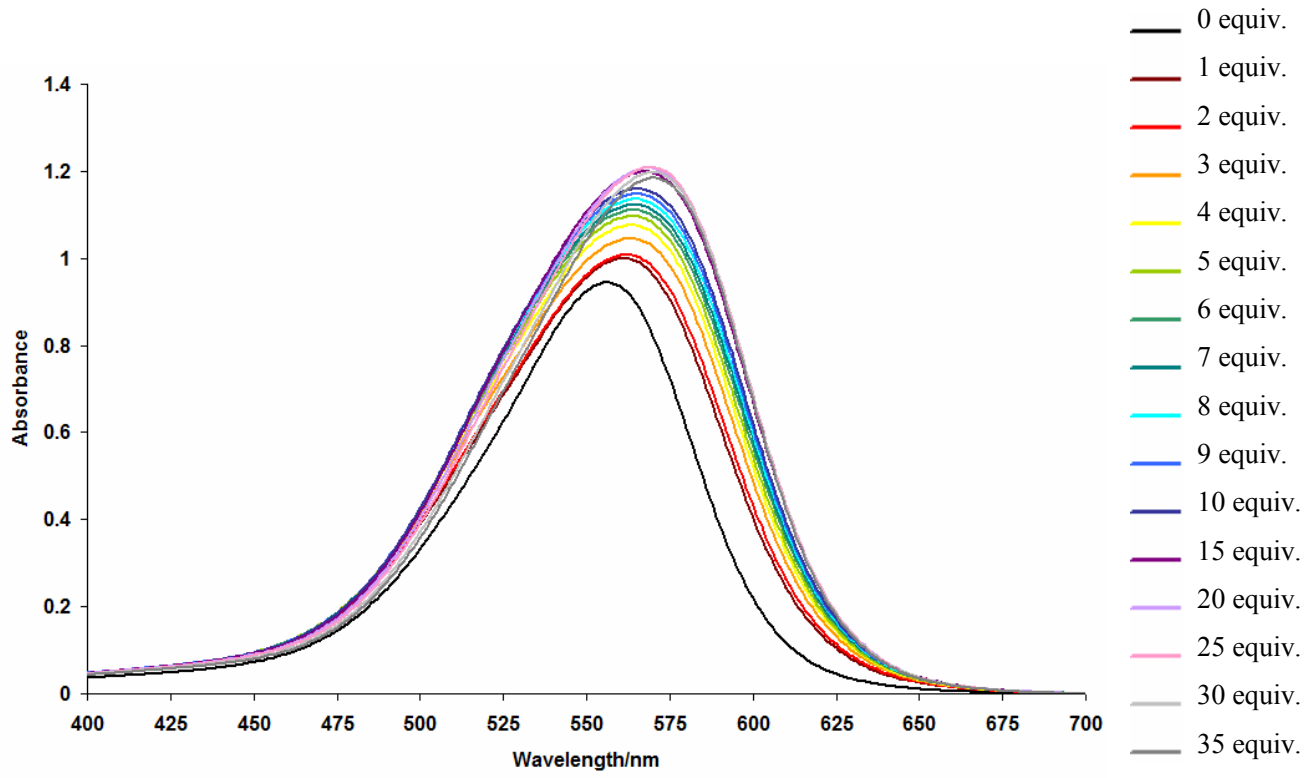

Figure 3.19 – UV/Vis spectroscopic titration plot for a 1 x 10^{-5} moldm^{-3} solution of **3.1** with tosylate in acetone, beginning at pH 1.

The other receptors behave in a similar manner with a few exceptions. The greatest difference between the receptors is found in their response to acetate. While **3.7** behaves in a similar manner to **3.1**, both **3.2** and **3.3** show a different behaviour during the acetate titration. Both the pyridyl-containing **3.2**, and ester-containing **3.3** show a visibly detectable discolouration and formation of a higher energy UV absorbance band corresponding to the alcohol form, however **3.3** responds almost immediately to the presence of acetate, with the change being caused in the first few additions of anion (Figure 3.20), while the change in **3.2** is more gradual, and the primary absorbance does show evidence of a red shift (11 nm) before the peak disappears.

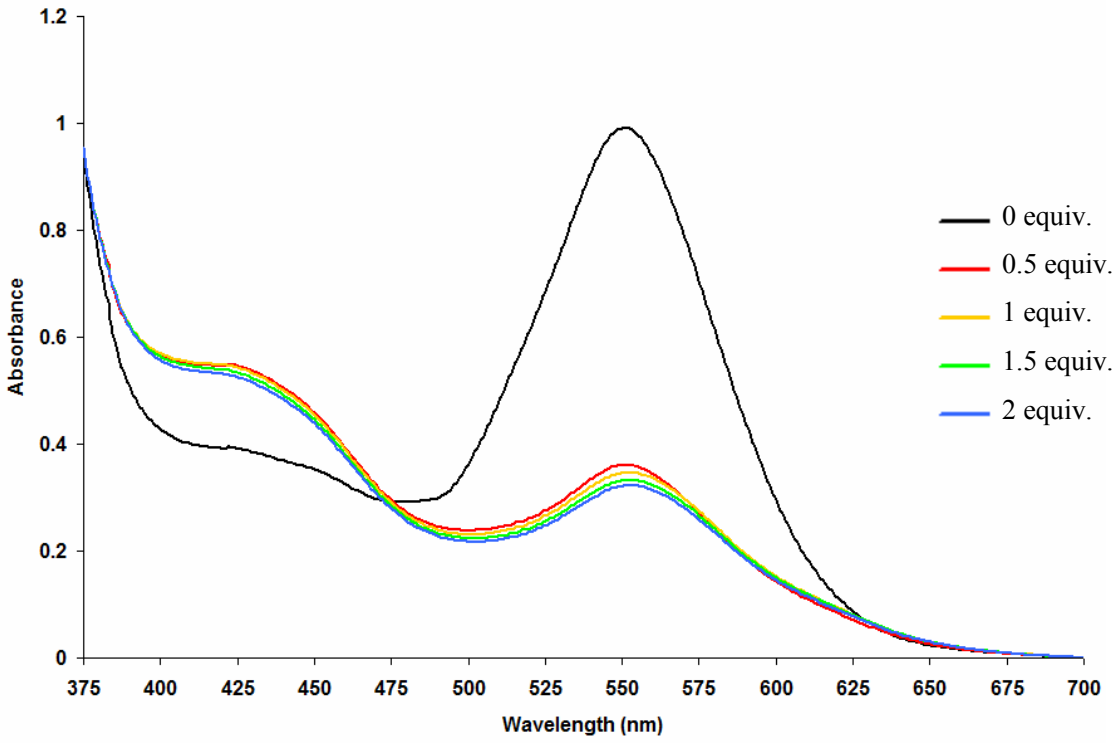

Figure 3.20 – UV/Vis spectroscopic titration plot for **3.3** with acetate.

This shift is detectable visibly, as the solution changes from a pink-red colour to pale yellow. This change is not caused by a change in pH, as there should still be an excess of the acid present – indeed the pH is still found to be < 1, and a spectrum of the alcohol form before addition of the acid shows no signal at 425 nm, which is perhaps attributable to a change in energy of the $\pi \rightarrow \pi^*$ excitation. Instead, the drastic change is assigned as being due to twisting of the receptor around the urea binding groups, a process by which the urea is freed from its intramolecular hydrogen bonds to more fully bind to the anion. This effect has been observed during the NMR experiments detailed in section 3.2. The rapidity of the change is likely caused by the much lower concentration here – in the NMR experiments it is difficult for an observer to see the paler yellow colour when it is overwhelmed by the residual pink colour. The reason for the change in **3.2** is less-well understood, since **3.2** should not

engage in intramolecular hydrogen bonding, and may instead be caused by a twisting of the receptor in order to better bind to a larger number of acetate anions, via interactions with pyridinium protons.

During the course of these first experiments, it became apparent that even with the excess of acid, the pH was not constant throughout the experiment, particularly when basic anions were added. To counter this, a pH 1 buffer solution was prepared using $HBF_4/NaBF_4$ in water, at a concentration high enough so that even with addition of an excess of acetate the pH remained at 1. A total of 2 μl of this buffer solution was sufficient to generate the coloured form and retain it throughout the experiment. Addition of a buffer solution had only a small effect on the binding to chloride and bromide attributable to the increased interference caused by competition with the buffer solution – the use of $NaBF_4$ in the buffer leads to formation of small quantities of NaCl and NaBr, but the poor solubility of these salts in acetone goes some way to preventing this. Weakly coordinating anions such as nitrate show almost no binding in the presence of buffer – the interactions between host and guest are too weak to favour complexation of the anion to the receptor with so much competition with the buffer. Binding to acetate differed only in the rate of colour loss – still no change in observed in the wavelength, suggesting that acetate is still most likely abstracting protons from the acidic solution than binding.

Difficulties in refining binding constants were found due to the complex equilibria present in the systems, identified by the lack of any isosbestic points in the absorbances. This is perhaps unsurprising, considering the potential of the receptors to bind to between one and three (or higher, in some cases) anions, as well as the natural equilibrium between each of these receptor:$anion_x$ complexes and their colourless alcohol forms.

3.5 Summary

In summary, a range of pararosaniline-based anion receptor compounds have been synthesised, and have been shown to successfully bind anions in both the neutral and cationic forms, although the acquisition of reliable numerical data on the strength of the binding in both forms is hampered by the low solubility of many of the alcohol forms and by the complex equilibria present in the cation forms. Indeed, even at a very low pH (< 1) the cationic form is still not found in 100% abundance, as evidenced by broad resonances and the presence of multiple species in the ^{1}H NMR spectrum and UV absorbance bands at around 250 nm consistent with the alcohol form of the receptors. We have shown that despite these difficulties, such receptors show some promise as anion receptors, and due to their rigidity can potentially form larger assemblies through intermolecular interactions. It may be possible to modify the properties further through the further functionalisation of the arms groups, or perhaps through replacement of the central OH group with other alkoxy fragments.

The range of receptors show promise as pH-sensitive detectors with innate anion binding properties, and can provide both a colourimetric and, in the case of receptors like **3.2**, a solubility switching response based on the pH. Indeed, systems such as **3.2** are potentially able to abstract anions from aqueous media by dissolution of the receptor with acid and then precipitation of the receptor-guest salt by neutralisation.

The ability to tune the colour of the receptor by modification of the arm functional groups should not be underestimated, as it is feasible that a tailored approach to receptor design could potentially produce a range of colours. Additional functionality at the arms has been also been shown to affect the hydrogen bonding pattern of the urea, and this effect can lead to interesting changes in the colour of the cation when

anion binding is strong enough to break the intramolecular interactions and distort the planarity of the structure.

Despite the synthesis of a number of receptors with innate metal binding functionality, no useful data could be gathered for interactions of any of these receptors with metals, since the already poor solubilities of these receptors are made worse by addition of a metal salt. While this suggests complexation of the metal to the receptor may be taking place, no useful data could be gathered to confirm this. The thioureas **3.5** and **3.6** were found to have particularly poor solubility, proving only partially soluble even in DMSO. This low solubility limited detailed studies on these receptors. None of the receptors have as yet been successfully crystallised, with or without the presence of any anions, instead forming an amorphous, clay-like material.

3.6 Experimental Details

***p*-Tolyl/*p*-rosaniline urea tripod 3.1**:

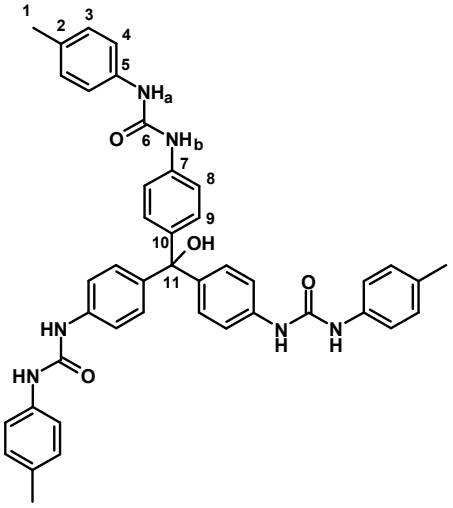

Pararosaniline base (1.00 g, 3.30 mmol) and *p*-tolyl isocyanate (1.20 g, 10.0 mmol) were mixed in 50ml acetonitrile and heated to reflux for 16 hours, resulting in the formation of a very deep violet-blue precipitate, which was filtered and washed with further acetonitrile to remove and excess starting material. Yield: 2.27 g, 3.20 mmol, 98%. ^{1}H NMR (acetone-d_6, J/Hz, δ/ppm): 2.25 (s, 9H, H1), 5.04 (s, 1H, OH), 7.07 (d, 8.2, 6H, H3), 7.21 (d, 8.6, 6H, H9), 7.41 (d, 8.2, 6H, H4), 7.46 (d, 8.6, 6H, H8), 8.01 (s, 3H, NH_a), 8.08 (s, 3H, NH_b). ^{13}C{^{1}H} NMR (DMSO-d_6, δ/ppm): 20.29 (CH_3, C1), 79.78 (C11), 117.17 (C3), 118.21 (C9), 128.14 (C4), 129.13 (C8), 130.54 (C2), 137.12 (C10), 138.11 (C5), 141.64 (C7), 152.56 (C6). ESI^{+}-MS: m/z 687 $[M\text{-}OH]^{+}$. Anal. Calc. for $C_{43}H_{40}N_6O_4$: C, 73.28; H, 5.72; N, 11.92. Found: C, 71.71; H, 5.67; N, 11.21. Recalculated for the possibility of water, likely from the solvent: Anal. Calc. for $C_{43}H_{40}N_6O_4.H_2O$: C, 71.45; H, 5.86; N, 11.63. IR (cm^{-1}): 3305 (O-H stretch), 2805 (N-H stretch), 1634 (Urea C=O stretch).

3-Pyridyl/*p*-rosaniline urea tripod 3.2:

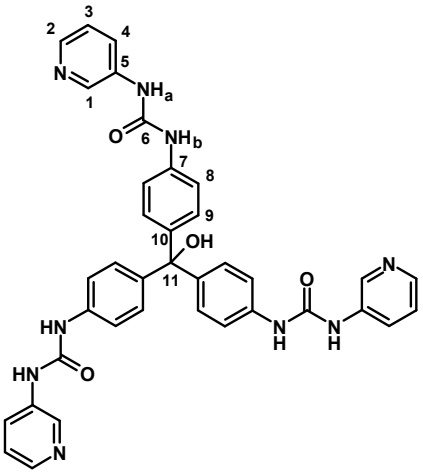

Nicotinic acid (10.0 g, 81.2 mmol) was suspended in 10ml DMF. Diphenylphosphoryl azide (17.6 ml, 81.6mmol) was added, followed by triethylamine (11.4 ml, 81.8 mmol). The mixture was stirred for 2 hours, and then the reaction quenched by addition of 50 ml H_2O. The solution was transferred to a separating funnel and extracted with diethyl ether (3 x 50 ml). The combined ether layers were then extracted with water (3 x 50 ml), and the ether removed under vacuum to give nicotinoyl azide as a white crystalline solid. Yield: 8.9 g, 60.1 mmol, 74%. ^{1}H NMR (DMSO-d_6, J/Hz, δ/ppm): 7.60 (dd, 4.8, 8.0, 1H, H2), 8.28 (ddd, 1.7, 2.1, 8.0, 1H, H3), 8.86 (dd, 1.7, 4.8, 1H, H1), 9.07 (d, 2.1, 1H, H4).

A portion of this nicotinoyl azide (2.00 g, 13.5 mmol) was dissolved in 25 ml acetone and heated to reflux for 2 hours. Pararosaniline base (1.20 g, 4.00 mmol), dissolved in a further 25 ml acetone was added and the reflux continued for a further 16 hours. The product precipitated slowly as an indigo powder which was filtered and washed with more acetone. Yield: 1.59 g, 2.40 mmol, 60%. ^{1}H NMR (DMSO-d_6, J/Hz, δ/ppm): 6.19 (s, 1H, OH), 7.10 (d, 8.6, 6H, H9), 7.28 (dd, 4.6, 8.2, 3H, H3), 7.36 (d, 8.6, 6H, H8), 7.92 (d, 8.2, 3H, H4), 8.16 (dd, 1.0, 4.6, 3H, H2), 8.56 (d, 2.2, 3H, H1), 8.81 (2s, 6H, NH_a/NH_b). $^{13}C\{^1H\}$ NMR (DMSO-d_6, δ/ppm): 80.48 (C11), 118.19, 124.28, 125.75, 128.89, 137.14, 138.48, 140.67, 142.67, 143.48, 153.26 (C6). ESI^+-

MS: m/z 666 $[M+H]^+$, 334 $[M+2H]^{2+}$, 223 $[M+3H]^{3+}$. Anal. Calc. for $C_{37}H_{31}N_9O_4$: C, 66.76; H, 4.69; N, 18.94. Found: C, 64.37; H, 4.99; N, 17.37. Recalculated for the possible presence of solvent: Anal. Calc. for $C_{37}H_{31}N_9O_4.H_2O+C_3H_6O$: C, 64.76; H, 5.30; N, 17.00. IR (cm^{-1}): 3313 (O-H stretch), 2816 (N-H stretch), 1642 (Urea C=O stretch).

Methyl benzoate/*p*-rosaniline urea tripod 3.3:

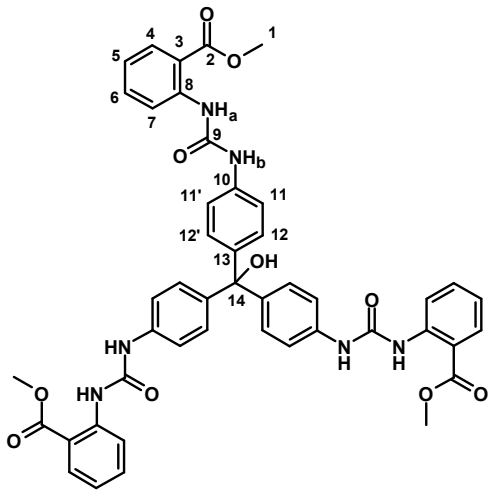

Pararosaniline base (1.00 g, 3.30 mmol) and methyl 2-isocyanatobenzoate (1.77 g, 10.0 mmol) were mixed in 50 ml acetone and heated to reflux for 16 hours. The resulting solution was cooled and the solvent removed under vacuum, leaving a purple precipitate. This precipitate was purified by washing with acetonitrile to remove any excess starting material. Yield: 1.76 g, 2.10 mmol, 70%. ^{1}H NMR (acetone-d_6, J/Hz, δ/ppm): 3.92 (s, 9H, H1), 5.11 (s, 1H, OH), 7.04 (d, 7.8, 3H, H6), 7.28 (d, 8.7, 6H, H12), 7.50-7.65 (m, 3H, H5), 7.58 (d, 8.7, 6H, H11), 8.00 (dd, 1.4, 7.8, 3H, H7), 8.62 (d, 8.5, 3H, H4), 9.16 (s, 3H, NH_b), 10.32 (s, 3H, NH_a). $^{13}C\{^1H\}$ NMR (acetone-d_6, δ/ppm): 52.2 (CH_3, C1), 114.5 (C, C14), 118.3 (CH, C12), 120.0 (CH, C12'), 120.8 (CH, C5), 128.6 (CH, C6), 128.7 (CH, C7), 129.8 (CH, C11), 130.8 (C-H, C11'), 134.3 (CH, C4), 138.7 (C13), 142.7 (C10), 143.3 (C3), 152.5 (C8), 168.6 (C9), 205.6 (C2). ESI^+-MS: m/z 819 $[M-OH]^+$, ESI^--MS: 835 $[M-H]^-$, 871 $[M+Cl]^-$. Anal. Calc. for $C_{46}H_{40}N_6O_{10}$: C, 66.02; H, 4.82; N, 10.04. Found: C,

65.78; H, 5.01; N, 10.22. IR (cm^{-1}): 3305 (O-H stretch), 2974 (N-H stretch), 1675 (Urea C=O stretch).

***p*-Tolyl/*p*-rosaniline thiourea tripod 3.5**:

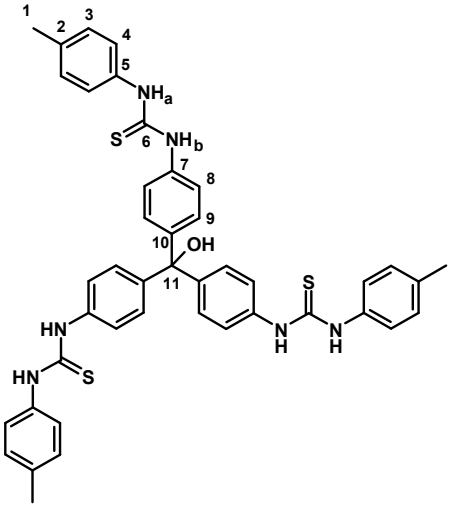

Pararosaniline base (0.31 g, 1.00 mmol) and *p*-tolyl isothiocyanate (0.45 g, 3.00 mmol) were mixed in 50 ml acetone and heated to reflux for 40 hours. The resulting solution was cooled and the solvent removed under vacuum. Washing the precipitate with acetonitrile and CH_2Cl_2 gave the product as a purple powder. Yield: 0.23 g, 0.30 mmol, 30%. ^{1}H NMR (DMSO-d_6, J/Hz, δ/ppm): 2.27 (s, 9H, H1), 6.04 (s, 1H, OH), 7.10 (d, 13.2, 6H, H3), 7.13 (d, 13.8, 6H, H9), 7.30 (d, 13.2, 6H, H4), 7.37 (d, 13.8, 6H, H8), 9.67 (s, 3H, NH_a), 9.70 (s, 3H, NH_b). ^{13}C{^{1}H} NMR (DMSO-d_6, δ/ppm): Unable to acquire suitable spectrum due to poor solubility. ESI$^+$-MS: m/z 775 $[M+Na]^+$. Anal. Calc. for $C_{43}H_{40}N_6O_1S_3$: C, 68.59; H, 5.35; N, 11.16. Found: C, 67.95; H, 4.99; N, 10.99. IR (cm^{-1}): 3321 (O-H stretch), 2820 (N-H stretch), 1462 (C=S stretch).

3-Pyridyl/*p*-rosaniline thiourea tripod 3.6:

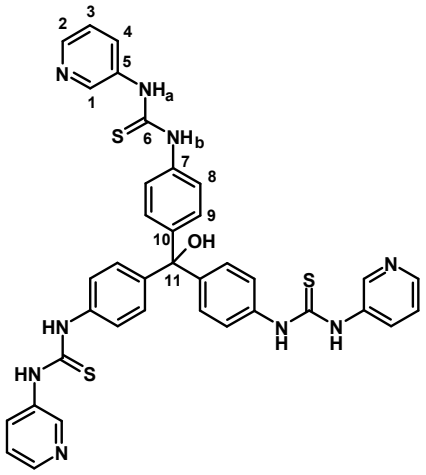

Pararosaniline base (0.15 g, 0.50 mmol) was mixed with 3-pyridyl isothiocyanate (0.20 g, 1.50 mmol) in 25 ml acetonitrile and heated to reflux for 18 hours, during which time the product was formed as a dark purple precipitate. This precipitate was filtered and washed with further amounts of acetonitrile. Yield: 0.30 g, 0.42 mmol, 84%. ^{1}H NMR (DMSO-d_6, J/Hz, δ/ppm): 6.58 (s, 1H, OH), 7.05-7.20 (m, 3H, H3), 7.30-7.40 (m, 12H, H8/9), 7.85-7.95 (m, 3H, H4), 8.25-8.35 (m, 3H, H2), 8.56 (s, 3H, H1), 10.04 (s, 6H, NH_a/NH_b). $^{13}C\{^{1}H\}$ NMR (DMSO-d_6, δ/ppm): 64.87 (C11), 122.78, 125.17, 127.84, 129.05, 131.53, 136.02, 145.46, 180.97 (C6). ESI^{+}-MS: m/z 715 $[M+H]^{+}$, 358 $[M+2H]^{2+}$, 239 $[M+3H]^{3+}$. Anal. Calc. for $C_{37}H_{31}N_9S_3O$: C, 62.24; H, 4.38; N, 17.66. Found: C, 62.35; H, 4.44; N, 17.38. IR (cm^{-1}): 3323 (O-H stretch), 2824 (N-H stretch), 1466 (C=S stretch).

Methylsulphanyl/*p*-rosaniline urea tripod 3.7:

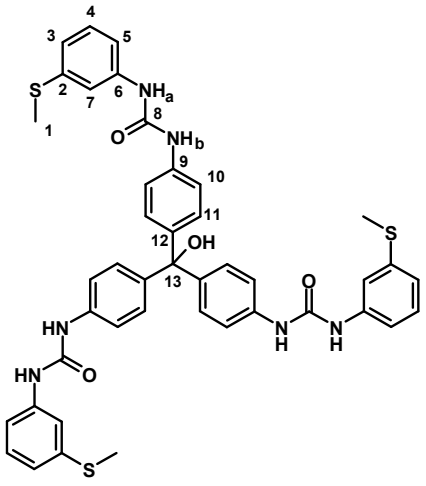

Pararosaniline base (0.31 g, 1.00 mmol) was mixed with 3-(methylthio)phenyl isocyanate (0.50 g, 3.00 mmol) in 50 ml acetone and heated to reflux for 8 hours. Cooling the solution and removal of the solvent under vacuum gave the crude product, which was purified by washing with acetonitrile and CH_2Cl_2, leaving the product as a dark purple powder. Yield: 0.74 g, 0.93 mmol, 93%. ^{1}H NMR (DMSO-d_6, J/Hz, δ/ppm): 2.45 (br. s., 9H, H1), 6.19 (s, 1H, OH), 6.85 (d, 7.6, 3H, Ar-H), 7.12 (d, 8.6, 6H, H11), 7.21 (t, 7.6, 3H, Ar-H), 7.36 (d, 8.6, 6H, H10), 7.46 (s, 3H, H7), 8.68 (s, 6H, NH_a/NH_b). ^{13}C{^{1}H} NMR (DMSO-d_6, δ/ppm): 15.28 (CH3, C1), 80.49 (C13), 115.55, 115.94, 118.07, 119.93, 128.88, 129.96, 138.62, 139.26, 140.89, 142.54, 153.18 (C8). ESI$^+$-MS: m/z 823 $[M+Na]^+$. Anal. Calc. for $C_{43}H_{40}N_6O_4S_3$: C, 64.48; H, 5.03; N, 10.49. Found: C, 64.22; H, 4.96; N, 10.87. IR (cm^{-1}): 3320 (O-H stretch), 2812 (N-H stretch), 1666 (C=O stretch).

3.7 References

1. I. A. Schrijver, M. J. Melief, M. van Meurs, A. R. Companjen and J. D. Laman, *J. Histochem. Cytochem.,* 2000, **48**, 95-103.
2. H. C. Biddle, *J. Am. Chem. Soc.,* 1913, **35**, 273-281.
3. W. Luck and H. Sand, *Angew. Chem. Intl. Ed.,* 1964, **3**, 570-580.
4. G. Vinitha, A. Ramalingam and P. K. Palanisamy, *Spectroc. Acta Pt. A-Molec. Biomolec. Spectr.,* 2007, **68**, 1-5.
5. D. R. Turner, E. C. Spencer, J. A. K. Howard, D. A. Tocher and J. W. Steed, *Chem. Commun.,* 2004, 1352-1353.
6. N. Qureshi, D. S. Yufit, J. A. K. Howard and J. W. Steed, *Dalton Trans.,* 2009, 5708-5714.
7. M. M. Kosanic and J. S. Trickovic, *J. Photochem. Photobiol. A-Chem.,* 2002, **149**, 247-251.
8. D. R. Turner, *PhD Thesis, King's College London,* 2004.
9. R. A. Binstead, *SPECFIT, (1996) Spectrum Software Associates, Chapel Hill, NC, USA.*

4. Metal-Templated Anion Receptors

4.1 Aims

As discussed in chapter one, substituted pyridines with attached anion binding functionalities can make for a wide range of potential anion receptors – the pyridine nitrogen atom can be used to displace bromide and attach a pyridyl urea substituent to a larger framework, such as a calixarene[1] or the tri-substituted benzene 'pinwheel' cores.[2-3] The pyridyl functionality can also be used to bind to a metal ion such as silver(I) or copper(II).[4-8] Previous work has focussed on substituted secondary aminopyridines[9] and 3-ureidopyridines,[10] with the ureas typically containing simple aryl or alkyl substituents. Work by Filby and colleagues[1] reported the synthesis of a number of receptors based on the simple pyrene-appended aminopyridine **4.1** (Figure 4.1) and found that the innate fluorescence of the pyrene group provided a strong detection method for anion binding. Upon binding to an anion, the receptor arms are brought closer together, and this leads to intramolecular π-π stacking between pyrene moieties. This leads to formation of an excimer complex, a dimer which is associative in the excited state and dissociative in the ground state.

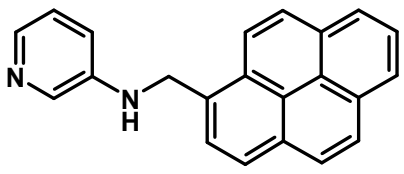

Figure 4.1 – Pyrene-appended aminopyridine **4.1**.

In a related effort, we have synthesised the related pyrene-appended ureidopyridine **4.2** (Figure 4.2), with the hope of creating similar receptors constructed around the 1,3,5-tribromomethyl-2,4,6-triethyl benzene core. In addition, we will also attempt to

replicate the ML_2 pincer complexes reported by Turner and coworkers on *p*-tolyl ureidopyridine,[10] and potentially even form ML_3 tripodal complexes based on facially-capped octahedral metal ions in a similar manner.

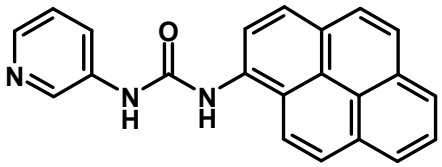

Figure 4.2 – Pyrene-ureidopyridine (PUP) ligand **4.2**.

Synthesis of **4.2** involved similar azide-based reaction to those detailed in the previous chapter, involving reaction of a carboxylic acid with diphenylphosphoryl azide (DPPA) to generate a carboxazide intermediate. While the azidation step can be carried out on the pyrene fragment, with reaction of DPPA with pyrenecarboxylic acid to give a pyrenyl azide for reaction with readily available aminopyridine, although it was found that the pyrenyl azide is highly unstable and is decomposed quickly by both air and light. Synthesis of **4.2** via the previously detailed nicotinoyl azide procedure (chapter 3) with aminopyrene gave much higher yields and purity (Figure 4.3). Small, aromatic azides are often found to be explosive when dry, thus the nicotinoyl azide was kept in solution at all times and no such difficulties were observed.

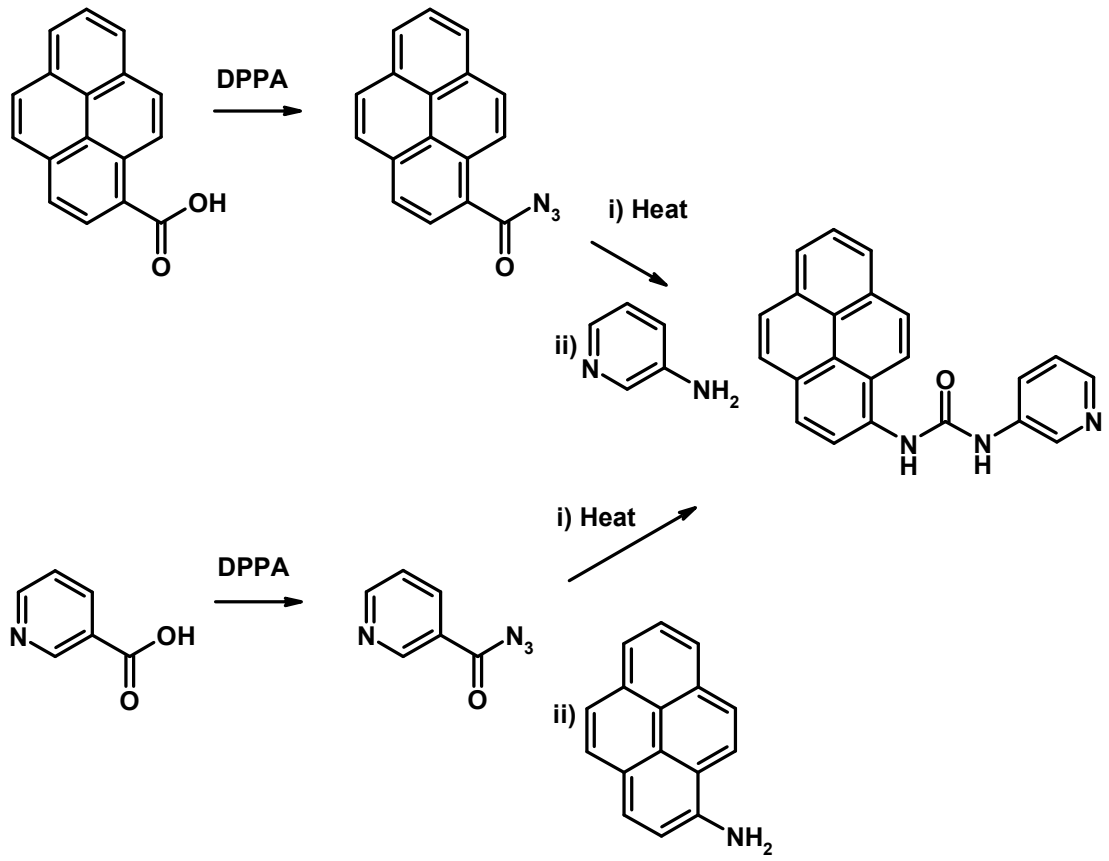

Figure 4.3 – Synthetic pathways to compound **4.2**.

Crystals of **4.2** were grown as long, thin needles by slow evaporation of the solvent from a 1:1 mixture of methanol and chloroform. The crystals are a solvate of **4.2**, containing water and methanol, and possess $P2_1/c$ symmetry. The molecule (Figure 4.4) is found to be twisted from the planar arrangement typical of similar pyridyl ureas,[5, 11-12] and displays the expected hydrogen-bonded urea tape common for simple urea-containing molecules,[13] but quite rare among aryl ureas with electron-withdrawing substituents. This interaction is reinforced by significant π stacking between pyrene groups and leads to particularly strong assembly in one dimension. This dominant π stacking is the reason for the twist in the molecule which breaks the usual planarity of the pyridyl urea group and thus reinitialises the urea tape hydrogen bonding.

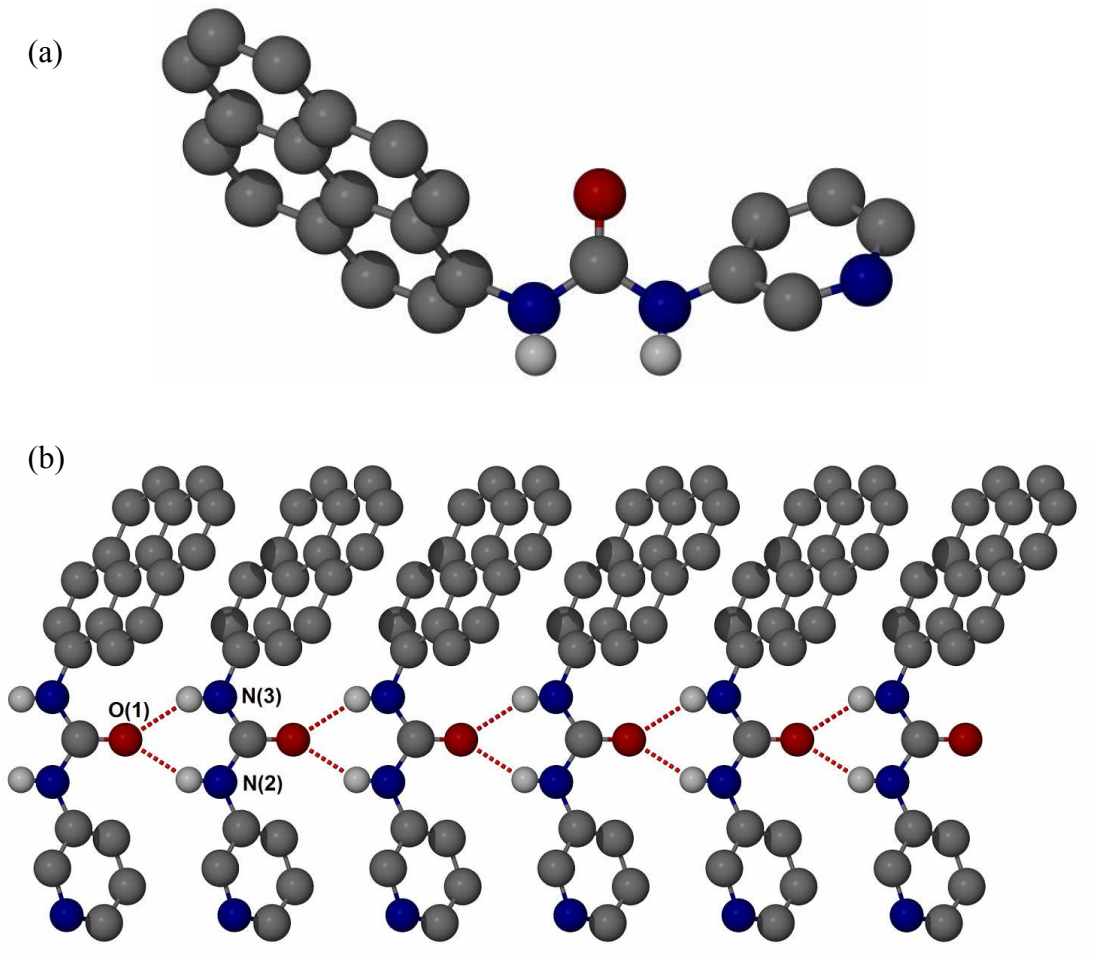

Figure 4.4 – (a) X-ray molecular structure of **4.2** and (b) linear packing interactions of **4.2** in the crystal. C-H atoms omitted for clarity. Selected hydrogen-bond distances: N(2)-O(1) = 2.28(2) Å; N(3)-O(1) = 2.29(3) Å.

These chains of molecules stack together in an anti-parallel fashion, held by pyrene-C-H – urea/pyridine π interactions, relating two molecules together across an inversion centre. This arrangement leads to sheets of molecules which are linked primarily by pyridyl-N···solvent interactions. The solvent molecules are methanol and water, which are localised in channels between pyrene groups in the structure and are filled with a regular arrangement of methanol molecules, held by hydrogen bonding to

the pyridyl nitrogen atoms and interacting with a string of water molecules (Figure 4.5).

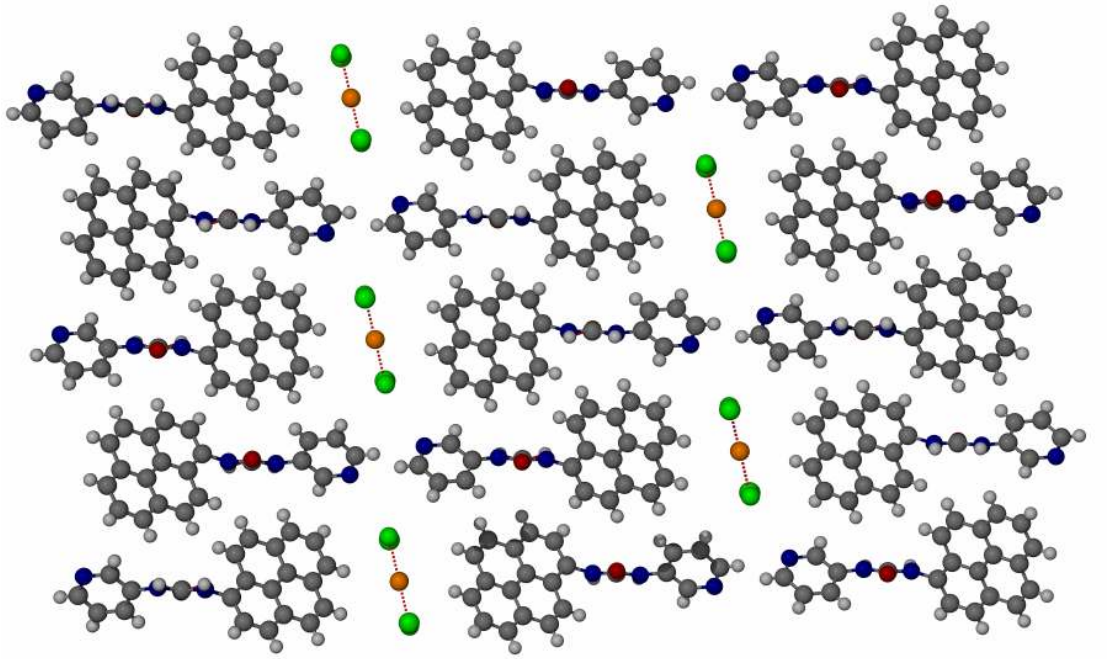

Figure 4.5 – Crystal packing in the x-ray structure of **4.2**. Methanol molecules are green, water oxygen atoms are orange. Pyridine N-Methanol O distance 3.56(2) Å.

Creating a multipodal receptor from **4.2** was far more challenging. Extremely poor solubility of the ligand made reacting it with the tripod core difficult, as even with **4.2** in a large excess over the core led to formation of an indistinguishable mixture of mono, di, and trisubstituted core, with apparent decomposition of the ligand also a problem. Attempts to repeat the synthesis in the solid phase by grinding in a ball-mill proved ineffective. It seems that the reaction conditions required to force the reaction between **4.2** and core are likely sufficient to destroy the pyrene substituent.

4.2 Metal-based Receptors

Due to the difficulties in reacting **4.2** with the tripod core, it was decided to discontinue development of organic-based receptor compounds with **4.2** and instead focus on metal-based receptors. The effect of a variety of transition metals on the behaviour of **4.2** was followed by both UV/Visible spectroscopy and fluorometry, since at the low concentrations used for these experiments the ligand was found to be sufficiently soluble in acetonitrile. The UV/Visible absorbance spectrum of **4.2** at a concentration of 2 x 10^{-5} mol dm^{-3} in acetonitrile is shown in figure 4.6.

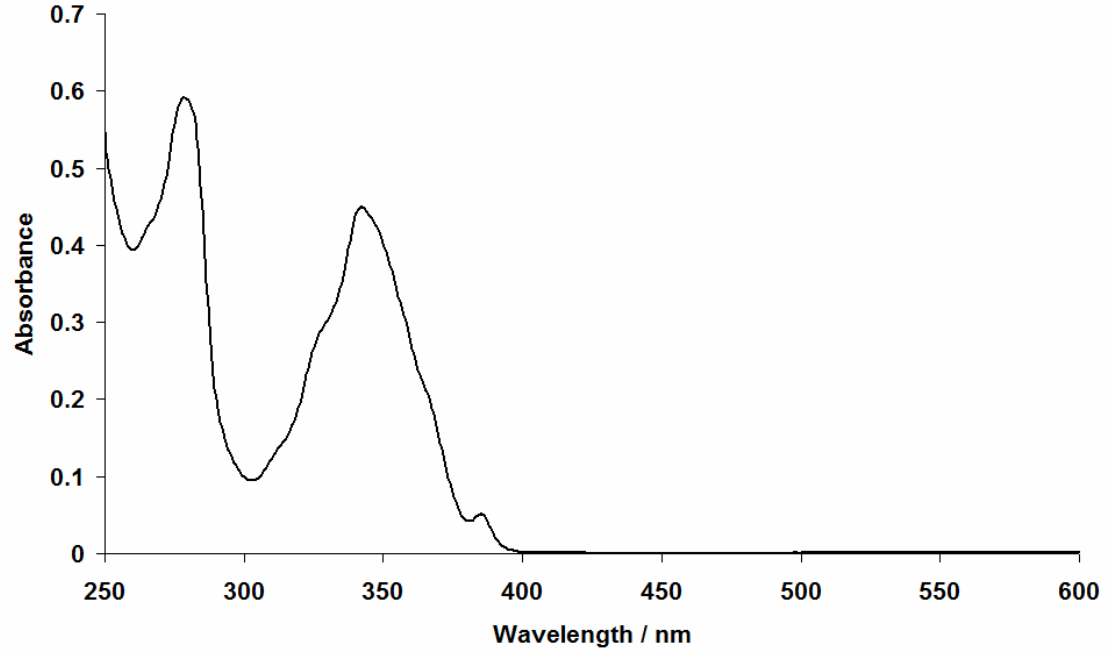

Figure 4.6 – UV/Visible absorption spectrum of **4.2** in MeCN (2 x 10^{-5} mol dm^{-3}).

Addition of metal salts to solutions of **4.2** causes a range of effects depending on the nature of the metal. For the sake of consistency, the metal salts chosen were all trifluoromethanesulphonate (triflate, OTf^-) salts, chosen for their solubility of the salts in acetonitrile and for the non-binding nature of the triflate anion. It was found that all of the metals cause a blue-shift in the absorbance spectra, typically in the region of 2 – 6 nm (Figure 4.7). Changes in intensity of peaks are also observed, with the peak

at 342 nm attributed to $\pi \rightarrow \pi^*$ excitation decreasing in favour of a band emerging in the trough at 300 nm, particularly for zinc salts. The peak at 278 nm, assigned as an intra-ligand charge transfer band, also tends to experience a loss in intensity, though when the metal is zinc (II), the intensity of this peak increases. When **4.2** interacts with copper (II) salts, the absorbance profile changes dramatically – the primary absorbance peaks are lost almost completely, in favour of an absorbance continuum stretching from 550 nm to lower then 250 nm. This forms almost immediately following addition of copper (II) triflate, requiring addition of only three equivalents for the change to be complete. The new solution is a pale yellow colour and was found to no longer fluoresce under ultraviolet light. Such a ratio seems odd, suggesting complexation of three metals to one ligand, but may be explainable by considering that the metal may be weakly bound at such low concentrations, and that three equivalents of metal are necessary to encourage complexation. Elemental analyses on prepared samples containing **4.2** with metal salts in a 2:1 ligand:metal ratio showed good agreement with formation of the 2:1 complex, but the resulting precipitates displayed poor solubility. Preparing a sample with metal and ligand in a 1:3 ligand to metal ratio gave similar elemental results, suggesting precipitation of the first available product is the driving force, though attempting to probe the ratio by MS showed no significant formation of any metal-bound ligand complexes, either due to their insolubility or the high lability causing decomposition in the mass spectrometer. The reason for the loss in intensity may be due to a ligand-metal charge transfer to vacant d orbitals of the copper, or to oxidative transfer of electrons to the copper. Such an effect has been seen before with similar fluorescent ligands.[14] The general loss of structure in the absorbance bands is likely caused by slow precipitation of the metal-ligand complex.

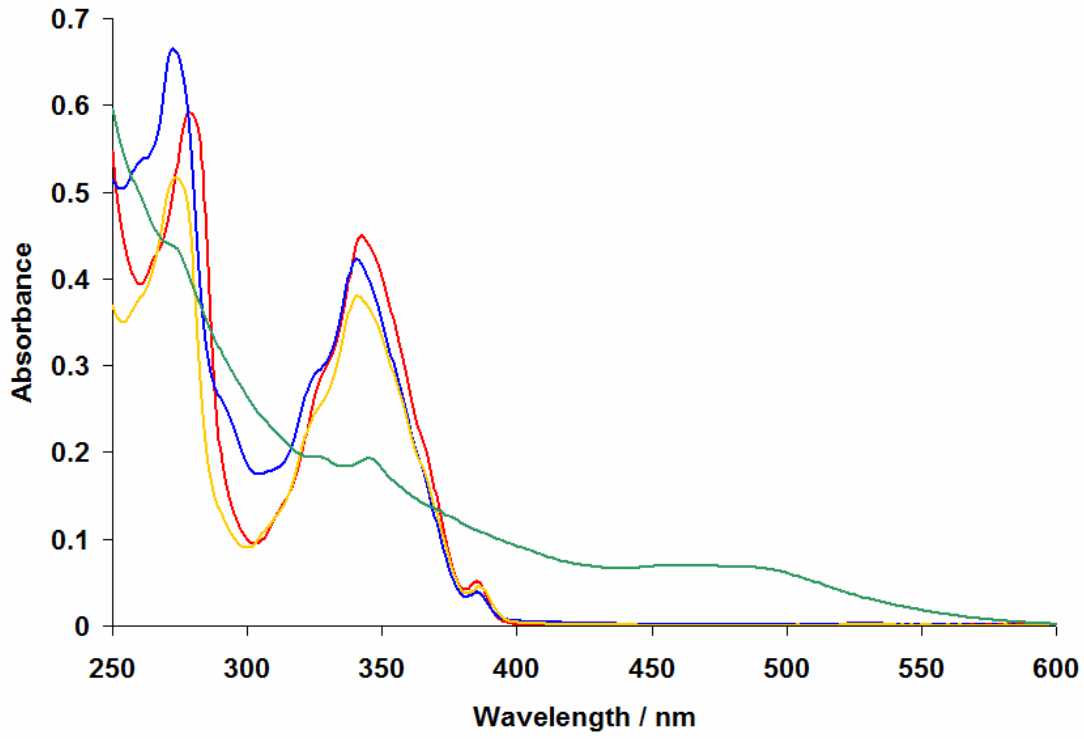

Figure 4.7 – UV/Visible absorbance profiles at 2 x 10^{-5} mol dm^{-3} concentrations in MeCN of **4.2** (red), with addition of 10 equivalents $Zn(OTf)_2$ (blue), AgOTf (yellow), and $Cu(OTf)_2$ (green).

Following the addition of metal salts by fluorometry showed negligible change in the innate fluorescence band of **4.2** for zinc(II) or silver(I), though addition of copper to the solution of **4.2** causes visible quenching of the emission band (Figure 4.8) as previously discussed. No shifting of the band wavelengths were observed.

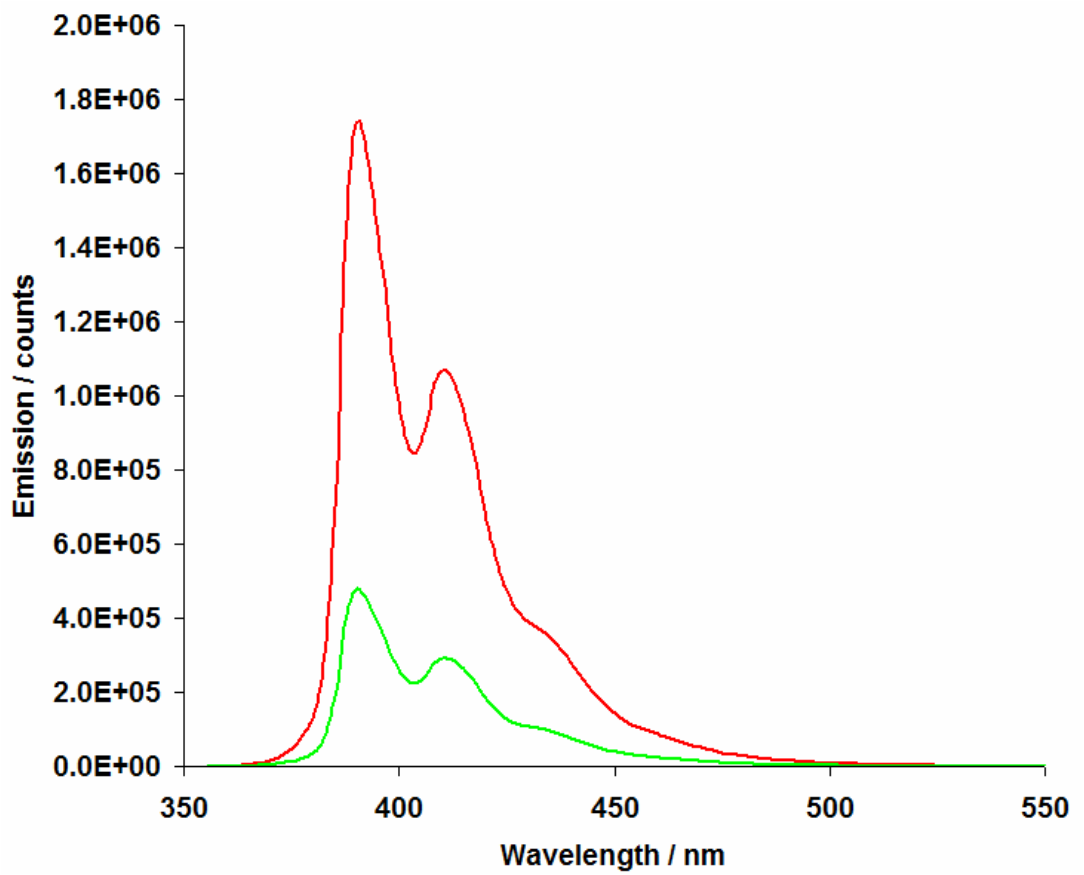

Figure 4.8 – Emission spectra for 2 x 10^{-5} mol dm^{-3} solutions in MeCN of **4.2** (red) and **4.2** + 3 equivalents of $Cu(OTf)_2$ (green) after excitation at 350 nm.

Since it appeared by UV/Visible methods that the metal and ligand were indeed interacting in some fashion, it was decided to carry out anion binding studies on both free **4.2** and **4.2** in the presence of metal salts by both UV/Visible spectroscopy and fluorimetry, in order to compare the anion binding capabilities of the free ligand and the metal-bound complex.

4.3 Anion Binding Studies

Firstly, as a standard, the anion binding properties of **4.2** without any additional metals were studied. Standard spectroscopic methods were used, with 3 ml of a stock solution of ligand at 2 x 10^{-5} mol dm^{-3} concentration added to a cuvette and guest solutions, made to a concentration such that 10 µl was equal to one equivalent, added using a microliter syringe. Addition of the anion solution showed no visible response by eye to the solution, but did show a visible response under UV light in some cases. In most cases, the UV/Visible absorption profile showed red-shifting upon addition of anion, with the absorbances passing through an isosbestic point indicating a simple host → host:guest equilibrium. Figure 4.9 shows an example titration plot (**4.2** with chloride), while figure 4.10 summarises the results, showing the endpoint of each titration (addition of 50 equivalents of anion).

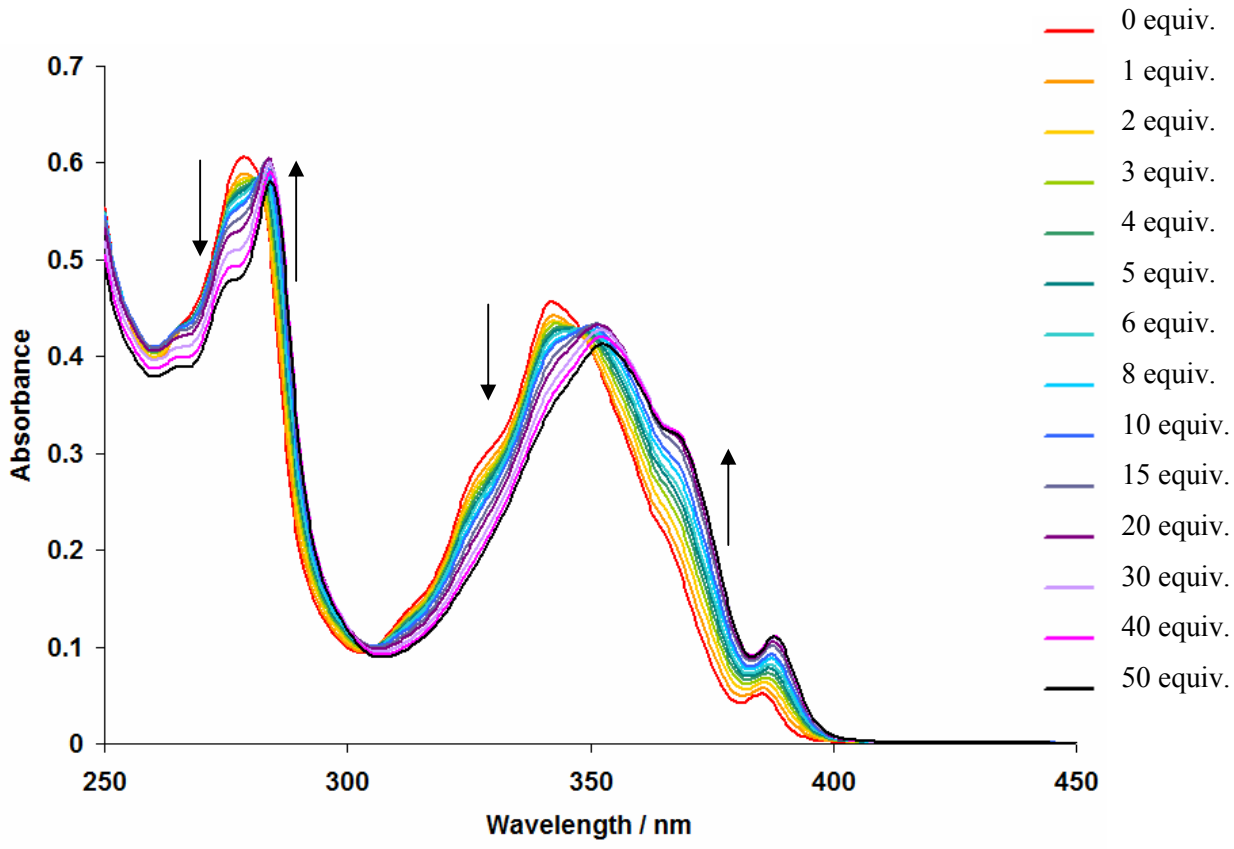

Figure 4.9 – UV/Visible titration plot for **4.2** with chloride in MeCN.

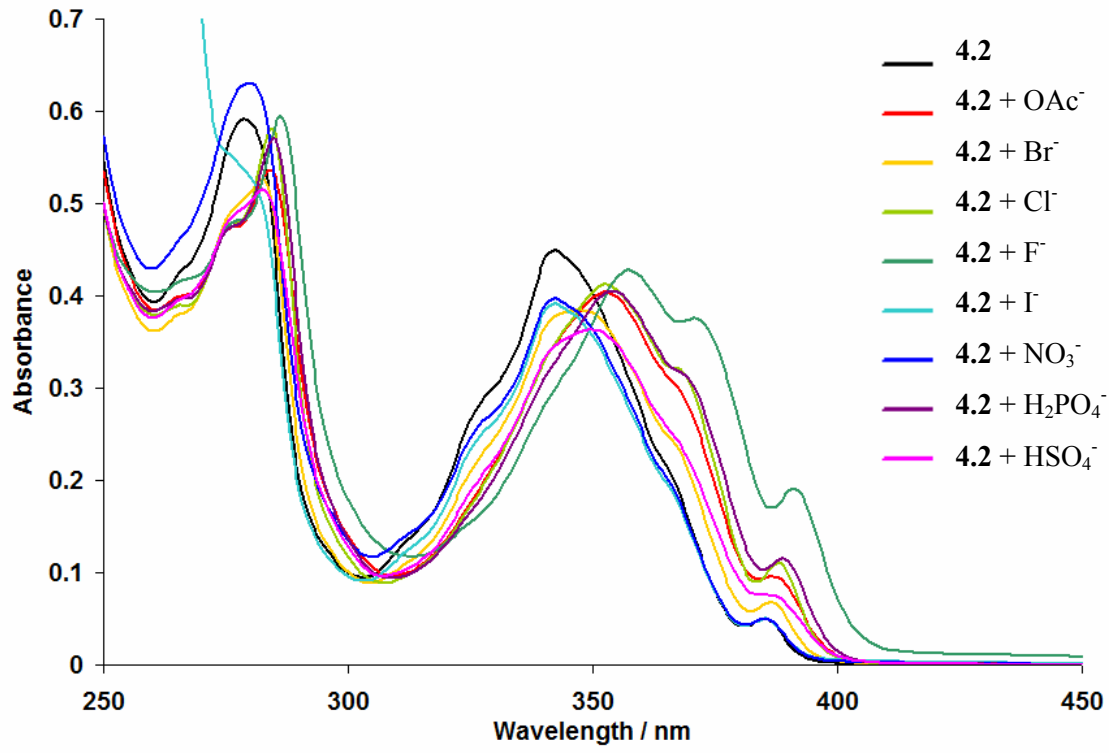

Figure 4.10 – UV/Visible absorption profiles for **4.2** in the presence of anions (50 equivalents).

Guest	β_1
Acetate	4.95(3)
Bromide	3.10(4)
Chloride	3.75(2)
Fluoride	4.22(5)
Iodide	2.8(2)
Nitrate	< 1
Dihydrogen Phosphate	4.41(2)
Hydrogen Sulphate	3.39(4)

Table 4.1 – Refined binding constants for **4.2** with a variety of anions in MeCN. Binding constants were determined using the SpecFit32 software.[15]

From a combinatorial plot such as figure 4.10, it is easier to draw attention to similarities and differences between anions. For example, nitrate and iodide both show little change in the band positions, but a small difference in the peak intensities are observed – the peak at 342 nm decreases slightly, while with nitrate the peak at 278 nm increases slightly. Iodide shows a large band appearing at 250 – 270 nm, which is identified as a natural absorbance of iodide and is not due to any host-guest interaction. The small changes are in accordance with the low binding strength of these anions. By contrast, addition of fluoride causes a dramatic change in the absorbance profile, with a large red shift observed. Chloride, acetate and dihydrogen phosphate all cause similar changes in the absorbance of **4.2** and all show similar binding strengths. Bromide and hydrogen sulphate also seem to behave in a similar manner in their interactions with **4.2**, causing a broadening of the 342 nm absorption band with a modest red-shift.

Repeating the titration experiments in a fluorescence cuvette and observing the changes in fluorescence caused by addition of anions highlighted further differences between anions (Figure 4.11).

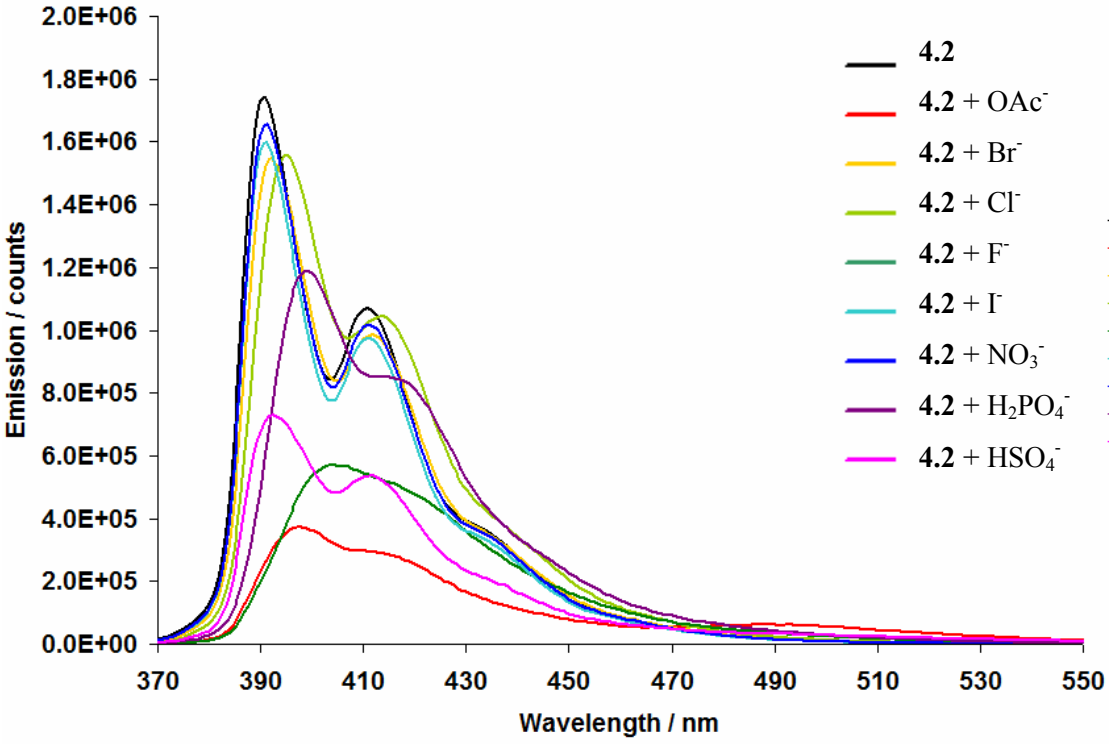

Figure 4.11 – Emission profiles for 2 x 10^{-5} mol dm^{-3} solutions of **4.2** in MeCN in the presence of anions (50 equivalents). Anions are TBA salts. Excitation wavelength 347 nm, solutions were found to possess the same absorbance intensity at this point.

From the fluorescence data, it is apparent that the weakly-coordinating anions (iodide and nitrate) also have only a small effect on the emission of **4.2**, as little change in the emission wavelength or intensity is observed. Bromide too displays only a small difference, causing a small (1 nm) red shift in the emission. Binding of chloride exhibits a more detectable change, with a red shift of 4 nm in the emission band detected. In terms of the extent of the band shift, the largest differenced are found for dihydrogen phosphate, with a larger shift (9 nm) coupled with a fairly significant decrease in intensity, and fluoride, which shows the greatest shift (14 nm) and a drastic loss in intensity. While the UV data suggests similar binding between HSO_4^- and bromide, the fluorescence data suggests otherwise – bromide, as mentioned

causes a small shift in the emission band, and has little effect on the intensity of that band. HSO_4^- causes a similarly small shift in the emission band, but strongly quenches the intensity of this band. Acetate, causes a modest shift in the position of the emission band, comparable to chloride, but has the largest quenching effect on the intensity of the band. When observing the solutions by eye under a UV lamp, the solutions of **4.2** unbound and in the presence of the majority of the anions are violet in colour, since their emission is on the far edge of the visible range (400 – 410 nm). Those anions which display the largest red-shift, particularly $H_2PO_4^-$ and acetate, appear pale blue in colour, and look to be brighter in colour due to a wider range of visible wavelength photons emitted.

The behaviour of **4.2** with anions was also probed in the presence of metal salts. 3 equivalents of the appropriate metal salt (copper, zinc, and silver triflates) were added to the solution of **4.2** before titration with anions. In the case of both silver and zinc, addition of anion stock solutions caused precipitation of the metal salt after three and six equivalents of anion added respectively, suggesting that the metal:**4.2** complex is weakly bound, at least at the low concentrations used here. Inclusion of copper triflate, thanks to the drastic impact on the UV/Visible spectrum of the ligand, shows evidence of complexation of **4.2** to metal. Figure 4.12 shows an example titration plot for the interaction of the metal-bound **4.2** with chloride.

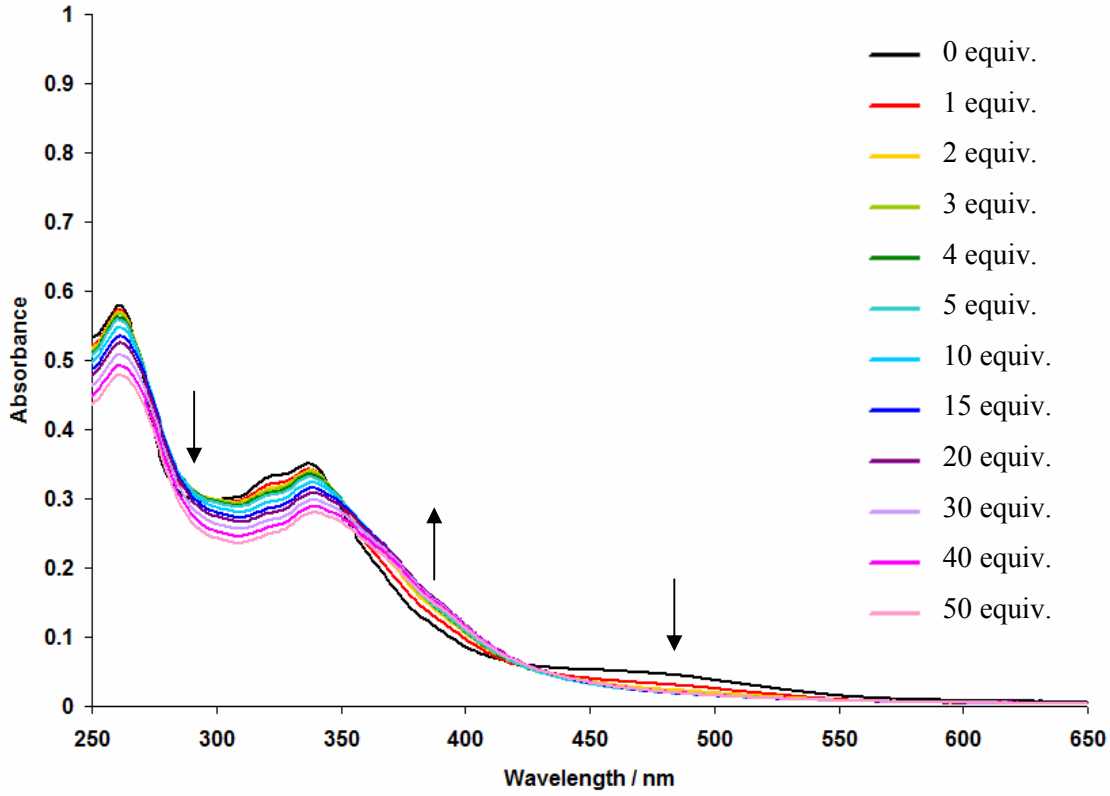

Figure 4.12 – Titration plot for **4.2** with chloride in presence of 3 equivalents of $Cu(OTf)_2$. Solution at 2 x 10^{-5} mol dm^{-3} in acetonitrile.

In a change of behaviour from the free ligand with chloride, addition of copper (II) causes a marked decrease in the red-shift observed through the titration. The steady change from ligand to ligand:guest complex is lost, or at least suppressed by interactions with copper. Growth of the shoulder at ~365 nm is still observed, but the presence of a sharp absorbance at ~285 nm is not. In addition, the broad absorbance at 450 – 500 nm, not found in the absorption spectra of either $Cu(OTf)_2$ or **4.2**, and therefore attributed as being due to a **4.2**-Copper complex, is reduced upon addition of most anions, suggesting removal of copper from the ligand and generation of copper salts.

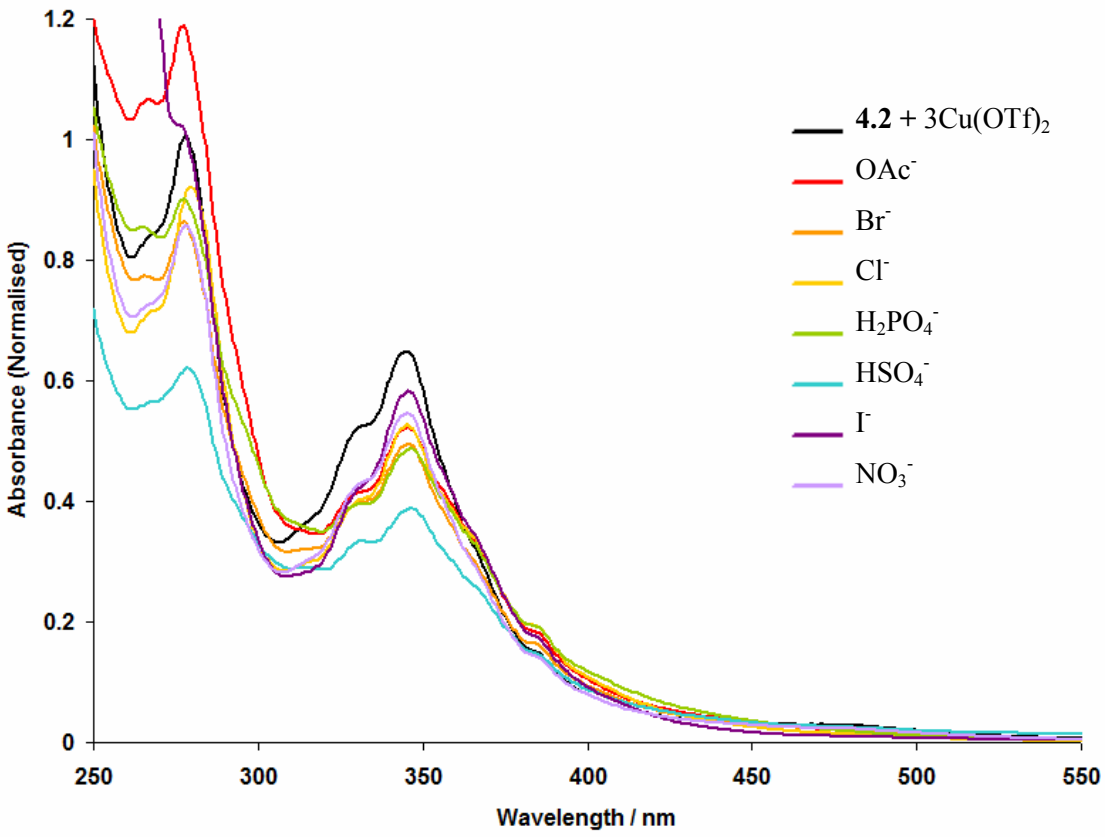

Figure 4.13 – Summarised titration data for **4.2**/Copper complex. All spectra normalised to the initial **4.2** + 3Cu(OTf)$_2$ spectrum. Solutions at 2 x 10^{-5} mol dm^{-3} concentration in acetonitrile.

Guest	β_1
Acetate	2.5(3)
Bromide	3.2(1)
Chloride	3.9(1)
Fluoride	4.0(2)
Iodide	2.4(1)
Nitrate	< 1
Dihydrogen Phosphate	4.2(2)
Hydrogen Sulphate	2.9(1)

Table 4.2 – Refined binding constants for **4.2** + 3Cu(OTf)$_2$ with anions.

Acetate, of all of the anions studied here, shows a particular increase in intensity of the band at ~285 nm. This increase is first observed after addition of 6 equivalents of acetate to the solution, and is likely caused by loss of the three equivalents of copper as copper (II) acetate, with the next acetate interacting with the urea of **4.2**. This could account for the lower binding observed with acetate, and perhaps sulphate too. Binding of the **4.2**/copper species with iodide and nitrate is weak – little change is observed in the absorbance spectra, save for dilution effects. What changes there are between the initial and final spectra follow a similar pattern to the free ligand, with only the loss of the broad band between 450 and 500 nm providing any evidence for the formation of a metal:ligand complex. Consideration of the fluorescence data for the same system shows no noticeable difference between the emissions of the free ligand and the ligand with metal apart from the lower intensity of emission due to quenching effects from the copper.

In both the free ligand and the metal-present system, addition of acetate results in the growth of a new emission band at ~490 nm (Figure 4.14). This band is attributed to the formation of an excimer formed by π-π interactions between ligands which is common for pyrene-containing species.[16]

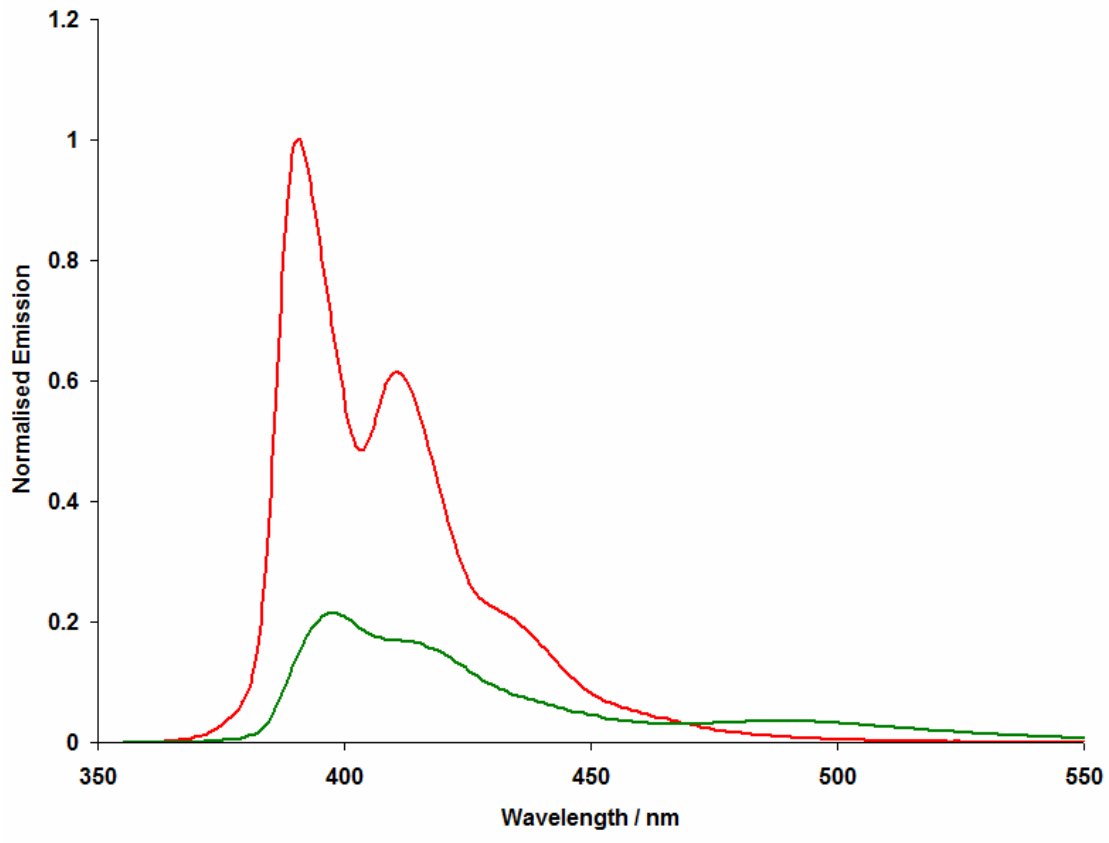

Figure 4.14 – Normalised emission spectra of free **4.2** (red) and with acetate (green).

4.4 Summary

In summary, we have successfully synthesised the pyrene-containing receptor molecule **4.2**, combining the optical response qualities of the pyrene group with the anion binding functionality of the urea, and further functionalised with a pyridine group for attachment to a core structure. While the low solubility and reactivity of **4.2** has prevented the successful attachment to an organic core, interactions with various metal salts have been investigated, and suggest that complexation of **4.2** to a metal centre is difficult, but possible, as UV/Visible absorbance spectroscopy shows the presence of a new absorbance band at 450-500 nm upon addition of copper (II) to the solution. This band is reduced upon addition of anions, as the anions interact more strongly with the metal, removing it before binding to the receptor. Fluorescence of **4.2** is modified by addition of anions, with more strongly bound anions causing a visible change in the wavelength of the emission, often coupled with a quenching by the majority of oxo-anions. Acetate seems able to encourage π-π interactions in solution, leading to the formation of a mildly fluorescent excimer even as it quenches the primary emission band.

Structurally, the presence of a pyrenyl functionality allows for a high degree of π stacking to occur, and this is the dominant interaction in the formation of the crystal, as evidenced by the twisting of the pyridyl-urea group and reformation of the urea tape motif, rare in aryl ureas containing electron-withdrawing substituents such as a pyridyl group.

Difficulties were found in the metal-binding studies in that it is difficult to conclusively prove which species is present in the solutions, whether binding occurs through a ML_n complex (where n can feasibly be any integer from 1 to 6), or even some more complex species. The presence of multiple equilibria caused by the

lability of the metal ion before anions are even considered highlights some of the problems that this method of creating an anion receptor by simple ligand-to-labile-metal interactions experiences. To try and avoid this issue, a range of well-definable capped ML_3 systems were considered, based on the much less labile ruthenium(II) metal ion. This work is detailed in the next chapter.

4.5 Experimental Details

Pyreneureidopyridine (PUP) 4.2:

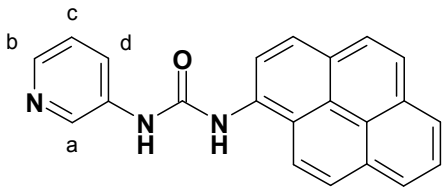

Nicotinoyl azide (0.31 g, 2.5 mmol), synthesised according to earlier method (Page 114), in solution in Et_2O, was added to acetonitrile (25 ml) and the ether removed under gentle vacuum. The acetonitrile solution was then heated to 70 ^oC with stirring for 30 mins. 1-Aminopyrene (0.5 g, 2.3 mmol) was added to the solution and the mixture heated to reflux for 18 hours with stirring, with the product precipitating from solution as a grey powder upon cooling, which was filtered and washed with diethyl ether. Yield 0.76 g, 2.25 mmol, 98%. ^1H NMR (DMSO-d_6, J/Hz, δ/ppm): 9.29 (s, 2H, NHa/b), 8.68 (s, 1H), 8.55 (d, J = 8.4, 1H), 8.33 (d, J = 9.3, 1H), 8.29 – 8.16 (m, 5H), 8.16 – 7.97 (m, 4H), 7.34 (dd, J = 4.7, 8.3, 1H). $^{13}C\{^1H\}$ NMR (DMSO-d_6, δ/ppm): 121.53 (C2), 124-132 (12 signals, pyrene Cs), 133.09 (C3), 136.77 (C1), 140.53 (C5), 143.43 (C4), 153.60 (C6). ESI^+-MS: m/z 338.3 $[M+H]^+$, 674.9 $[2M+H]^+$. Anal. Calc. for $C_{22}H_{15}N_3O$: C, 78.32; H, 4.48; N, 12.46. Found: C, 77.61; H, 4.55; N, 12.33. IR (cm^{-1}): 2987 (N-H stretch), 1624 (C=O stretch).

Metal-bound PUP Systems:

Synthesis of metal-templated systems involved dissolution of PUP (0.05 g, 0.015 mmol) into acetonitrile (5 ml), with the aid of heating to ensure complete dissolution. Addition of a metal salt in a 2:1 PUP:metal ratio generally caused precipitation of a powder, analysed by elemental analysis.

2 PUP + $AgNO_3$ → $Ag(PUP)_2.NO_3$: Anal. Calc. for $C_{44}H_{30}N_7O_5Ag$: C, 62.57; H, 3.58; N, 11.61. Found: C, 57.93; H, 3.81; N, 10.48. Anal. Calc. for $C_{44}H_{30}N_7O_5Ag.4H_2O$: C, 57.65; H, 4.18; N, 10.70.

2 PUP + $CuCl_2$ → $Cu(PUP)_2.Cl_2$: Anal. Calc. for $C_{44}H_{30}N_6O_2CuCl_2$: C, 65.30; H, 3.74; N, 10.39. Found: C, 60.54; H, 3.77; N, 10.48. Anal. Calc. for $C_{44}H_{30}N_6O_2CuCl_2.CH_3CN.3H_2O$: C, 61.09; H, 4.35; N, 10.84.

2 PUP + $Cu(BF_4)_2$ → $Cu(PUP)_2.(BF_4)_2$: Anal. Calc. for $C_{44}H_{30}N_6O_2Cu(BF_4)_2$: C, 57.95; H, 3.32; N, 9.22. Found: C, 58.21; H, 3.81; N, 9.08.

MS: Attempts to detect the active species in the PUP + 3 $M(OTf)_2$ solutions used during the spectroscopic titrations using mass spectrometry showed only the presence of the $[PUP+H]^+$ species at m/z 338.1 and the $[(PUP)_2+H]^+$ species at m/z 675.3 under positive mode. Negative mode showed only the presence of triflate at m/z 149.1.

Crystal Data:

Crystals were grown from **4.2** in Methanol/Chloroform (1:1 ratio, 2 ml) by slow evaporation of the solvent.

Crystal data for **4.2**: $C_{22}H_{15}N_3O_2$, M = 353.37, yellow needles, 0.02 × 0.01 × 0.2 mm^3, monoclinic, space group $P2_1/c$ (No. 14), a = 18.480(5), b = 4.5835(12), c = 23.532(6) Å, β = 112.718(5)°, V = 1838.6(8) $Å^3$, Z = 4, D_c = 1.277 g/cm^3, F_{000} = 736, MoKα radiation, λ = 0.71073 Å, T = 173(2)K, $2\theta_{max}$ = 56.4º, 8029 reflections collected, 3423 unique (R_{int} = 0.0750). Final *GooF* = 1.788, *R1* = 0.1371, *wR2* = 0.3228, *R* indices based on 1829 reflections with I >2σ(I) (refinement on F^2), 245 parameters, 0 restraints. Lp and absorption corrections applied, μ = 0.084 mm^{-1}.

4.6 References

1. M. H. Filby, S. J. Dickson, N. Zaccheroni, L. Prodi, S. Bonacchi, M. Montalti, C. Chiorboli, M. J. Paterson, T. D. Humphries and J. W. Steed, *J. Am. Chem. Soc.*, 2008, **130**, 4105-4113.
2. C. Walsdorff, W. Saak and S. Pohl, *J. Chem. Res. (S)*, 1996, 282 - 283.
3. L. O. Abouderbala, W. J. Belcher, M. G. Boutelle, P. J. Cragg, M. Fabre, J. Dhaliwal, J. W. Steed, D. R. Turner and K. J. Wallace, *Chem. Commun.*, 2002, 358-359.
4. V. Amendola, L. Fabbrizzi, C. Mangano, P. Pallavicini and M. Zema, *Inorg. Chim. Acta*, 2002, **337**, 70-74.
5. P. Blondeau, A. van der Lee and M. Barboiu, *Inorg. Chem.*, 2005, **44**, 5649-5653.
6. V. J. Catalano, M. A. Malwitz and A. O. Etogo, *Inorg. Chem.*, 2004, **43**, 5714-5724.
7. S. K. Ghosh, J. Ribas and P. K. Bharadwaj, *Cryst. Eng. Comm.*, 2004, **6**, 250-256.
8. D. R. Turner, E. C. Spencer, J. A. K. Howard, D. A. Tocher and J. W. Steed, *Chem. Commun.*, 2004, 1352-1353.
9. K. J. Wallace, W. J. Belcher, D. R. Turner, K. F. Syed and J. W. Steed, *J. Am. Chem. Soc.*, 2003, **125**, 9699-9715.
10. D. R. Turner, M. J. Paterson and J. W. Steed, *J. Org. Chem.*, 2006, **71**, 1598-1608.
11. N. Qureshi, D. S. Yufit, J. A. K. Howard and J. W. Steed, *Dalton Trans.*, 2009, 5708-5714.
12. A. Camerman, A. Hempel, D. Mastropaolo and N. Camerman, *Acta Cryst. C-Crystal Structure Communications*, 2006, **62**, O190-O192.
13. Y. L. Chang, M. A. West, F. W. Fowler and J. W. Lauher, *J. Am. Chem. Soc.*, 1993, **115**, 5991-6000.
14. S. J. Dickson, A. N. Swinburne, M. J. Paterson, G. O. Lloyd, A. Beeby and J. W. Steed, *Eur. J. Inorg. Chem.*, 2009, 3879-3882.
15. R. A. Binstead, *SPECFIT*, (1996) Spectrum Software Associates, Chapel Hill, NC, USA.
16. F. M. Winnik, *Chem. Rev.*, 1993, **93**, 587-614.

5. Octahedral Metal-Templated Tripodal Receptors

5.1 Aims

The use of octahedral metal centres as the core of a tripodal anion receptor compound has already received some attention owing to the well-defined geometries possible with the inclusion of a metal.[1-4] Generation of a symmetric ML_3 receptor can be achieved in one of two ways. One is to coordinate three ditopic ligands in a manner related to the well-documented ruthenium or iridium tris-bipy complexes.[5-7] Substitution onto the bipy (2,2-bipyridine)[8-11] or replacement of one bipy group with a similar species, for example biimidazole,[12-13] can allow for pendant functional groups which can contain anion binding moieties in a suitable arrangement to allow binding to occur. The second method for generating a ML_3 receptor complex can be more difficult, since it relies on blocking three coordination sites in a facial (*fac*) manner such that the opposite three sites are positioned correctly to give the best organisation for a receptor species. The best method for achieving such blocking is through the use of a tridentate face-capping ligand, often an aromatic species,[14-16] heterocycle,[17-18] or claw-like tridentate ligand.[19-20] Such a capped metal leads to the range of complexes known as 'half-sandwich' or 'piano-stool' complexes, named for their distinctive three-legged and often flat-topped appearance (Figure 5.1).

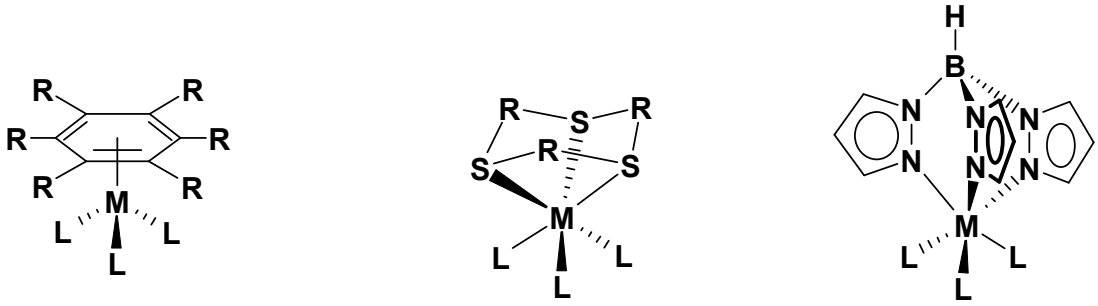

Figure 5.1 – Examples of 'piano-stool' coordination complexes.

The choice of metal is also important – smaller metals tend to favour formation of simple MX_n salts over ML_n complexes, and generally very little has been attempted in basing such a receptor on any of the first-row transition metals, instead focussing on the less labile heavier metals, such as iridium, platinum and ruthenium. Such metals have a history in catalysis,[21-22] and coordinate a wide array of potential ligands.

Based on previous work by Dickson and colleagues,[23] it was decided to synthesise a range of similar ruthenium-based tripodal receptor complexes. This earlier work looked into coordination of a number of substituted pyridines to an aryl-coordinated ruthenium(II) core. They found that formation of the full tri-substituted $[ML_3]^{2+}$ receptor was hampered by the low affinity to attachment of a third ligand to the metal, leading instead to formation of the favoured $[ML_2X]^+$ dipodal complex. Thus, our aim was to circumvent this problem by replacing the aromatic p-cymene capping group with the 1,4,7-trithiacyclononane ([9]ane-S_3) heterocycle first reported by Schröder *et al*.[24] and later by Roche and coworkers[25-26] who were the first to report coordination of three pyridines to the capped ruthenium centre. Their crystallographic evidence showed the retention of the octahedral nature of the Ru(II) core, with the three pyridines remaining at 90^o to one another, to the extent that the use of 4,4-bipyridine as the ligating species led to the formation of a self-assembled cubic structure, with the ([9]ane-S_3)Ru(II) fragments forming the vertices of this cube.[25] It was hoped, therefore, that the use of this ([9]ane-S_3)Ru(II) core would allow for the synthesis of tripodal receptors of well-defined geometry. To that end, a number of 3-substituted pyridine ligands were synthesised (Figure 5.2), containing either a secondary amine or a urea as the anion binding functionality.

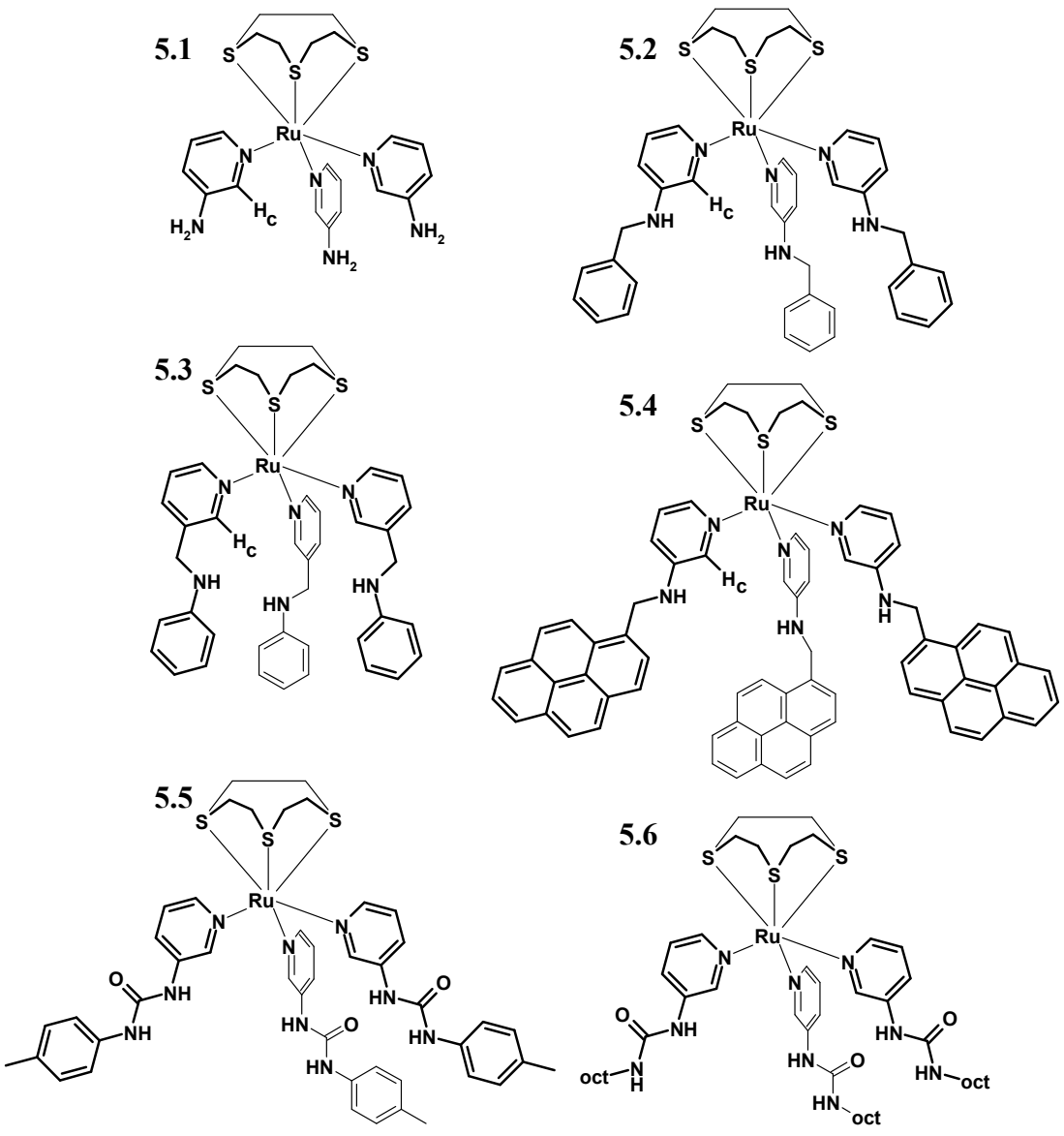

Figure 5.2 – $\{([9]ane\text{-}S_3)Ru\}^{2+}$ receptor complexes synthesised in this study. Counter-ions are PF_6.

Synthesis of the [9]ane-S_3-capped ruthenium precursor is achieved fairly readily by reacting $[RuCl_2(DMSO)_4]$, formed by reaction between $RuCl_3$ and DMSO,[27] with the thioether ring. The thioether displaces three of the coordinated DMSO molecules and has been shown to remain coordinated to the ruthenium centre with a high degree of stability, though coordinated pyridines can be displaced in the presence of

acetonitrile, due to the more favourable formation of the acetonitrile-coordinated complex.[26] Metathesis of the counter anions from chloride to hexafluorophosphate was achieved through addition of $AgPF_6$ and subsequent removal of the precipitated AgCl, and was carried out before the receptor ligands were added. In most cases, the complexes appear various shades of green in colour, with the exception of the pyrene-containing **5.4**, which is yellow-ochre in colour. Some problems with purification arose during synthesis of the urea-based receptors **5.5** and **5.6** due to the similar solubilities of receptor complex and unbound ligand. These difficulties arose due to the need to have an excess of the ligand present in solution during the reaction to favour formation of the tripod – a threefold excess was found to be insufficient, producing a mixture of three-armed receptor, two-armed receptor, and free ligand. Addition of 3.5-4 equivalents led to a greater yield of three-armed receptors, but required removal of the excess ligand. For complex **5.5** this was achieved by dissolution of the crude product in acetone and addition of cold diethyl ether until the complex precipitated. Complex **5.6** required more careful solvent balance, eventually involving a mixture of acetone, ether and ethyl acetate to remove the majority of the excess ligand by recrystallisation, although some ligand is still found to be present by ^{1}H-NMR.

Receptors **5.2** and **5.3** are isomers of one another, the difference being in the placement of the N-H group. Complex **5.3** potentially has a smaller binding pocket within the receptor due to the extra distance from the core and the flexibility provided by the methylene bridge allowing a greater degree of encapsulation of an anion. Receptor **5.4**, with its pyrene functionalities, was hoped to possess similar fluorescent properties to related pinwheel compounds.[28]

While related *p*-cymene containing complexes were found to be stable as the dipodal species,[23] formation of the tripodal receptor proved difficult, as the dipodal species was found to be more stable. By constrast, our receptors, based on the [9]ane-S_3-capped ruthenium, are found to be stable to this solvent decomposition to a far greater degree. Studies by ^{1}H-NMR over a period of time showed that even after a period of one week, only a small proportion (<10%) of the tripodal complex had degraded. Even after a number of weeks, this ratio remains fairly constant, suggesting equilibration between dipod and tripod.

During the synthesis of **5.1**, the final complex was seen to crystallise from the ethanol:water (1:1) mix used during the synthesis as dark green needles (Figure 5.3).

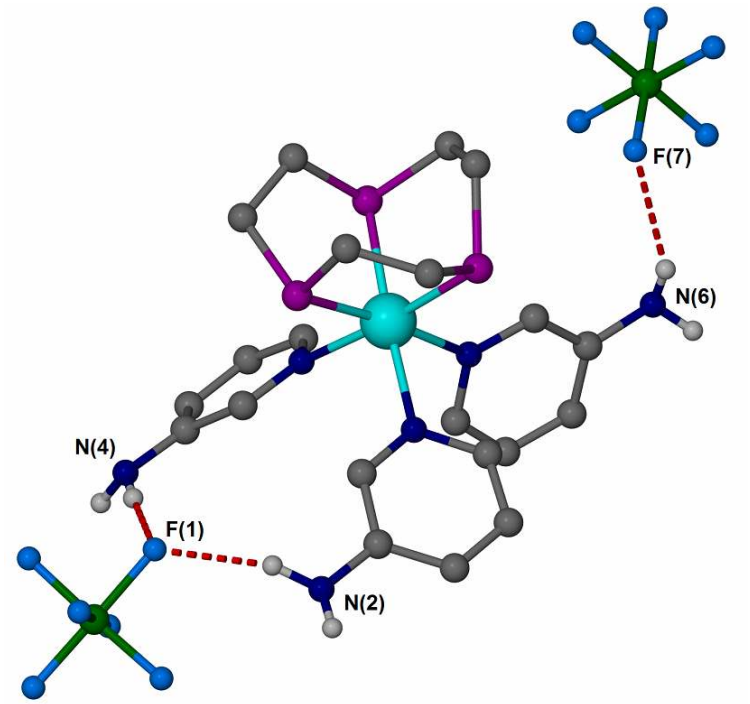

Figure 5.3 – X-ray molecular structure of **5.1**.$(PF_6)_2$ complex. Carbon hydrogen atoms removed for clarity. Selected H-bond distances (Å): N(4)H-F(1) 3.359(3); N(2)H-F(1) 3.138(3); N(6)H-F(7) 3.408(3).

The structure adopts space group $P\bar{1}$, with an inversion centre inside the desired binding pocket generated by the three aminopyridine arms (Figure 5.4). These two symmetry-equivalent complexes are held together by the hydrogen bond interactions between the aminopyridine amine groups and one of the PF_6 counterions (and its symmetry-equivalent through the point of inversion). This same anion also interacts with the thioether ring of another equivalent of receptor, in a similar manner to that first described by Bedford and coworkers,[29] such that the anion is involved in six hydrogen bonds, three from N-H groups and three from C-H groups (CH-anion distances in the range of 3.1 – 3.5 Å). The second PF_6 anion only experiences one N-H hydrogen bond (that to N(6)H), but is surrounded by three thioether rings, with which the anion can interact through potentially six C-H bonds.

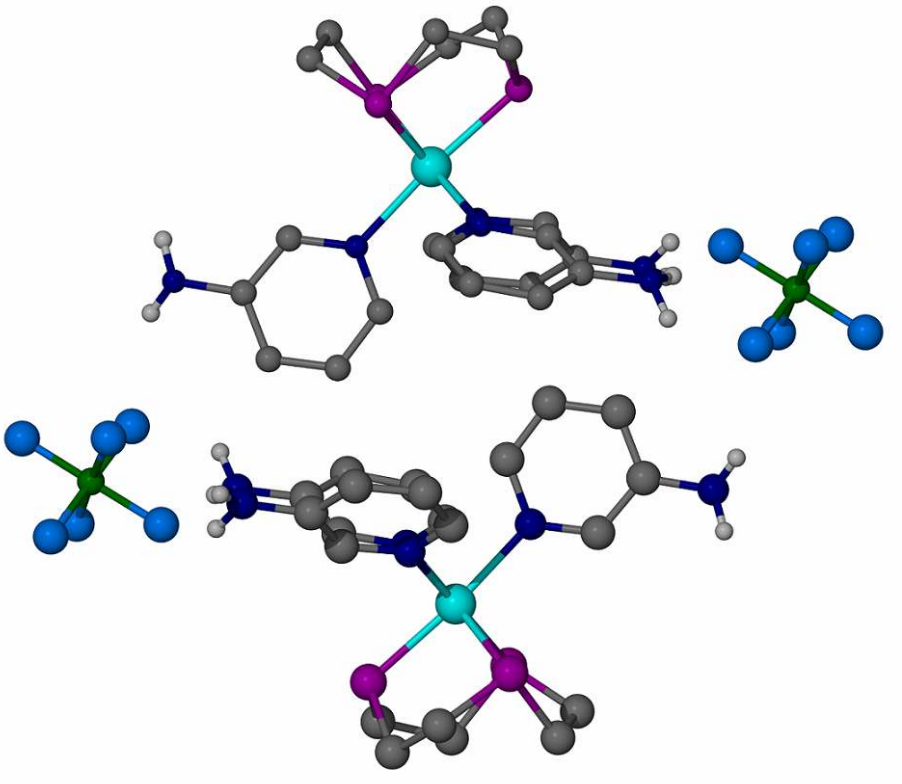

Figure 5.4 – Packing arrangement of two **5.1** complexes around a common cavity. C-H atoms and second PF_6 counter anion removed for clarity.

The structure shows that the receptor complex, at least in the solid state, exists in the opposite conformation to that expected, with the aminopyridine N-H groups pointing away from a common cavity beneath the metal centre, though this may be an effect of the solid state packing or the increased size of a PF_6 anion. It seems plausible that rotation about the Ru-N axes could lead to a situation in which three amine N-H groups point to a central position, although such an arrangement may prove unfavourable due to the possibility of steric interference between the C-H protons adjacent to both the pyridine nitrogen atom and the amine.

5.2 Anion Binding Studies

Binding studies were performed on the receptor complexes using ^{1}H-NMR spectroscopic titrations, using the same methods as for other receptors. The solvent system chosen was 30% DMSO-d_6 in $CDCl_3$. The inclusion of DMSO was essential to retain solubility of receptor **5.1** during the titration, as addition of anions to the solution in $CDCl_3$ or acetone-d_6 caused precipitation of the complex. For comparison's sake, the same solvent system was used throughout the experiments.

Complex **5.1** showed severe broadening of the amine N-H resonances due to rapid exchange upon addition of anions caused either by rotation of the amine group about the C-N bond or by dissociation of H^+ from the amine. Similar difficulties were found during experiments with **5.3**, which also experiences an increasingly significant exchange process as the titration progresses. In these cases, the neighbouring pyridyl C-H signal (Hc, Figure 5.2) alone was followed during the titration, while with the other amine receptors (**5.2, 5.4**) the N-H resonance remained sharp in the NMR spectrum and thus could be followed. In titrations with **5.4**, only the N-H resonances were plotted, as the pyridyl C-H resonance is obscured by the pyrene C-H resonances.

Titrations with urea-based receptor **5.5** followed the urea N-H resonances exclusively. Titration curves are shown below (Figures 5.5-5.9) and results tabulated collectively (Table 5.1). Due to purification issues detailed earlier, no titration data on **5.6** could be collected.

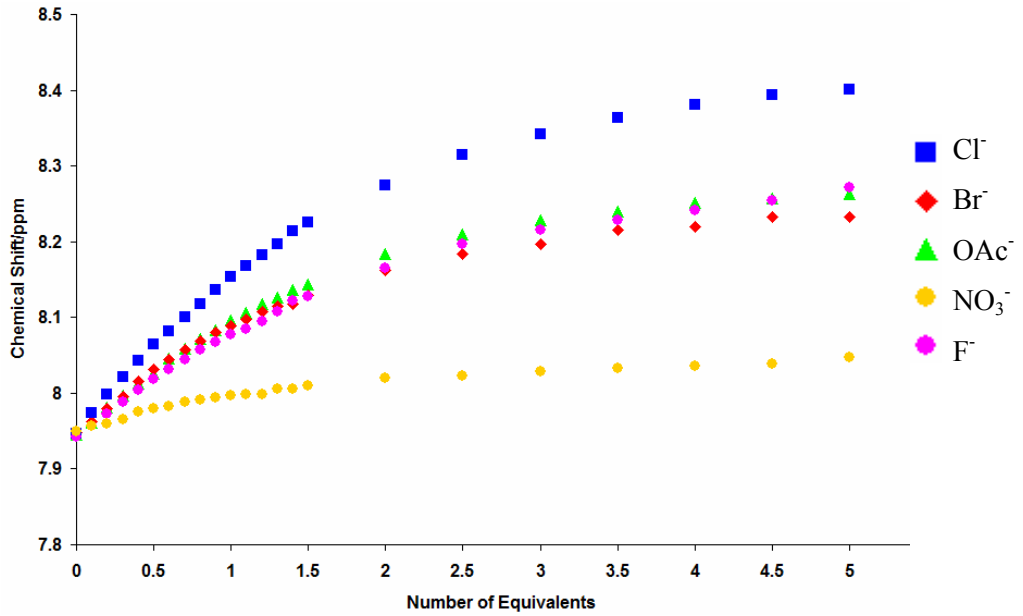

Figure 5.5 – Chemical shift changes of pyridine C-H proton of **5.1** with a variety of anions.

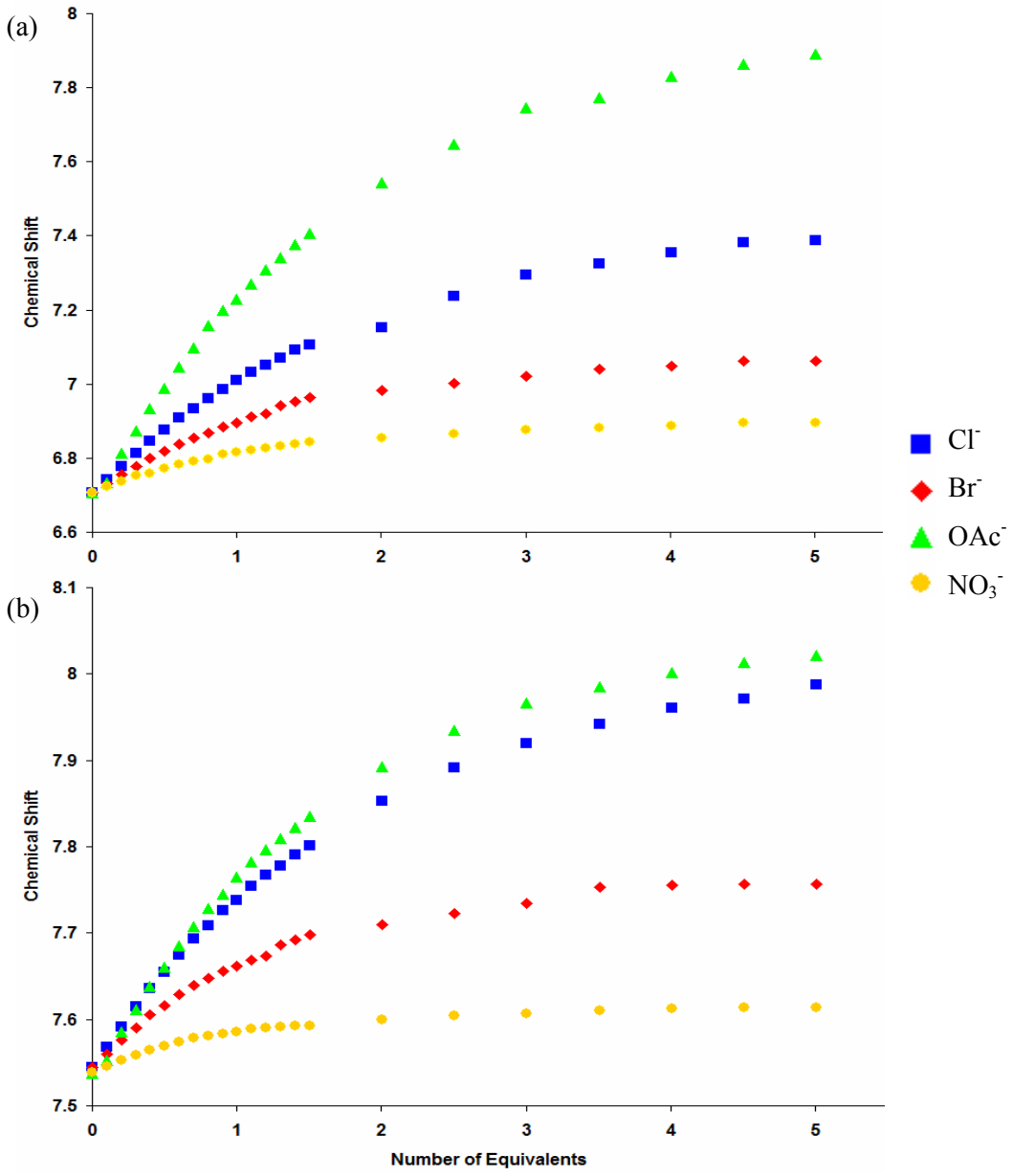

Figure 5.6 - Chemical shift changes of (a) amine N-H and (b) pyridyl C-H protons of **5.2** with a variety of anions.

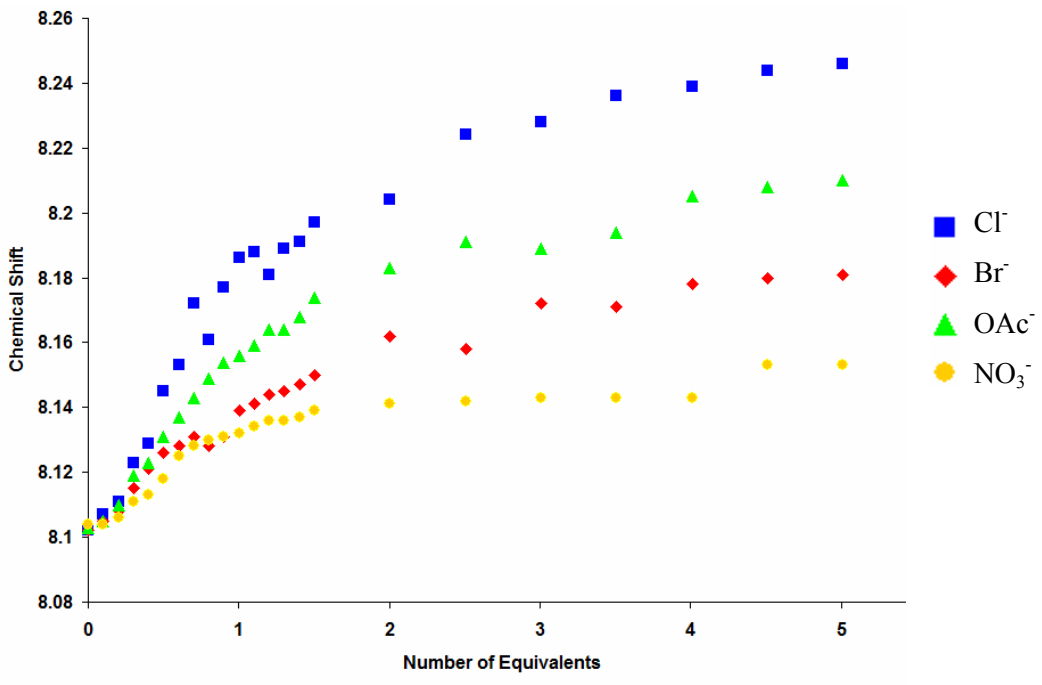

Figure 5.7 - Chemical shift changes of pyridyl C-H protons of **5.3** with a variety of anions.

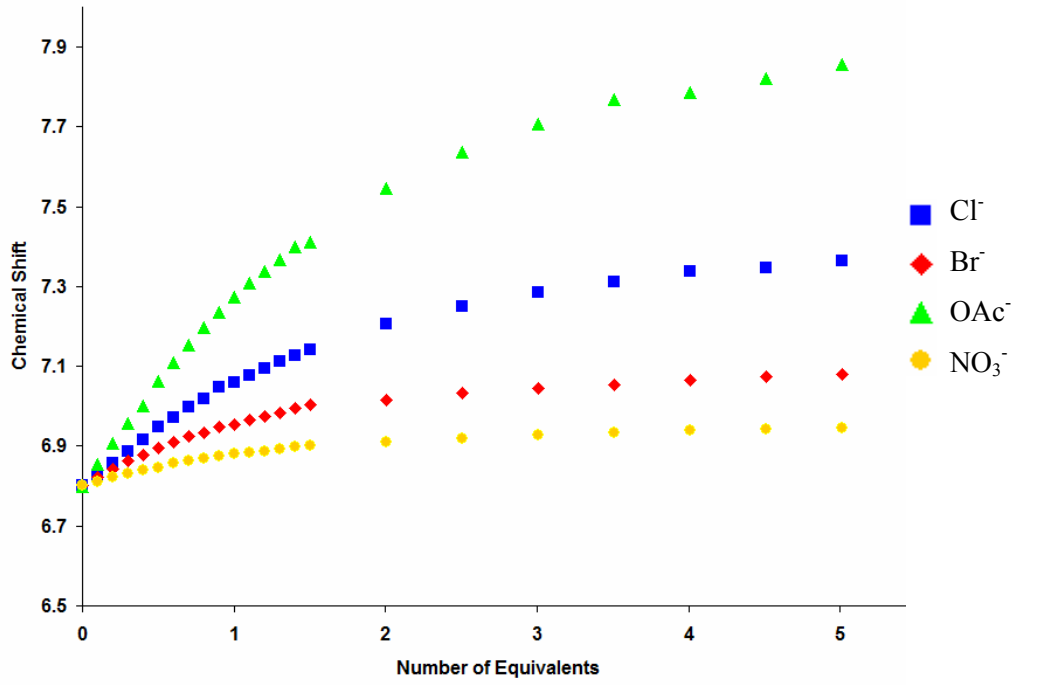

Figure 5.8 - Chemical shift changes of amine N-H protons of **5.4** with a variety of anions.

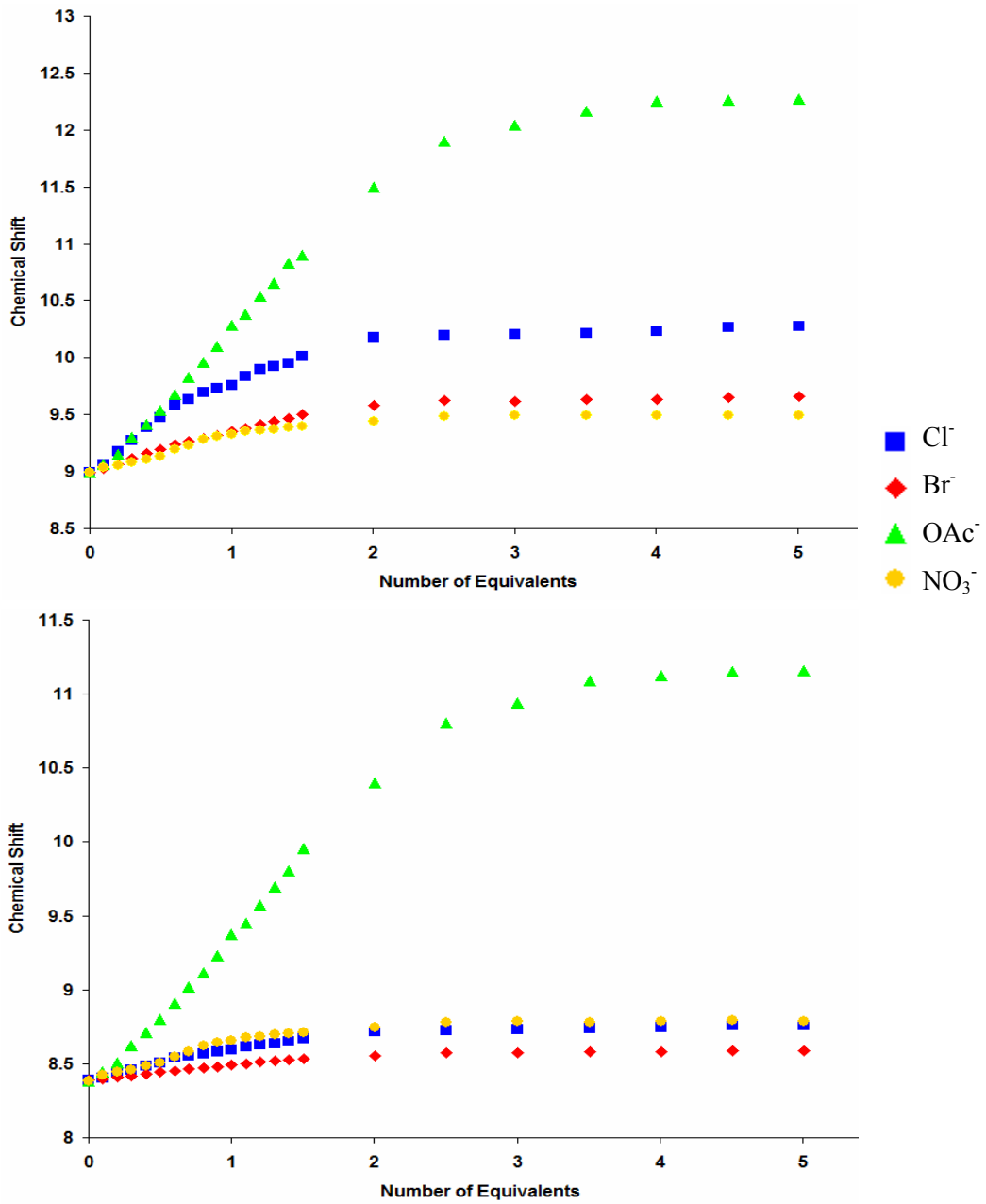

Figure 5.9 - Chemical shift changes of urea N-H protons of **5.5** with a variety of anions.

Guest		Host **5.1**	**5.2**	**5.3**	**5.4**	**5.5**
Acetate	β_1	2.02(1)	2.05(1)	2.03(1)	2.36(1)	2.5(1)
	β_{12}	3.83(1)	3.90(2)	N/A	4.05(1)	5.84(3)
	(β_2)	1.81	1.85	-	1.69	3.34
Bromide	β_1	2.04(8)	2.29(8)	1.82(1)	2.13(2)	3.38(5)
	β_{12}	N/A	N/A	N/A	N/A	6.52(3)
	(β_2)	-	-	-	-	3.14
Chloride	β_1	1.76(1)	1.73(1)	2.11(8)	2.62(1)	2.32(3)
	β_{12}	3.52(1)	3.46(9)	N/A	4.10(1)	5.9(1)
	(β_2)	1.76	1.73	-	1.48	3.58
Fluoride	β_1	< 1	N/A	N/A	N/A	N/A
Nitrate	β_1	1.86(2)	2.33(6)	2.5(1)	2.05(2)	2.05(2)

Table 5.1 – β values for ([9]ane-S_3)Ru-based hosts, showing 1:1 and 1:2 binding modes, refined using the HypNMR 2006 software.[30] Titrations of receptor **5.1** with fluoride showed poor binding, so this anion was omitted from further studies. β_2 is calculated by subtracting β_1 from β_{12} (where applicable) and represents the second binding step.

From the titration data, it is possible to compare the anion affinities of the receptor complexes. There is only a small difference between the binding affinities of **5.1** and **5.2**, suggesting that the addition of a benzyl group to the receptor amine has only a marginal effect on the anion binding of the receptor. If anything, the benzyl-appended **5.2** shows a lower affinity for acetate and chloride and a higher affinity for bromide and nitrate over the reference compound **5.1**. Interestingly, binding of both of these anions shows little variation in strength for the addition of the first and second equivalent of anion, especially for chloride, which shows that complexation to

the second anion is equally as likely as binding to the first. This effect may be due to replacement of the PF_6 counterions and balancing of the 2+ charge of the complex, favoured by chloride and acetate being more strongly bound than the hexafluorophosphate.

Changing the position of the N-H group has a much more pronounced effect on the receptor properties –anions are typically found to bind slightly weaker with **5.3** than **5.2**, likely due to the more enclosed cavity of the receptor binding site, though **5.3** seems to show a rather unusually high binding to nitrate over the other anions, although when considering such small shifts the magnitude of the error may make this an erroneous result. The inclusion of the sterically more demanding pyrenyl functionality seems to favour binding of the receptor to chloride (and to a lesser extent acetate), with chloride binding to receptor **5.4** approximately ten-fold stronger compared to the smaller **5.1** – **5.3** receptors. Unusually, receptor **5.5** appears to show strongest binding with bromide over the other anions studied, despite this anion showing only a small chemical shift throughout the titration. Likewise, acetate was found to give the greatest chemical shift but yields relatively low binding constants. This may seem counter-intuitive, but the strength of the binding is not dependent on the extent of the chemical shift, but rather on the degree of curvature – a strongly bound anion may cause a small shift, but will arrive at this maximum value quickly. The higher binding to bromide over acetate is likely due to the size and shape complementarity of the receptor to the anion – the spherical bromide is able to interact better with the three binding groups, but has only a small effect on the electronic shielding of the binding protons.

The complexes show greater binding than similar monopodal receptors,[23] which are found to bind only very weakly, if at all.

Job plot analyses on the receptors suggested primarily 1:1 binding, consistent with expected values, but with the maxima slightly skewed toward 1:2 binding in many cases (Figure 5.10), in good agreement with the refined binding constants.

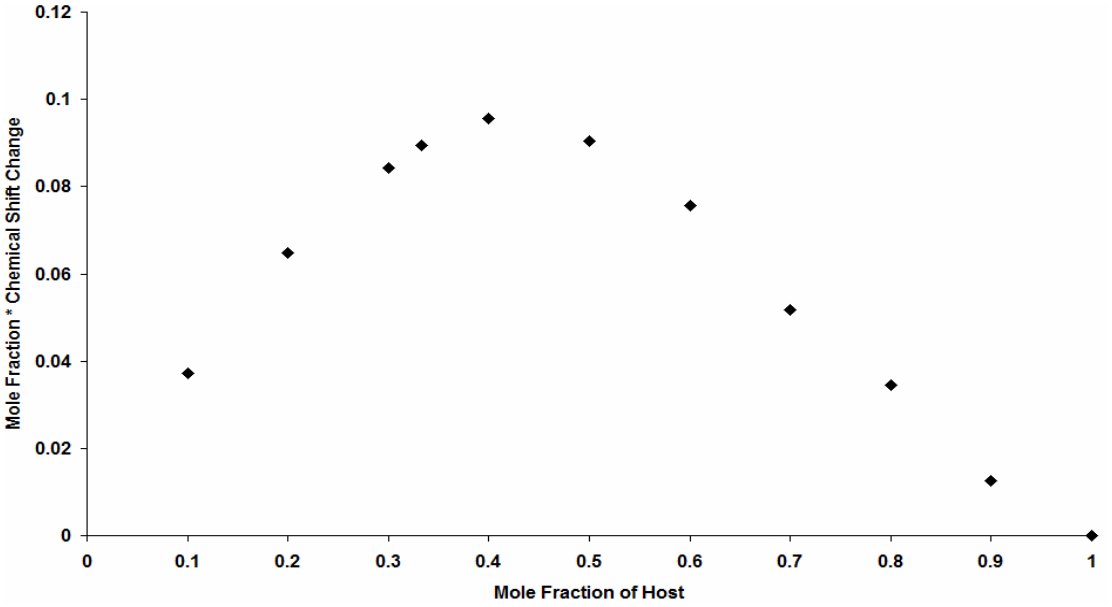

Figure 5.10 – Example Job plot for receptors with chloride, bromide and acetate (example shown is **5.1** with chloride).

The presence of a 1:2 host:guest species in many cases may indicate the possibility of externally coordinated anions similar to the crystal structure of **5.1**, and such an arrangement would be expected to give a noticeable differentiation in the chemical shifts of N-H groups between the single N-H---anion and the bifurcated N-H---anion---H-N interactions, or at least a broadening of the signal consistent with exchange processes experienced by the three binding groups as they average between the two binding states. Since such an effect is observed in the case of receptors 5.1 and 5.3, it may be that such is the method of binding, though the fact that there is only one visible N-H resonance for receptors **5.2**, **5.4** and **5.5**, and that it remains sharp suggests that this external binding is not the correct mode for these receptors, unless such a process occurs faster than the NMR timescale. Instead, it seems likely that

there exists a second binding site in the thioether heterocycle used as the capping group, as suggested by the crystal structure of receptor **5.1**, and originally postulated by Bedford and colleagues of a related (9)ane-S_3-templated palladium complex.[29] This ring, owing to its geometry when coordinated to the metal centre, possesses a potential of six hydrogen-bond donor atoms in the C-H bonds which are made more acidic due to their proximity to the ring's sulphur atoms. Indeed, examining the change in environment experienced by these protons during the NMR titration experiments showed that they undergo noticeable shift of up to 0.5 ppm, though due to the presence of multiple signals from the tetrabutylammonium cations in the 1-3 ppm range, these shifts could not be followed accurately enough to provide additional data for the determination of binding constants.

5.3 Photometric Studies

Receptor **5.4** is expected to be fluorescent due to the presence of pyrenyl groups. Because of this, and with the well-defined geometry around the ruthenium core, it was possible to study the changes in the absorbance and emission spectra of the receptor with addition of anions. The complex shows an absorbance similar in structure to that of the free ligand from which it is assembled, albeit red-shifted slightly (Figure 5.11), suggesting a lowering in the excitation energy caused by coordination to the metal. As expected, absorbance intensity of **5.4** is approximately three times greater than that of the free ligand, due to the complex containing three ligand arms.

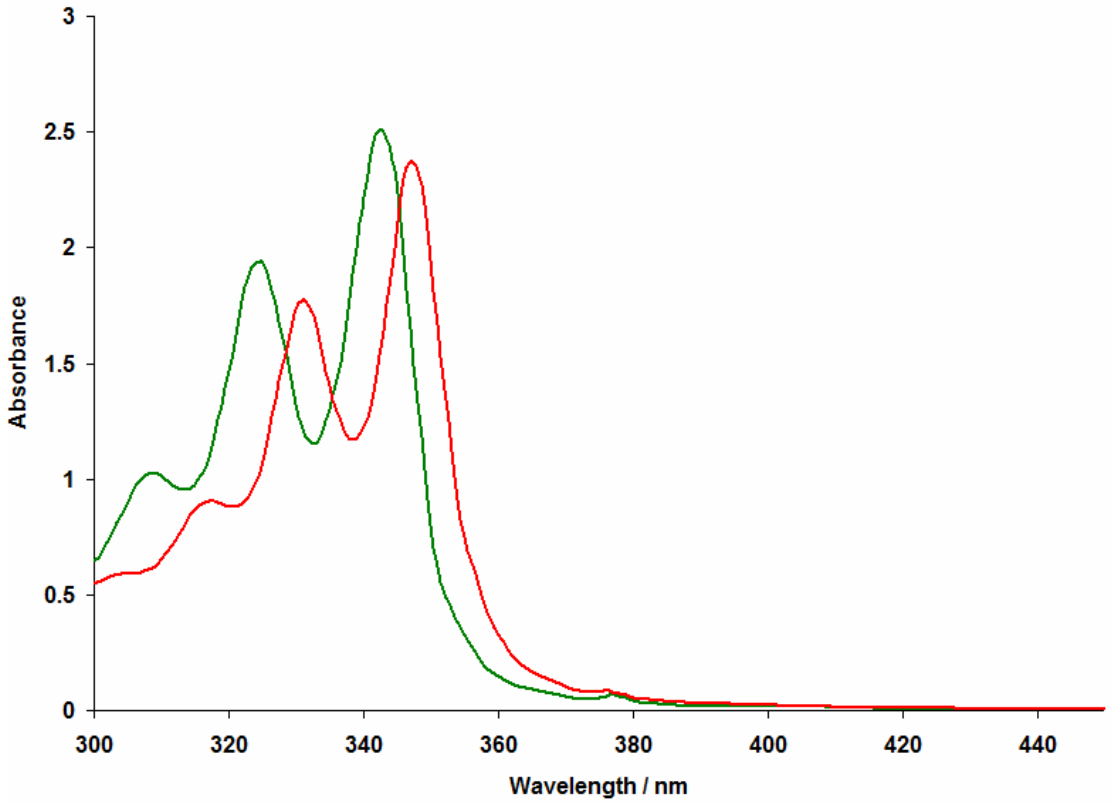

Figure 5.11 – UV/Visible absorption profiles of **5.4** (2 x 10^{-5} moldm^{-3}, red) and unbound 3-(1-pyrenemethylamino)pyridine (6 x 10^{-5} moldm^{-3}, green) in 30% DMSO in $CHCl_3$ solvent.

Addition of anions to the solution had a negligible impact on the absorbance of the complex (Figure 5.12), with only a slight difference in intensities observed, attributable to measurement error. This lack of detectable response to the addition of most anions indicates that binding of the complex to an anion does not affect the region of the complex responsible for the absorbance by any appreciable amount, perhaps unsurprising as binding takes place away from the pyrene functionality, with no accessible electronic pathway between the pyrene and the receptor core due to the bridging methylene, although it does imply that the expected pyrene-pyrene interactions either do not occur, or are perhaps already in place and are unaffected by the addition of anions.

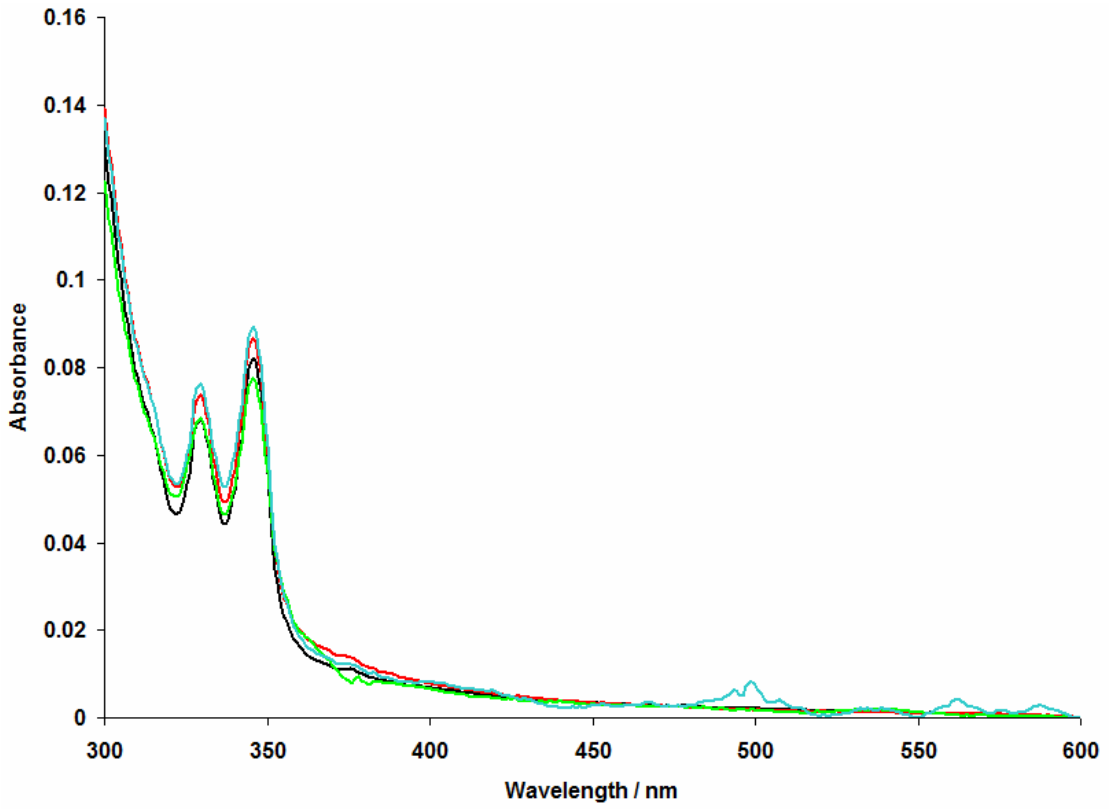

Figure 5.12 – UV/Visible absorbance profiles of **5.4** as the PF_6 salt (black), and with addition of 500 equivalents of chloride (green), acetate (blue) and bromide (red) at a concentration of 4 x 10^{-6} mol dm^{-3} in 30% DMSO in $CHCl_3$. Anions are TBA salts.

While the absoption spectra of **5.4** with most of the anions suggest that nothing detectable is happening, the emission spectra suggest quite the opposite. Addition of anions to **5.4**, when followed by fluorimetry, shows a remarkable change in the emission profile of the receptor complex. Excitation at the primary absorbance wavelength at 347 nm gives the initial emission profile of the complex, which shares similarities to the free ligand (Figure 5.13), with many of the emission bands remaining present at approximately the same wavelength, with the primary difference being in the intensities of the bands.

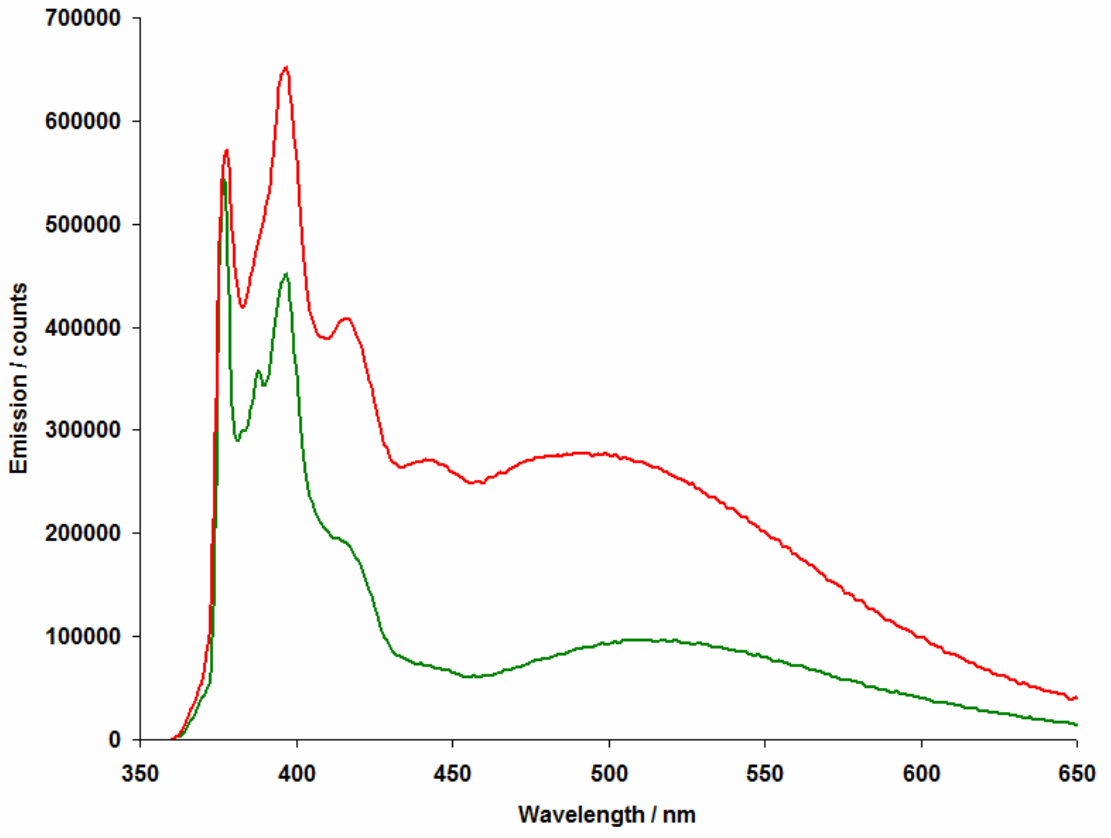

Figure 5.13 – Emission profiles for **5.4** (4 x 10^{-6} moldm^{-3}, red) and unbound 3-(1-pyrenemethylamino)pyridine (1.2 x 10^{-5} moldm^{-3}, green) in 30% DMSO in $CHCl_3$ solvent, excitation wavelength of 347 nm.

The most noticeable difference is in the drastic growth of the broad emission band around 500 nm. This is identified as an emission band from a pyrene-pyrene excimer, which is associative in the excited state and dissociative in the ground state, and is a common feature in pyrene-containing species.[31] The presence of this band is therefore not surprising, but rather it is the dramatically different intensity of this band that is of interest, since the amount of pyrene chromophore present in the solution should be the same in both cases. The most feasible explanation is that the band is enhanced by the pyrene groups being forced into close proximity to one another through their coordination to the metal, thus encouraging formation of this excimer complex.

Addition of anions to the solution of **5.4**, when followed by fluorimetry, at first glance appears to have a switch-on effect on the emission of the complex, with the emission intensity increasing to almost double the initial value, accompanied by a similar increase in the 500 nm excimer band. Further investigation into this enhancement, however, showed that this is not purely an anion driven enhancement – a similar emission to those found with anions is found from the complex alone at the reduced concentration experienced at the end of the titration experiment (Figure 5.14). The increase in emission at lower concentration suggests that some degree of self-quenching is taking place for receptor **5.4**, since the same effect is not observed for the free ligand.

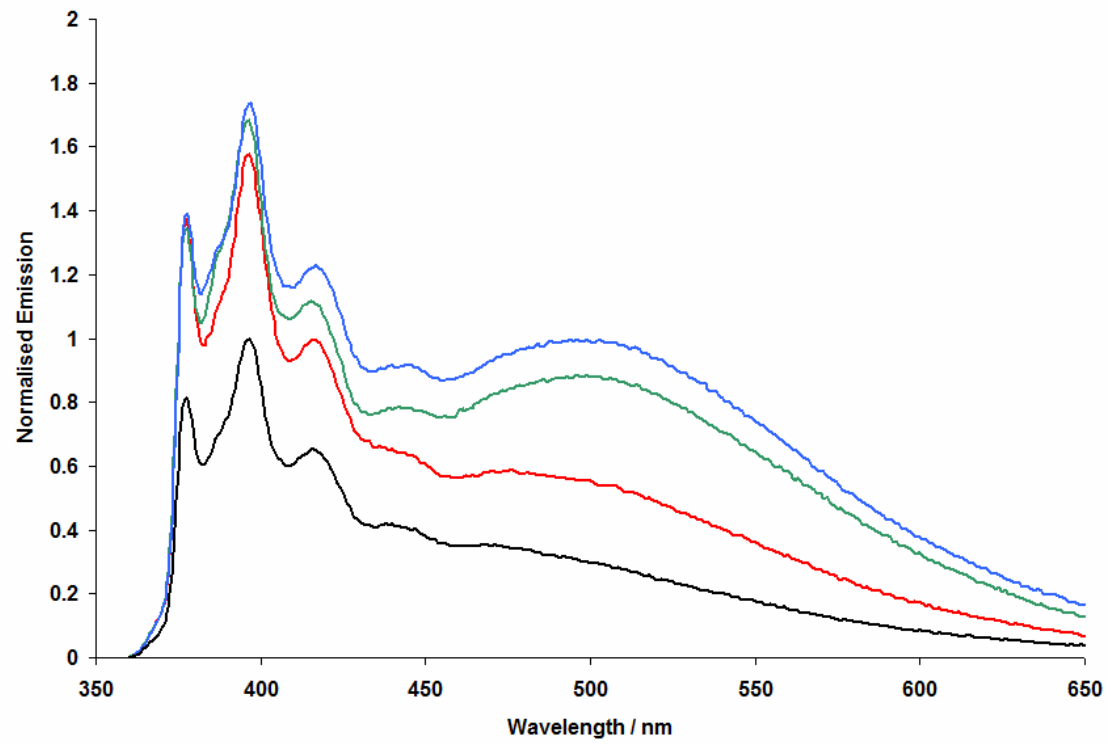

Figure 5.14 – Normalised emission profiles for **5.4** (red) and with chloride (green) and acetate (blue) at 4.3 x 10^{-5} moldm^{-3} in 30% DMSO in $CHCl_3$. All three normalised to the same standard (**5.4** at 5 x 10^{-5} moldm^{-3}, black).

In order to determine the degree of this self-quenching, the emission intensity of the complex was recorded at a wide range of concentrations, and in a varying ratio of solvent. Dilution of the complex, keeping the solvent ratio the same, was found to follow a non-linear progression, with the highest intensity of emission being observed at extremely low complex concentration (Figure 5.15). Lower than this critical concentration and the emission intensity falls off rapidly. Collecting absorbance data over the same range of concentrations shows a linear change in the absorbance with concentration.

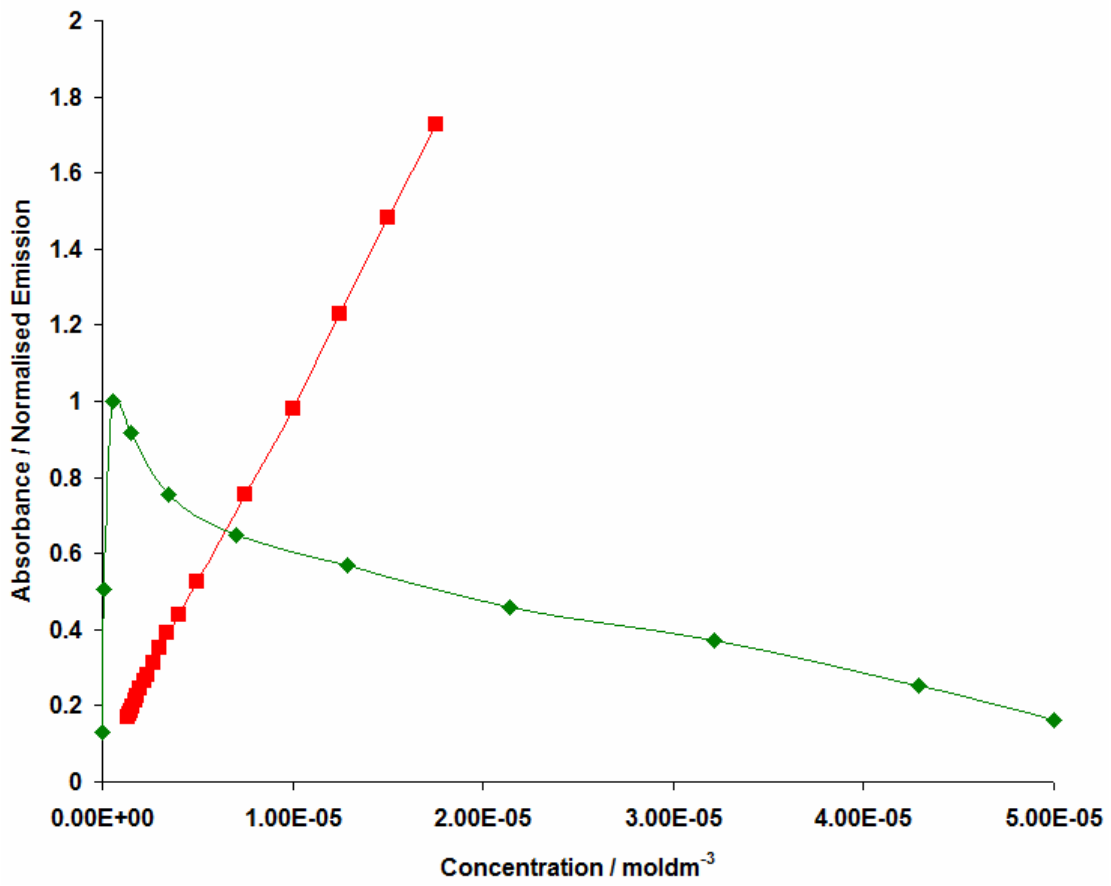

Figure 5.15 – Linear plots of 347 nm absorbance (red) and 397 nm emission (normalised, green) of **5.4** at varying concentrations in 30% DMSO in $CHCl_3$.

It was also found that the quenching was greater at lower DMSO content, and weaker with higher DMSO content, since the degree of solvation is an important factor – with more DMSO providing greater solvation of the complex, the quenching process is less pronounced. This concurs well with the concentration data, since lower concentrations are equivalent to greater solvation.

While the primary emission of the complex is thus mostly unaffected by the presence of anions, but rather by the concentration of the complex, the excimer emission band is certainly affected by anions, as can be seen in Figure 5.14. A large increase in the intensity of this band is observed, indicating that the pyrene-pyrene interactions are enhanced by binding to an anion, and since the same effect is not observed by titration

of anions into a solution of free 3-(1-pyrenemethylamino)pyridine, it must be caused by the close proximity of the pyrene groups in the complex. If the proposed binding model is to be believed, whereby one anion can bind in the cavity generated by the three amine groups, then inclusion of an anion within this cavity must in some manner orient the ligand arms in such a way as to enhance pyrene-pyrene interactions. Molecular modelling of the complex in the presence and absence of anions was carried out in an effort to find a likely method for this to occur. Figure 5.16 shows a postulated dimeric species formed by the interdigitation of the arms of two distinct **5.4** complexes around an encapsulated chloride anion, and displays evidence of π–π interactions between two of the six pyrene groups, with additional interactions between some pyrene and pyridine groups. The anion is held in place by a ring of six N-H···Cl hydrogen bonds.

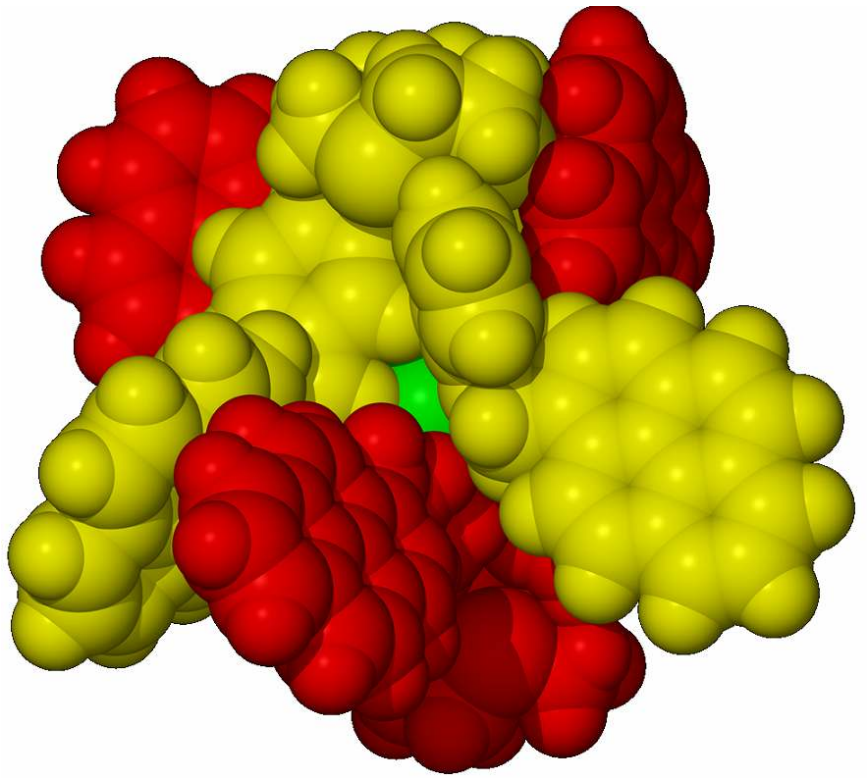

Figure 5.16 – Molecular model of the $[(\mathbf{5.4})_2.Cl]^{3+}$ clathrate, calculated using a HF/STO3G level of theory. Individual receptor **5.4** complexes coloured red and yellow, chloride is green, for clarity.

The formation of this capsule seems to agree with the crystal data found for receptor **5.1**, which shows two receptor complexes related across the central cavity by a inversion symmetry element in a similar manner, and it may be that Job plot analyses of the ^{1}H-NMR data, which showed a maximum between 0.33 and 0.5 mol. fraction, may in fact be pointing to the formation of this 2:3 host:anion species, with the other two anions binding through the exposed thioether C-H rings.

5.4 Summary

In summary, a range of 1,4,7-trithiacyclononane-capped ruthenium(II)-based anion receptor complexes have been synthesised. These receptors, in contrast to similar aromatic-capped ruthenium complexes, show a high resistance to degradation from the tripodal ML_3 species to a dipodal ML_2X species by solvent or anion, and often reach an equilibrium between the two forms, with the tripodal species favoured. Many of these receptors show two potential anion binding sites, one in the cavity generated between the three ligand arms and the second in the capping thioether ring, as evidenced by structural data of the reference receptor compound **5.1**.

The possible formation of a capsule compound in which the pyridine arms of each complex interdigitate, potentially encapsulating a small anion such as chloride through multiple N-H---anion hydrogen bond interactions is suggested by molecular modelling of the more pyrene-appended receptor **5.4**, which is reinforced by the evidence of the existence of an excimer in the emission spectra which is enhanced by addition of anions, and further reinforced by crystallographic data of receptor **5.1**. Receptor **5.4** also shows a degree of self-quenching which is more pronounced at higher concentrations, evidenced by the higher emission at lower concentrations down to a maximum emission at around 5×10^{-7} mol dm^{-3}. It may be that formation of the proposed capsule is the driving force for this fluorescent quenching, providing a radiative decay pathway that is not fluorescent.

5.5 Experimental Details

Synthesis of components:

Pyridine-containing ligands were synthesised according to pre-reported literature methods.[23, 28, 32-33]

([9]ane-S_3)$RuCl_2$.DMSO

$RuCl_3$ trihydrate (1 g, 3.8 mmol) was dissolved in the minimum amount of DMSO (2-3 ml) and the solution heated to boiling to remove any water from the solution. The DMSO solution was cooled and acetone (25 ml) was added, leading to precipitation of a dark orange material. Filtration of this material left an orange solution which gave the desired $RuCl_2(DMSO)_4$ as yellow crystals upon drying. Repeated dissolution of the dark orange precipitate with more DMSO/acetone with heating produced more of the yellow product. Highest yield 0.8 g, 1.6 mmol, 43%. Anal. Calc. for $C_8H_{24}S_4O_4RuCl_2$: C, 19.83; H, 4.99. Found: C, 19.84; H, 4.90.

This $RuCl_2(DMSO)_4$ (0.48 g, 1 mmol) was then dissolved in $CHCl_3$ (25 ml) in a round-bottomed flask fitted with a reflux condenser. 1,4,7-trithiacyclononane ([9]ane-S_3) (0.2 g, 1.1 mmol) was added and the solution heated to reflux for 90 mins with stirring, leading to the precipitation of the capped ([9]ane-S_3)$RuCl_2$.DMSO as a yellow-orange solid. Highest yield 0.36 g, 0.84 mmol, 84%. Anal. Calc. for $C_8H_{18}S_4ORuCl_2$: C, 22.32; H, 4.21. Found: C, 22.05; H, 4.08.

Synthesis of receptors:

([9]ane-S_3)Ru(3-aminopyridine)$_3$.2PF_6:

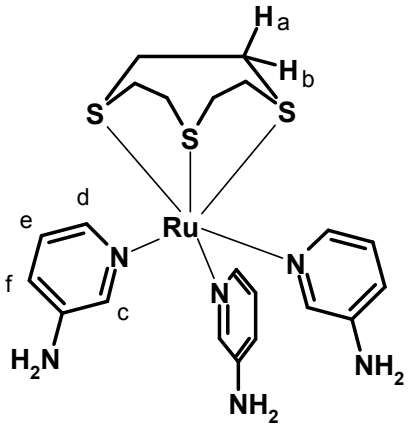

([9]ane-S_3)$RuCl_2$.DMSO (0.17 g, 0.4 mmol) was dissolved in ethanol/water (1:1, 30 ml) with slight warming of the solution. Silver hexafluorophosphate (0.21 g, 0.85 mmol) was added and the solution stirred at 60°C for 1 hour, over which time the formation of silver chloride could be observed as a silvery-grey precipitate. Filtration of this salt left a yellow solution, to which was added 3-aminopyridine (0.11 g, 1.2 mmol). The solution was then heated to reflux for 16 hours, during which the colour was observed to go from yellow to blue-green. Cooling and slow evaporation of the solvent led to the formation of the product as deep green needle-shaped crystals. Yield 0.13 g, 0.15 mmol, 37%. ^{1}H NMR (DMSO-d_6, J/Hz, δ/ppm): 2.53 – 2.90 (m, 12 H, H_a/H_b), 5.79 (s, 6 H, NH_2), 6.98 – 7.14 (m, 6 H, H_e/H_f), 7.41 (d, J = 4.5, 3 H, H_d), 7.73 (d, J = 2.2, 3 H, H_c). ^{13}C{^{1}H} NMR (DMSO-d_6, δ/ppm): 33.68 (Thioether C), 122.46 (C_e), 126.40 (C_f), 139.96 (C_d), 142.31 (C-NH_2), 146.96 (C_c). ESI$^+$-MS: m/z 708.8 {([9]ane-S_3)Ru(3-aminopyridine)$_3$.PF_6]$^+$, 281.7 [([9]ane-S_3)Ru(3-aminopyridine)$_3$]$^{2+}$. Anal. Calc. for $C_{21}H_{30}N_6S_3Ru(PF_6)_2$: C, 29.54; H, 3.54; N, 9.85. Found: C, 29.68; H, 3.60; N, 9.52. IR (cm^{-1}): 3391 (ν(N-H)).

([9]ane-S_3)Ru(3-(benzylamino)pyridine)$_3$.2PF_6:

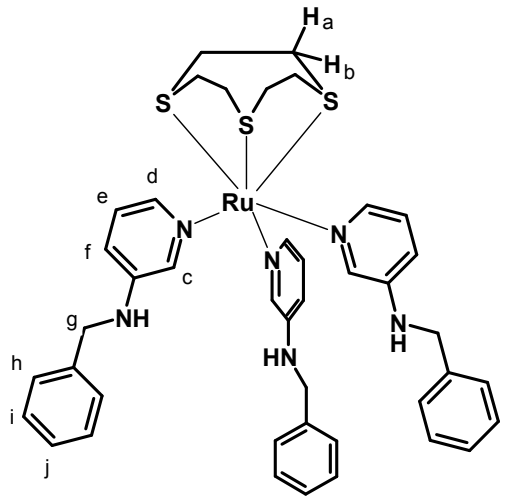

([9]ane-S_3)$RuCl_2$.DMSO (0.16 g, 0.38 mmol) was dissolved in ethanol/water (1:1, 30 ml) with slight warming of the solution. Silver hexafluorophosphate (0.19 g, 0.76 mmol) was added and the solution stirred at 60^{o}C for 1 hour, over which time the formation of silver chloride could be observed as a silvery-grey precipitate. Filtration of this salt left a yellow solution, to which was added 3-(benzylamino)pyridine[32] (0.21 g, 1.1 mmol). The solution was then heated to reflux for 16 hours, during which the colour was observed to go from yellow to green. Cooling the solution and removal of the solvent *in vacuo* led to the formation of the product as a green powder. Yield 0.31 g, 0.27 mmol, 72%. ^{1}H NMR (Acetone-d_6, J/Hz, δ/ppm): 2.59-3.02 (2 m, 12 H, Ha/Hb), 4.24 (d, J = 5.6, 6 H, Hg), 6.41 (t, J = 5.6, 3 H, NH), 7.13 – 7.38 (m, 15 H, H_e, H_f, H_h, H_i, H_j), 7.56 (d, J = 2.5, 3 H, H_d), 7.78 (d, J = 5.5, 3 H, H_c). $^{13}C\{^1H\}$ NMR (Acetone-d_6, δ/ppm): 33.57 (Thioether C), 46.70 (Cg), 121.73, 126.36, 126.99, 127.42, 128.85, 138.37, 138.67, 141.77, 146.57 (C_c). ESI$^+$-MS: m/z 979.1 $[M–PF_6]^+$. Anal. Calc. for $C_{42}H_{48}N_6S_3Ru(PF_6)_2$: C, 44.87; H, 4.30; N, 7.48. Found: C, 45.15; H, 4.44; N, 7.36. IR (cm^{-1}): 3442 (ν(N-H)).

([9]ane-S_3)Ru(3-(phenylaminomethyl)pyridine)$_3$.2PF_6:

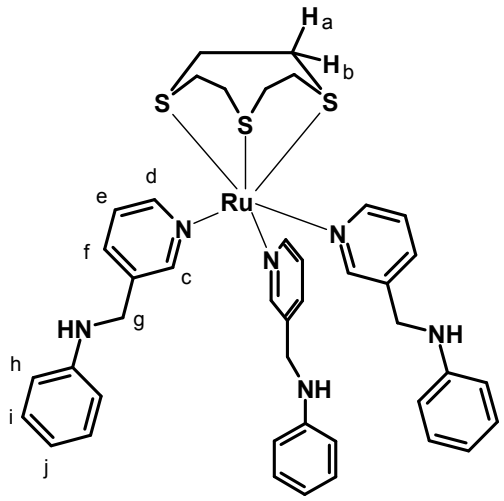

Formation of the ([9]ane-S_3)Ru(PF_6)$_2$ intermediate was achieved via the same method as before. Addition of 3-(phenylaminomethyl)pyridine[23] (0.21 g, 1.1 mmol) to the solution of this intermediate, followed by heating to reflux for 16 hours, led to a similar green colour. Cooling and removal of the solvent led to the formation of the product as a green powder. Yield 0.24 g, 0.22 mmol, 59 %. ^{1}H NMR (Acetone-d_6, J/Hz, δ/ppm): 2.55-2.70 (m, 6H, H_b), 2.80-2.95 (m, 6H, H_a), 4.39 (d, J = 6.2, 6H, H_g), 5.60 (t, J = 6.2, 3H, NH), 6.40-6.55 (m, 6H, H_h), 6.64 (t, J = 5.7, 3H, H_j), 7.09 (dd, J = 7.5, 8.3, 6H, H_i), 7.39 (dd, J = 5.7, 7.8, 3H, H_e), 8.03 (d, J = 7.7, 3H, H_f), 8.31 (d, J = 5.5, 3H, H_d), 8.39 (s, 3H, H_c). ^{13}C{^{1}H} NMR (Acetone-d_6, δ/ppm): 33.57 (Thioether Cs), 44.15 (C_g), 112.61, 117.26, 126.64, 129.38, 138.15, 139.72, 147.74, 152.41. ESI$^+$-MS: m/z 979.2 [M-PF_6]$^+$. Anal. Calc. for $C_{42}H_{48}N_6S_3Ru(PF_6)_2$: C, 44.87; H, 4.30; N, 7.48. Found: C,45.07; H, 4.42; N, 7.39. IR (cm^{-1}): 3444 (ν(N-H)).

([9]ane-S_3)Ru(3-(1-pyrenemethylamino)pyridine)$_3$.2PF_6:

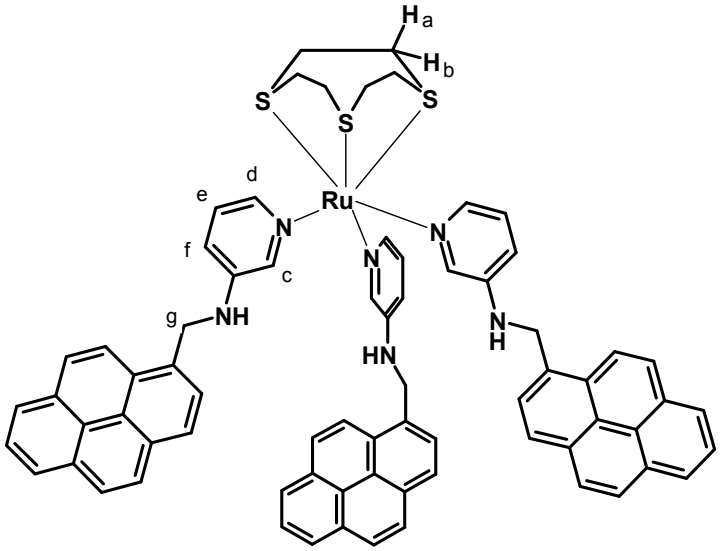

In situ formation of the ([9]ane-S_3)Ru(PF_6)$_2$ (0.22 g, 0.5 mmol) intermediate was achieved via the same method as before. This time, 3-(1-pyrenemethylamino)pyridine[28] (0.46 g, 1.5 mmol) was added to the solution and again heated to reflux for 16 h, causing the colour of the solution to go yellow-ochre in colour. Cooling and removal of the solvent led to the formation of the product as an ochre powder. Yield 0.59 g, 0.39 mmol, 79%. ^{1}H NMR (Acetone-d_6, J/Hz, δ/ppm): 1.96 – 2.50 (m, 12 H, H_a/H_b), 4.64 (d, J = 5.5, 6 H, H_g), 6.43 (t, J = 5.5, 3 H, NH), 6.68 (dd, J = 5.5, 8.6, 3 H), 7.02 (d, J = 5.5, 3 H), 7.14 (d, J = 8.4, 3 H), 7.27 (d, J = 5.5, 3 H), 7.81 (d, J = 7.9, 3 H), 8.00 – 8.28 (m, 18 H), 8.34 (dd, J = 1.9, 7.7, 3 H). ^{13}C{^{1}H} NMR (Acetone-d_6, δ/ppm): 33.06 (Thioether Cs), 44.55 (C_g), 122.38, 124.58, 124.66, 124.94, 125.19, 125.55, 125.66, 125.72, 126.51, 127.40, 127.62, 127.94, 128.13, 130.78, 130.85, 131.11, 131.47, 137.49, 141.36, 146.07. ESI$^+$-MS: m/z 1351.5 [M-PF_6]$^+$. Anal. Calc. for $C_{72}H_{60}N_6S_3Ru(PF_6)_2$: C, 57.78; H, 4.04; N, 5.62. Found: C, 57.10; H, 4.03; N, 5.52. IR (cm^{-1}): 3428 (ν(N-H)).

([9]ane-S_3)Ru(3-(*p*-tolylureido)pyridine)$_3$.2PF_6:

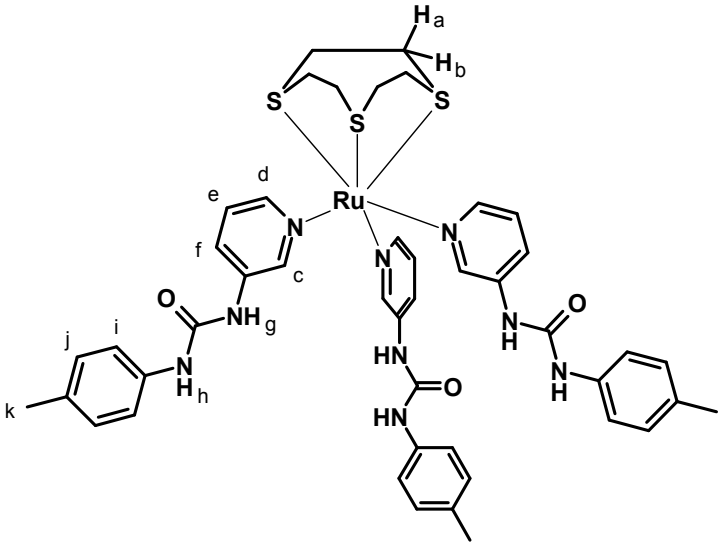

Formation of the ([9]ane-S_3)Ru(PF_6)$_2$.DMSO intermediate was achieved via the same method as before. 3-(*p*-tolylureido)pyridine (TUP)[33] (0.27 g, 1.2 mmol) was added to the solution and again heated to reflux for 16 h, causing the colour of the solution to go dark green in colour. Cooling and removal of the solvent led to the formation of the crude product as a dark green powder. Purification was achieved by recrystallisation of this green powder with acetone/diethyl ether to remove excess TUP. The final product was a lighter shade of green than the crude. Yield 0.23 g, 0.19 mmol, 46%. ^{1}H NMR (Acetone-d_6, J/Hz, δ/ppm): 1.11 (s, 9 H, H_k), 2.25-2.89 (m, 12 H, H_a/H_b), 7.10 (d, J = 8.6, 6 H, H_j), 7.37 (d, J = 8.6, 6 H, H_i), 7.45 (dd, J = 5.7, 8.3, 3 H, H_e), 7.99 (d, J = 5.7, 3 H, H_f), 8.05 (d, J = 8.1, 3 H, H_d), 8.24 (s, 3H, H_c), 8.72 (s, 3 H, H_h), 9.35 (s, 3 H, H_g). ^{13}C{^{1}H} NMR (Acetone-d_6, δ/ppm): 19.96 (Ck), 33.85 (Thioether Cs), 119.36, 126.82, 127.54, 129.51, 132.47, 136.43, 139.14, 144.38, 147.60, 152.46. MALDI-ToF$^+$-MS: m/z 755.1 [([9]ane-S_3)Ru(TUP)$_2$F]$^+$. Anal. Calc. for $C_{45}H_{51}N_9O_3S_3Ru(PF_6)_2$: C, 43.13; H, 4.10; N, 10.06. Found: C, 42.94; H, 4.35; N, 9.49. IR (cm^{-1}): 2923 (ν(N-H)), 1717 (ν(C=O)).

([9]ane-S_3)Ru(3-(*n*-octylureido)pyridine)$_3$.2PF_6:

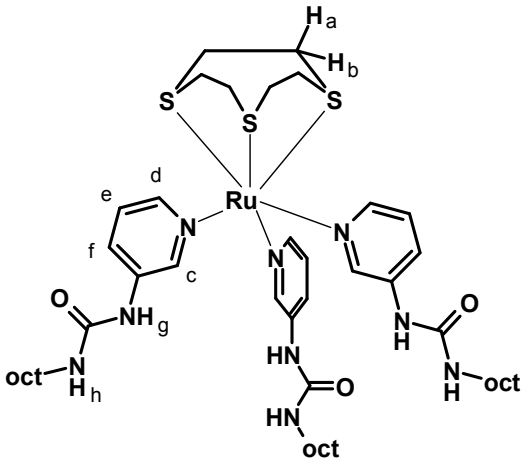

Formation of the ([9]ane-S_3)Ru(PF_6)$_2$.DMSO intermediate was achieved via the same method as before. 3-(*n*-octylureido)pyridine (OUP)[33] (0.22 g, 0.9 mmol) was added to the solution, containing 0.3 mmol of ([9]ane-S_3)Ru(PF_6)$_2$.DMSO and again heated to reflux for 16 h, causing the colour of the solution to go dark green in colour. Cooling and removal of the solvent led to the formation of the crude product as a dark green powder. Purification was difficult due to the high solubility of both OUP and the complex. Repeated recrystallisation of the crude product with acetone/cold diethyl ether was required to remove the majority of the starting material. Yield 0.22 g, 0.17 mmol, 55%. ^{1}H NMR (DMSO-d_6, J/Hz, δ/ppm): 0.83 – 3.03 (m, 51 H, octyl C-Hs), 6.41 (s, 3 H, H_h), 7.31 (dd, J = 5.6, 8.4, 3 H, H_e), 7.73 (d, J = 5.6, 3 H, H_f), 7.91 (d, J = 8.4, 3 H, H_d), 8.75 (s, 3 H, H_c), 9.06 (s, 3 H, H_g). ^{13}C{^{1}H} NMR (DMSO-d_6, δ/ppm): 14.33 – 40.71 (8 C, octyl Cs), 34.66 (thioether Cs), 127.41, 127.65, 140.49, 144.63, 147.64, 155.74 (urea C). ESI$^+$-MS: m/z 799.1 [([9]ane-S_3)Ru$(OUP)_2F]^+$. Anal. Calc. for $C_{48}H_{81}N_9O_3S_3Ru(PF_6)_2$: C, 43.69; H, 6.19; N, 9.56. Found: C, 42.78; H, 5.97; N, 9.26. IR (cm^{-1}): 2928 (ν(N-H)), 1680 (ν(C=O)).

Crystal Data:

Crystals were grown from **5.1** in Ethanol/water (1:1 ratio, 2 ml) by slow evaporation of the solvent.

Crystal data for **5.1**.2PF_6: $C_{21}H_{30}F_{12}N_6P_2RuS_3$, M = 853.70, green needles, 0.02 × 0.02 × 0.2 mm^3, triclinic, space group $P\bar{1}$ (No. 2), a = 11.7238(11), b = 11.7563(11), c = 13.1508(12) Å, α = 109.9560(10), β = 94.499(2), γ = 110.922(2)°, V = 1549.4(2) $Å^3$, Z = 2, D_c = 1.830 g/cm^3, F_{000} = 856, MoKα radiation, λ = 0.71073 Å, T = 120(2)K, $2\theta_{max}$ = 61.0º, 27777 reflections collected, 8829 unique (R_{int} = 0.0280). Final *GooF* = 0.920, *R1* = 0.0306, *wR2* = 0.1072, *R* indices based on 7873 reflections with I >2σ(I) (refinement on F^2), 430 parameters, 0 restraints. Lp and absorption corrections applied, μ = 0.910 mm^{-1}.

5.6 References

1. S. G. Telfer, G. Bernardinelli and A. F. Williams, *Chem. Commun.*, 2001, 1498-1499.
2. S. G. Telfer, G. Bernardinelli and A. F. Williams, *Dalton Trans.*, 2003, 435-440.
3. B. Wu, X. J. Yang, C. Janiak and P. G. Lassahn, *Chem. Commun.*, 2003, 902-903.
4. S. Nieto, J. Pérez, V. Riera, D. Miguel and C. Alvarez, *Chem. Commun.*, 2005, 546-548.
5. N. C. A. Baker, N. McGaughey, N. C. Fletcher, A. V. Chernikov, P. N. Hortonb and M. B. Hursthouse, *Dalton Trans.*, 2009, 965-972.
6. B. Geisser, A. Ponce and R. Alsfasser, *Inorg. Chem.*, 1999, **38**, 2030-2037.
7. P. L. Arnold and A. C. Scarisbrick, *Organometallics*, 2004, **23**, 2519-2521.
8. L. H. Uppadine, F. R. Keene and P. D. Beer, *J. Chem. Soc., Dalton Trans.*, 2001, 2188-2198.
9. X. D. Yu, H. Lin and H. K. Lin, *Transit. Met. Chem.*, 2008, **33**, 829-834.
10. A. Ghosh, S. Verma, B. Ganguly, H. N. Ghosh and A. Das, *Eur. J. Inorg. Chem.*, 2009, 2496-2507.
11. X.-F. Shang, J. Li, H. Lin, P. Jiang, Z.-S. Cai and H.-K. Lin, *Dalton Trans*, 2009, 2096-2102.
12. S. Derossi, H. Adams and M. D. Ward, *Dalton Trans.*, 2007, 33-36.
13. Y. Cui, Y. L. Niu, M. L. Cao, K. Wang, H. J. Mo, Y. R. Zhong and B. H. Ye, *Inorg. Chem.*, 2008, **47**, 5616-5624.
14. K. J. Wallace, R. Daari, W. J. Belcher, L. O. Abouderbala, M. G. Boutelle and J. W. Steed, *J. Organomet. Chem.*, 2003, **666**, 63-74.
15. L. Ion, D. Morales, J. Pérez, L. Riera, V. Riera, R. A. Kowenicki and M. McPartlin, *Chem. Commun.*, 2006, 91-93.
16. M. Auzias, B. Therrien, G. Suss-Fink, P. Stepnicka, W. H. Ang and P. J. Dyson, *Inorg. Chem.*, 2008, **47**, 578-583.
17. A. L. Hector and A. F. Hill, *Inorg. Chem.*, 1995, **34**, 3797-3800.
18. M. Newell, J. D. Ingram, T. L. Easun, S. J. Vickers, H. Adams, M. D. Ward and J. A. Thomas, *Inorg. Chem.*, 2006, **45**, 821-827.

19. S. Bolano, J. Bravo, J. Castro, M. M. Rodriguez-Rocha, M. da Silva, A. J. L. Pombeiro, L. GonsalVi and M. Peruzzini, *Eur. J. Inorg. Chem.*, 2007, 5523-5532.
20. I. Kuzu, D. Nied and F. Breher, *Eur. J. Inorg. Chem.*, 2009, 872-879.
21. B. Boardman, M. J. Hanton, H. van Rensburg and R. P. Tooze, *Chem. Commun.*, 2006, 2289-2291.
22. Z. Y. Bian, K. Sumi, M. Furue, S. Sato, K. Koike and O. Ishitani, *Dalton Trans.*, 2009, 983-993.
23. S. J. Dickson, S. C. G. Biagini and J. W. Steed, *Chem. Commun.*, 2007, 4955-4957.
24. M. N. Bell, A. J. Blake, M. Schroder, H. J. Kuppers and K. Wieghardt, *Angew. Chem. Int. Ed. Eng.*, 1987, **26**, 250-251.
25. S. Roche, C. Haslam, H. Adams, S. L. Heath and J. A. Thomas, *Chem. Commun.*, 1998, 1681-1682.
26. S. Roche, H. Adams, S. E. Spey and J. A. Thomas, *Inorg. Chem.*, 2000, **39**, 2385-2390.
27. I. P. Evans, A. Spencer and Wilkinso.G, *J. Chem. Soc.-Dalton Trans.*, 1973, 204-209.
28. M. H. Filby, S. J. Dickson, N. Zaccheroni, L. Prodi, S. Bonacchi, M. Montalti, C. Chiorboli, M. J. Paterson, T. D. Humphries and J. W. Steed, *J. Am. Chem. Soc.*, 2008, **130**, 4105-4113.
29. R. B. Bedford, M. Betham, C. P. Butts, S. J. Coles, M. B. Hursthouse, P. N. Scully, J. H. R. Tucker, J. Wilkie and Y. Willener, *Chem. Commun.*, 2008, 2429-2431.
30. P. Gans, *HypNMR 2006*, (2006) University of Leeds, Leeds.
31. F. M. Winnik, *Chem. Rev.*, 1993, **93**, 587-614.
32. K. J. Wallace, W. J. Belcher, D. R. Turner, K. F. Syed and J. W. Steed, *J. Am. Chem. Soc.*, 2003, **125**, 9699-9715.
33. D. R. Turner, E. C. Spencer, J. A. K. Howard, D. A. Tocher and J. W. Steed, *Chem. Commun.*, 2004, 1352-1353.

Appendices

List of abbreviations

Cp	=	Cyclopentadienyl anion ($C_5H_5^-$)
OTf	=	Trifluoromethane sulphonate anion (Triflate, $CF_3SO_3^-$)
OTs	=	*p*-toluene sulphonate anion (Tosylate, *p*-$CH_3C_6H_4SO_3^-$)
Tren	=	Tris(2-aminoethyl)amine
AMP	=	Adenosine Monophosphate
ADP	=	Adenosine Diphosphate
ATP	=	Adenosine Triphosphate
O3Tm	=	Trimesylate trianion (1,3,5-benzenetricarboxylate)
Et	=	Ethyl (CH_3CH_2) group
Me	=	Methyl (CH_3) group
Ph	=	Phenyl (C_6H_5) group
Bz	=	Benzyl ($C_6H_5CH_2$) group
PUP	=	3-(1-pyrenylureido)pyridine
TUP	=	3-(*p*-tolylureido)pyridine
OUP	=	3-(*n*-octyluriedo)pyridine
DPPA	=	Diphenylphosphoryl azide, $(PhO)_2P(O)N_3$
MeCN	=	Acetonitrile
DMSO	=	Dimethyl sulphoxide
Bipy	=	2,2-bipyridine
[9]ane-S_3	=	1,4,7-trithiacyclononane
TBA	=	Tetrabutylammonium cation

Instrumental Details

All NMR spectra were performed using a Varian Mercury-400 (400 MHz for ^{1}H, 100MHz for ^{13}C) spectrometer. MALDI-MS data was collected using an Applied Biosystems Voyager-DE STR instrument. ES^{+}-MS data was collected using a Thermo-Finnigan LTQ FT instrument. UV/Vis absorption wavelengths were recorded using a Perkin-Elmer Lambda 35 instrument. Fourier transform infrared spectra were recorded with a Perkin-Elmer Spectrum 100 ATR instrument, recording 64 scans over a spectral range of 4000 to 600 cm^{-1} with a resolution of 4 cm^{-1}. The analysis was carried out with the Spectrum Express 1.01 software. Elemental analysis was performed using an Exeter Analytical inc. CE-400 Elemental Analyser. Emission and excitation spectra were obtained using a Jobin-Yvon Horiba Fluorolog 3-22 Tau-3 spectrofluorimeter with a right angle illumination method and were corrected for the spectral response of the instrument. Commercial reagents were purchased from Sigma Aldrich or Alfa Aesar, and were used as supplied, without further purification. Deuterated solvents for NMR experiments were purchased from Goss Scientific Instruments Ltd., and were used as supplied.